FUNCTIONAL ADAPTATION OF THE RUMINAL EPITHELIUM

A Thesis Submitted to the

College of Graduate Studies and Research

in Partial Fulfillment of the Requirements

for the Degree of Master of Science

in the Department of Animal and Poultry Science

University of Saskatchewan

Saskatoon

By

Brittney L. Schurmann

December 2013

PERMISSION TO USE

In presenting this thesis in partial fulfillment of the requirements for a Master of Science degree from the University of Saskatchewan, I agree that the Libraries of this University may make it freely available for inspection. I further agree that permission for copying of this thesis in any manner, in whole or in part, for scholarly purposes may be granted by the professor or professors who supervised my thesis work, or in their absence, by the Head of the Department or Dean of the College in which my thesis work was done. It is understood that any copying or publication or use of this thesis or parts of thereof for financial gain shall not be allowed without my written permission. It is also understood that due recognition shall be given to me and to the University of Saskatchewan in any scholarly use which may be made of any material in my thesis.

Request for permission to copy or make other use of material in this thesis in whole or in part should be addressed to:

Head of the Department of Animal and Poultry Science

University of Saskatchewan

Saskatoon, Saskatchewan, Canada S7N 5A8

ABSTRACT

Short chain fatty acids (SCFA) synthesized in the rumen from carbohydrate fermentation are an essential energy source for ruminants. Current literature supports that SCFA are absorbed across the rumen epithelium via passive diffusion or protein-mediated transport, however, the rate and degree to which these pathways adapt to a change in diet fermentability is unknown. Furthermore, Na^+ flux is partially determined by SCFA absorption, and thus is a key indicator of functional changes in the rumen epithelium. The objectives of this study were to determine the time required for a change in SCFA and Na^+ absorption across the bovine rumen epithelium and to evaluate the rate and degree to which absorption pathways adapt to an increase in diet fermentability relative to changes in surface area. Twenty-five weaned Holstein steer calves were blocked by body weight and randomly assigned to either the control diet (CON; 91.5% hay and 8.5% vitamin/mineral supplement) or a moderately fermentable diet (50% hay; 41.5% barley grain, and 8.5% vitamin/mineral supplement) fed for 3 (G3), 7 (G7), 14 (G14), or 21 d (G21). All calves were fed at 2.25% BW at 0800 h. Reticular pH was recorded every 5 min for 48 h prior to killing (1000 h). Ruminal tissue was collected for Ussing chamber, barrier function, surface area measurements, and gene expression. Net $^{22}Na^+$ flux ($J_{NET\text{-}Na}$; 80 kBq/15 mL), the rate and pathway of mucosal to serosal ^{3}H-acetate ($J_{MS\text{-}acetate}$; 37 kBq/15 mL) and ^{14}C-butyrate ($J_{MS\text{-}butyrate;}$ 74 kBq/15 mL) flux, and serosal to mucosal flux of ^{3}H-mannitol ($J_{SM\text{-}mannitol}$; 74 KBq/15 mL) and tissue conductance were measured. Half of the chambers assigned to measure $J_{MS\text{-}acetate}$ and $J_{MS\text{-}butyrate}$ were further assigned to 1 of 2 acetate and butyrate concentration treatments: 10 m*M* (Low) and 50 m*M* (High). Furthermore, $J_{SM\text{-}mannitol}$ flux was also measured during an acidotic and hyperosmotic challenge (CHAL) and recovery (REC) to measure barrier function of ruminal tissue. Mean reticular pH, which was positively correlated with ruminal pH (R^2 = 0.5477), decreased from 6.90 for CON to 6.59 for G7 then increased. Net Na^+ flux increased 125% within 7 d. Total $J_{MS\text{-}acetate}$ and $J_{MS\text{-}butyrate}$ increased from CON to G21, where passive diffusion was the primary SCFA absorption pathway. Total $J_{MS\text{-}acetate}$ and $J_{MS\text{-}butyrate}$ were greater when incubated in High vs. Low. Effective surface area of the ruminal epithelium was not affected by dietary treatment. Increased $J_{SM\text{-}mannitol}$, tissue conductance, and increased expression of IL-1β and TLR2 (tendencies) with increased days fed the moderate grain diet indicated reduced rumen epithelium barrier function. Furthermore, the CHAL treatment reduced barrier function, which was not reversible during REC. This study indicates that a moderate

increase in diet fermentability increases rumen epithelium absorptive function in the absence of increased SA, but reduces barrier function. Data from this study also suggests that absorption and barrier function follow different timelines, posing a challenge for ruminant diet adaptation to moderately to highly fermentable diets.

ACKNOWLEDGEMENTS

First, I would like to acknowledge my supervisor, Dr. Greg Penner. From the start, I am extremely thankful for his encouragement and confidence in me pursuing a Master's degree. In particular, I am grateful for his guidance during the early stages of planning my experiment, generous hands-on help throughout my project, assistance during data analysis, and constructive criticism during the writing phase. I admire his ambition, as it constantly encouraged me to strive for more. I truly enjoyed my time with him along the way and have been fortunate to be part of the exciting learning environment of "Team Rumen".

I would also like to thank my other committee members: Dr. Fiona Buchanan, Dr. Dave Christensen, Dr. Steve Hendrick, and Dr. John McKinnon. In particular, I greatly appreciate their suggestions and contributions during the planning of my experiment. I also want to recognize Dr. Tim Mutsvangwa for his laboratory assistance, and Dr. Matthew Loewen and C. Ching for their aid in gene expression analysis.

Furthermore, without my fellow students and friends I would not have been able to complete my experiment. I am extremely grateful for the generous support from members of Team Rumen who helped me in various aspects from feeding and cleaning in the barn to mounting tissue in the laboratory: G. Chibisa, R. Claassen, P. Górka, G. Gratton, F. Joy, C. Rosser, T. Schwaiger, and M. Walpole. Specifically, I would like to thank M. Walpole for his guidance and patience in the Ussing chamber laboratory.

I would also like to show my appreciation to my parents, R. Schurmann and T. Schurmann, and my siblings, B. Schurmann, K. Schurmann, N. Schurmann, and R. Schurmann, and last but not least, my fiancé, E. Buyer, for their love and encouragement throughout this journey.

TABLE OF CONTENTS

LIST OF TABLES

LIST OF FIGURES

LIST OF ABBREVIATIONS

ACAT	acetyl-CoA acetyl transferase
ADF	acid detergent fibre
BASE	*ex vivo* initial flux period
BHBA	β-hydroxybutyric acid
CHAL	*ex vivo* acidotic challenge flux period
CON	control diet
CP	crude protein
C_T	PCR cycle threshold
DM	dry matter
DMI	dry matter intake
G3	fed moderate grain diet for 3 d
G7	fed moderate grain diet for 7 d
G14	fed moderate grain diet for 14 d
G21	fed moderate grain diet for 21 d
GPR41	G protein-coupled receptor 41
GPR43	G protein-coupled receptor 43
G_t	tissue conductance
High	high *ex vivo* acetate and butyrate concentration treatment
IGFBP3	insulin-like growth factor binding protein 3
IGFBP5	insulin-like growth factor binding protein 5
IL-1β	interleukin 1β
IL-4	interleukin 4

IL-8	interleukin 8
IL-10	interleukin 10
IL-13	interleukin 13
IL-22	interleukin 22
I_{SC}	short circuit current
$J_{MS\text{-}acetate}$	mucosal to serosal acetate flux
$J_{MS\text{-}butyrate}$	mucosal to serosal butyrate flux
$J_{MS\text{-}Na}$	mucosal to serosal sodium flux
$J_{NET\text{-}Na}$	net sodium flux
$J_{SM\text{-}mannitol}$	serosal to mucosal mannitol flux
$J_{SM\text{-}Na}$	serosal to mucosal sodium flux
Low	low *ex vivo* acetate and butyrate concentration treatment
MCT1	monocarboxylate transporter 1
NDF	neutral detergent fibre
NHE1	sodium-hydrogen exchanger 1
NHE3	sodium-hydrogen exchanger 3
OM	organic matter
PBS	phosphate buffered saline
qRT-PCR	quantitative real-time PCR
REC	*ex vivo* flux period following challenge and mucosal buffer replacement
SA	surface area
SARA	subacute ruminal acidosis
SCFA	short chain fatty acid

TLR2	toll-like receptor 2
TLR4	toll-like receptor 4
TNFα	tumor necrosis factor α

1.0. GENERAL INTRODUCTION

The gastrointestinal tract of ruminants is different relative to monogastric species, as it is comprised of 3 distinct regions prior to acidic digestion in the abomasum; the reticulum, rumen, and omasum. The reticulo-rumen facilitates microbial fermentation and absorption of the end-products (short-chain fatty acids; SCFA) arising from carbohydrate fermentation (Aschenbach et al., 2011). While fermentation of complex carbohydrates provides ruminants a dietary niche unavailable to monoagstric animals, the consumption of rapidly fermentable substrates predisposes cattle to ruminal acidosis. Ruminal acidosis occurs when the accumulation of fermentation acid products reduce ruminal pH below the physiological norm (pH < 5.8 to 6.2; Nocek, 1997; Penner et al., 2007). As such, ruminal acidosis is a concern on commercial operations where cattle are rapidly transitioned to diets with increasing fermentability in order to promote rapid growth, such as from backgrounding to finishing in feedlots, or to maximize milk production on dairy farms (Lesmeister and Heinrichs, 2004; Bevans et al., 2005; Penner et al., 2007). Therefore, recent research has focused in part on mitigation of ruminal acidosis.

Short chain fatty acids are the primary energy metabolite arising from carbohydrate fermentation in the rumen and provide up to 75% of the ruminant's total metabolizable energy requirements, relative to 10% in humans and 5 to 42% in various other monogastric and hind-gut fermenting species (Bergman, 1990). It has been suggested that, following fermentation, 50-85% of SCFA are absorbed across the ruminal epithelium (Bergman, 1990; Kristensen et al., 1998). Previous studies have suggested that absorption of SCFA occurs via passive diffusion with absorption rates largely dictated by the absorptive surface area (Bugaut, 1987; López et al., 2003). However, more recent studies have proven that SCFA absorption also occurs through facilitated transport (Kramer et al., 1996; Sehested et al., 1999b; Penner et al., 2009a; Aschenbach et al., 2009) with data suggesting that facilitated transport may play a prominent role in regulating the concentration of SCFA in the rumen and ruminal pH. The latter suggestion is based on a recent study demonstrating that lambs with greater rates of SCFA uptake are less susceptible to reduced ruminal pH, induced by an oral glucose challenge, than lambs with lower rates of SCFA uptake (Penner et al., 2009a).

While promoting the flux of specific molecules such as SCFA and Na^+ (Gäbel et al., 1991a,b; Etschmann et al., 2009; Aschenbach et al., 2009; Penner et al., 2009a), the structure of the ruminal epithelium concurrently acts as a protective barrier preventing harmful compounds from entering the portal circulation (Aschenbach and Gäbel, 2000; Plaizier et al., 2012). However, rapidly transitioning ruminants to a highly fermentable diet elevates ruminal SCFA production. As a result of the increased ruminal SCFA concentration and corresponding reduction in ruminal pH, tight junction stability may also be reduced leading to an increase in ruminal epithelium permeability (Steele et al., 2011; Liu et al., 2013). However, it is clear that the ruminal epithelium adapts in response to a change in diet. Documented adaptive responses include increases in Na^+ transport mediated at the cellular level (Etschmann et al., 2009) and increases in the absorptive surface area of the ruminal epithelium (Dirksen et al., 1985).

Previous studies have focused on understanding the mechanisms for SCFA transport across the ruminal epithelium (Sehested et al., 1999b; Aschenbach et al., 2009), the linkage of SCFA and Na^+ transport (Gäbel et al., 1991b; Sehested et al., 1996; Sehested et al., 1999b), and how individual animals may differ in their physiologic capability for SCFA uptake (Penner et al., 2009a), but these studies did not evaluate the rate of adaptation for these pathways in response to a change in diet fermentability. Furthermore, passive diffusion of undissociated SCFA has previously shown to increase Na^+ absorption (Gäbel et al., 1991b; Etschmann et al., 2009), therefore, Na^+ flux is another indicator of increased functional activity of the ruminal epithelium. Adaptation of the ruminal epithelium for Na^+ transport rates have been measured in sheep following an increase in dietary fermentability (Etschmann et al., 2009); however, this model has not been evaluated in cattle. The intent of the current study was to evaluate the timeline needed for a change in SCFA and Na^+ absorption across the bovine rumen epithelium following a change in diet fermentability and also to assess the rate and degree to which transport pathways adapt to diet adaptation in relation to epithelial surface area changes.

2.0. LITERATURE REVIEW

2.1. Ruminal Epithelium Structure and Function

2.1.1. Organization and Characterization of Cell Strata, Cell Type and Function

The ruminal epithelium is characterized as having 4 distinct strata, described as a stratified squamous epithelium (Graham and Simmons, 2005). From the apical (luminal-facing) membrane to the basolateral (blood-facing) membrane, the 4 strata include the stratum corneum, stratum granulosum, stratum spinosum, and stratum basale with each stratum performing unique roles promoting the function of the syncytium.

The outermost stratum, the stratum corneum, is in direct contact with the ruminal lumen and is comprised of flat, cornified keratinocytes that frequently undergo sloughing and replacement (Lavker and Matoltsy, 1970; Graham and Simmons, 2005). Although past studies have suggested that the stratum corneum contributes to the barrier function and regulation of SCFA transport of the ruminal epithelium (Hinders and Owen, 1965), this has been questioned. Studies evaluating the microstructure of the stratum corneum have revealed that cells are loosely connected (Graham and Simmons, 2005; Steele et al., 2011). While one study has reported expression of monocarboxylate transporters in the stratum corneum (Kirat et al., 2006), the relevance for this finding is not clear given that the stratum corneum is devoid of intracellular organelles. Due to the physical properties of the stratum corneum, it is likely that the primary role is physical protection of underlying strata from the abrasive contents of the reticulo-rumen (Graham and Simmons, 2005).

The stratum granulosum, located below the stratum corneum, is comprised of granular cells connected to one another via tight cell junctions. Tight cell junctions are composed of two principal proteins, claudin-1 and zonula occluden-1 (ZO-1; Graham and Simmons, 2005). These tight cell junction proteins function together to form a protective barrier that limits translocation of large molecules such as pathogens (Klevenhusen et al., 2013) and antigens (lipopolysaccharide; LPS; Emmanuel et al., 2007) across the ruminal epithelium. However, tight cell junctions may be permeable to smaller compounds such as K^+ and sugars (Graham and Simmons, 2005). As granulosum cells migrate and differentiate from the stratum granulosum to the stratum corneum, an increasing quantity of keratin granules accumulate within the cells,

leading to the formation of keratinocytes (Steven and Marshall, 1970; Graham and Simmons, 2005). There is also a reduction in the concentration of intracellular organelles, Na^+/H^+ exchange proteins, and Na^+/K^+-ATPase as cells move from the strata granulosum to corneum (Graham and Simmons, 2005; Graham et al., 2007). Although organelles and exchange proteins are located in the stratum granulosum, they are much more densely located in the stratum spinosum and stratum basale (Graham and Simmons, 2005; Graham et al., 2007). Due to the close relationship between SCFA absorption and Na^+/H^+ exchange (Gäbel et al., 1991b; Sehested et al., 1996; Sehested et al., 1999a) the localization of Na^+/H^+ exchangers is abundant in the stratum granulosum (Graham et al., 2007) suggesting that this stratum may play an important role in SCFA absorption regulation.

The stratum spinosum is located below the stratum granulosum of the ruminal epithelium. Comprising the stratum spinosum are cells capable of metabolic activity, as indicated by the presence of organelles such as nuclei, mitochondria, ribosomes, endoplasmic reticulum, golgi apparatus, and vesicles (Graham and Simmons, 2005). The stratum spinosum contains gap junctions between cells, including proteins such as connexion 26 and 43, which are responsible for cell signalling and cell-to-cell movement of small molecules such as small ions, sugars, lactate, and butyrate (White, 2003; Graham and Simmons, 2005). Furthermore, this stratum is rich in desmosomes which link neighbouring cells and also contains tight-cell junction proteins claudin-1 and ZO-1, though at a much lower concentration relative to the stratum granulosum (Graham and Simmons, 2005). Given the rich density of intracellular organelles located in the stratum spinosum, the primary role is likely metabolism of SCFA and subsequent transport of the end products via gap junctions to adjacent cells for cellular energy use or to the stratum basale for extrusion of metabolites into arterial circulation.

The stratum basale borders the lamina propria and is in close contact with arterioles. The stratum basale is comprised of columnar cells that are linked to stratum spinosum cells via desmosomes (Graham and Simmons, 2005). Similar to spinosum cells, basale cells contain nuclei, mitochondria and other intracellular organelles, however, nuclei are larger and mitochondria are more abundant, indicating a high capacity for metabolic activity (Graham and Simmons, 2005; Steele et al., 2011). In fact, the Na^+/K^+ ATPase, an ATP-dependent transporter, exhibits its highest density in the stratum basale, suggesting that the stratum basale plays a

prominent role in regulating the electrochemical gradient across the ruminal epithelium (Graham and Simmons, 2005). Suitably, the large quantity of mitochondria in basale cells corresponds with the profound energy requirements of the Na^+/K^+-ATPase (Graham and Simmons, 2005). As the stratum basale is rich in intracellular organelles, metabolism of energy molecules such as SCFA is a likely responsibility of this stratum. In addition, the abundance of Na^+/K^+-ATPase found in the stratum basale indicates its powerful driving force for the uptake of apical nutrients. It has been shown that increasing the fermentability of the diet initiates an increased rate of cellular differentiation and proliferation, which occur in the stratum basale (Goodlad, 1981).

2.1.2. Mechanisms of Ion Transport across the Ruminal Epithelium

The stratified squamous epithelium of the rumen epithelia acts as a selectively permeable membrane between the lumen of the rumen and arterial circulation. The rumen epithelium accomplishes this by regulating the absorption of molecules from the apical to basolateral membrane and secretion from the basolateral membrane to the apical membrane (Gäbel et al., 2002; Aschenbach et al., 2009; Leonard- Marek et al., 2007). Such molecules include ions such as SCFA (Gäbel et al., 2002; Aschenbach et al., 2009; Penner et al., 2009a), Na^+ (Gäbel et al., 1991b; Lodemann and Martens, 2006; Etschmann et al., 2009), Cl^- (Gäbel et al., 1991b; Leonhard-Marek et al., 2007), K^+ (White et al., 2003; Leonhard-Marek et al., 2007), Ca^{2+} (Leonhard-Marek et al., 2007; Wilkens et al., 2011), Mg^{2+} (Leonhard-Marek et al., 2007; Schweigel et al., 2009), HCO_3^- (Aschenbach et al., 2009; Penner et al., 2009a), glucose (Gäbel and Aschenbach, 2002), ammonia (NH_3/NH_4^+; Obara et al., 1991; Aschenbach et al., 2011), urea (Gozho et al., 2008; Doranalli et al., 2011), and peptides and amino acids (Matthews and Webb, 1995; Faix and Faixova, 2001). Regarding this thesis, SCFA and Na^+ flux are the focus, and as such these molecules will be emphasized for the remainder of this review.

2.1.2.1. Short Chain Fatty Acid Absorption across the Ruminal Epithelium

Early research on the rumen suggested that the ruminal epithelium facilitated dietary carbohydrate fermentation, but did not have the ability to absorb fermentation end products or other nutrients (Tappeiner, 1884). However, in the 1940's, it was discovered that SCFA are capable of crossing the epithelium (Barcroft et al. 1944). Following this discovery, there was

evidence suggesting that SCFA are not only able to move across the epithelium, but they are the primary energy source for ruminants (Bergman et al. 1965). Furthermore, it was originally thought that SCFA absorption across the ruminal epithelium occurred via passive diffusion (Bugaut, 1987). However, more recent research has shown using isolated ruminal epithelia from cattle (Sehested et al. 1999b) and sheep (Aschenbach et al. 2009; Penner et al. 2009a) that a portion of SCFA absorption is bicarbonate-dependent. Additionally, it has been suggested that there is a mechanism of absorption that is dependent on bicarbonate but is also sensitive to nitrate (Figure 2.1.; Aschenbach et al. 2009; Penner et al. 2009a).

Principal SCFA produced in the rumen include acetate, propionate, and butyrate (Bergman, 1990). Out of the total quantity of SCFA produced in the reticulo-rumen, approximately 50 to 85% are absorbed across the reticulo-rumen epithelium (Bergman, 1990; Kristensen et al. 1998). Furthermore, short-chain fatty acids exist in the ruminal lumen in the un-dissociated (HSCFA) or dissociated ($SCFA^-$) form. As mentioned above, one method of ruminal SCFA absorption is passive diffusion, in which case the SCFA diffuses across the epithelium in the undissociated form (Gäbel et al. 2002; Graham et al. 2007; Aschenbach et al. 2009). The luminal presence of H^+ most predominantly favors passive diffusion of protonated SCFA. In the ruminal lumen, SCFA are able to bind with H^+, resulting in HSCFA, a lipophilic molecule which is able to diffuse across the lipid membrane (Figure 2.1.; Aschenbach et al. 2009). Upon reaching the cytosol, HSCFA is dissociated into SCFA and H^+ due to the high cytosolic pH value (Gäbel et al. 1991). However, relative to dissociated SCFA, protonated SCFA comprise a small proportion of total ruminal SCFA and also a minority (~ 15%) of the total SCFA absorbed by the epithelium (Allen, 1997). Furthermore, non-protonated SCFA are lipophobic, and thus are not able to diffuse across the apical membrane (Gäbel et al. 2002).

The low ruminal concentration of protonated SCFA and low permeability of non-protonated $SCFA^-$ to the lipid bilayer membrane indicates that other absorption mechanisms must exist fornon-protonated SCFA. With the secretion of a bicarbonate anion, $SCFA^-$ can be transported across the epithelium via $SCFA^-/HCO_3^-$ exchange proteins (Figure 2.1.; Gäbel et al. 2002; Aschenbach et al. 2009; Penner et al. 2009a). Candidate $SCFA^-/HCO_3^-$ transporters

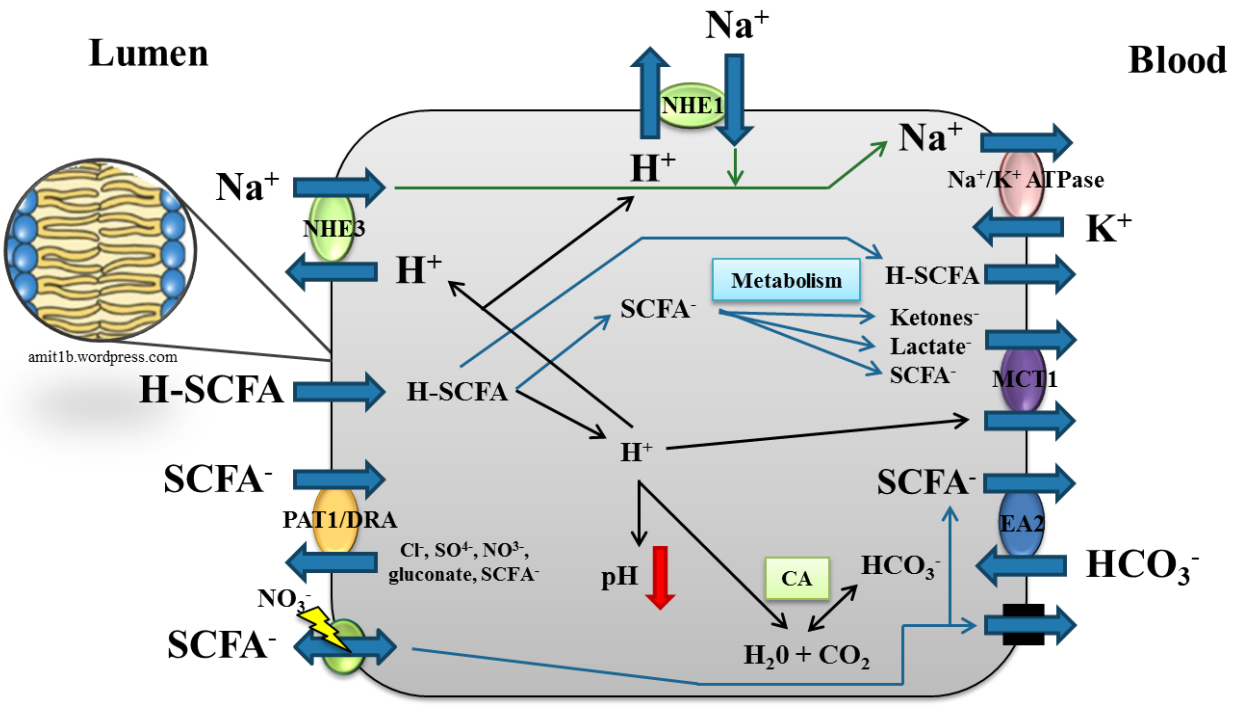

Figure 2.1. Apical and basolateral short chain fatty acid absorption and intra-epithelial metabolism, H^+ secretion, and Na^+ absorption. This is a simplified ruminal epithelium, as there are 4 strata with multiple cell layers per strata. Figure is adapted from Aschenbach et al., 2011.

include putative anion transporter 1 (PAT1), downregulated in adenoma (DRA) and anion exchanger 2 (AE2; Bilk et al., 2005). Both PAT1 and DRA have been expressed apically, whereas AE2 has been shown to be located on the basolateral membrane (Bilk et al., 2005). Furthermore, PAT1 and DRA exchange proteins generally secrete bicarbonate and absorb chloride; however, a SCFA anion may be exchanged in place of chloride (Kramer et al., 1996). The intracellular bicarbonate that exits at the apical membrane is sourced from the basolateral membrane, where it enters through AE2 (Bilk et al., 2005) or it may be produced by the hydration of carbon dioxide, a reaction performed by the enzyme carbonic anhydrase (CA): $H_2O + CO_2 \leftrightarrow H_2CO_3^-$ (Figure 2.1.; Gäbel and Sehested, 1997). The extra H^+ atom is removed from the molecule to form bicarbonate: $H_2CO_3^- \rightarrow HCO_3^- + H^+$ (Gäbel and Sehested, 1997). Cellular carbonic anhydrase therefore plays an important role in SCFA absorption by synthesizing bicarbonate for $SCFA^-/HCO_3^-$ exchange.

Furthermore, $SCFA^-$ flux independent of bicarbonate has been recently revealed. This pathway has shown to be sensitive to nitrate, however, the mechanism for this bicarbonate-independent SCFA uptake pathway is not well understood (Figure 2.1.; Aschenbach et al., 2009; Penner et al., 2009a). Perhaps the presence of nitrate causes a transformation of the protein exchanger, resulting in a reduction in SCFA transport. In summary, there are currently three known pathways for SCFA absorption across the ruminal epithelia: passive diffusion, bicarbonate-dependent, and bicarbonate-independent. However, considering that up to 85% of SCFA are absorbed across the ruminal epithelium, it is possible that more absorption pathways exist for this essential process.

Once a SCFA molecule has crossed the apical membrane into the epithelium, undissociated SCFA are dissociated in the cytosol to $SCFA^-$ and H^+ (Aschenbach et al., 2011). The $SCFA^-$ may then be metabolized within the cell for epithelial energy use. However, the proportion of SCFA metabolized are not equivalent among acetate, butyrate, and propionate, rather, the extent of SCFA metabolism is determined partially by lipophilic permeability of the SCFA, which is largely dependent on carbon chain length (Sehested et al., 1999a; Aschenbach et al., 2011). Acetic, propionic, and butyric acid exhibit carbon chain lengths of 2, 3 and 4, respectively, and it has been estimated that metabolism within the ruminal epithelium occurs at 30, 50, and 90% for each SCFA, respectively (Bergman, 1990). Numerous acyl-CoA synthetases

can be found which possess unique characteristics that determine which SCFA substrate they exploit and thus it is possible acyl-CoA synthetases play a regulatory role in epithelial metabolism (Ash and Baird, 1973; Penner et al., 2011). After SCFA uptake by the epithelium, oxidation of SCFA may occur as a specific acyl-CoA synthetase family, which initiates metabolism, adds CoA ester. Another explanation for the variability in epithelial metabolism of each SCFA is that there is a SCFA conductance channel on the basolateral membrane that has a greater permeability for acetate > propionate > butyrate (Stumpff et al., 2009). Interestingly, apical SCFA permeability is in the reverse order, meaning that butyrate accumulates within the epithelium for a greater period of time, and thus is more extensively metabolized. Apart from oxidation, $SCFA^-$ may be metabolized and repackaged via ketogenesis into ketone bodies for export into portal circulation. For example, butyrate may be re-packaged into the ketone beta-hydroxybutyric acid (BHBA) via ketogenesis before basolateral extrusion from the epithelium into the circulatory system (Kristensen and Harmon, 2004; Penner et al., 2011).

Dissociated SCFA or their metabolites, such as lactate and BHBA, in the epithelium may be extruded across the basolateral membrane into the blood, and subsequently metabolized by the liver or peripheral tissues for maintenance, growth, lactation, or lipogenesis (Bergman, 1990). The transport protein, mono-carboxylate transporter-1 (MCT1) is one mechanism of basolateral extrusion of dissociated SCFA and SCFA metabolites (Müller et al., 2002; Kirat et al., 2006). As mentioned above, the basolateral SCFA conductance channel is another absorption method of SCFA into the blood (Stumpff e al. 2009). Furthermore, a $SCFA^-/HCO_3^-$ exchanger, similar to that on the apical membrane, aids in basolateral extrusion of SCFA. And lastly, it has been suggested that lipophilic diffusion on the basolateral membrane may occur, when SCFA are in the undissociated form (Aschenbach et al., 2011). These basolateral $SCFA^-$ and SCFA metabolite extrusion pathways are shown in Figure 2.1.

Furthermore, diet is the largest determinant of SCFA absorption, as it largely influences ruminal SCFA concentration and pH (Allen 1997; Aschenbach et al., 2011). Numerous studies have shown increased SCFA absorption rates with elevated ruminal SCFA concentrations and reduced pH (Kristensen et al., 1996; Aschenbach et al., 2009). However, the rate and extent to which each SCFA absorption pathway adapts to changes in diet is not well understood.

2.1.2.2. Other Factors Regulating SCFA Absorption

In the ruminal epithelium, G protein-coupled receptors-41 and -43, GPR41 and GPR43, are expressed, which sense and bind acetate, propionate, and butyrate and may subsequently induce rumen development, as well as pancreatic insulin and glucagon secretion (Wang et al., 2009b). Epithelial cells are able to produce cyclic adenosine monophosphate (cAMP), a molecule used in intracellular signalling and activates cell surface receptors, such as GPR41 and GPR43 (Wang et al., 2009b, 2012). However, when SCFA bind to GPR41 or GPR43 proteins on the epithelium, there is a reduction in intracellular cAMP production and signalling (Wang et al., 2012). Furthermore, SCFA, in the absence of GPR41 and GPR43, have been shown to stimulate the expression of a cAMP response element (CRE)-reporter construct (Wang et al., 2009b, 2012). The CRE-reporter construct is the primary signaling molecule that initiates phosphorylation of CRE-binding protein, increases cAMP-protein kinase A (PKA) activity, and finally, increases the cAMP levels in cells, a process that can be abbreviated as cAMP-PKA-CREB signalling (Wang et al., 2012). The CRE-reporter construct is therefore the primary signaling molecule that initiates the elevated production of cAMP, which acts as a secondary messenger to activate GPR41 and GPR43 when cAMP recognizes extracellular signaling, and subsequently increases rumen epithelial development and hormone secretion from the pancreas. It has been shown that cAMP inhibits Na^+ and Cl^- transport across rumen epithelial tissue (Gäbel et al., 1999). The inhibition of Na^+ absorption via Na^+/H^+ exchangers has implications for regulation of intracellular pH, as protons within the cytosol cannot leave via the Na^+/H^+ exchangers when Na^+ absorption via this transporter is blocked (Gäbel et al., 1999). Furthermore, cAMP is able to inhibit Na^+/K^+-ATPase on the basolateral membrane that, if blocked, is not able to drive the Na^+/H^+ exchange proteins. Inhibition of Cl^- absorption by cAMP (Gäbel et al., 1999) may also cause a reduction in SCFA absorption. The $SCFA^-/HCO_3^-$ anion exchanger is also permeable to Cl^- (Cl^-/HCO_3^-; Sehested et al., 1999b), and when inhibited may cause a reduction in SCFA absorption.

As discussed above, SCFA may be metabolized within the cell prior to basolateral extrusion. Intracellular metabolism can also act as a driving force for SCFA absorption in 2 ways. First, SCFA absorption will increase due to the increase in SCFA concentration gradient between the ruminal lumen and inside the cell following metabolism of SCFA (Gäbel et al.,

2002). Additionally, the conversion of CO_2 within the cytosol to HCO_3^- by the enzyme carbonic anhydrase, creates a anion exchange mechanism where bicarbonate is driven out of the cell into the lumen and $SCFA^-$ are absorbed (Gäbel and Sehested, 1997; Gäbel et al., 2002; Bondzio et al., 2011).

2.1.2.3. Sodium Absorption across the Ruminal Epithelium

Sodium (Na^+) transport across epithelial tissue was originally measured using frog skin in the 1950's (Ussing and Zerahn, 1951). To date, however, Na^+ is an ion well known to be transported across the ruminal epithelium (Gäbel et al., 1989; Etschmann et al., 2009). Interestingly, Na^+ transport is closely related to SCFA flux across the ruminal epithelium (Gäbel et al., 1991b; Yang et al., 2012). Following ruminal absorption of HSCFA across the apical membrane, dissociation of the SCFA occurs within ruminal epithelial cells due to its low pKa value (Gäbel et al., 1991b) and the high intracellular pH. The release of H^+ increases intracellular acidity, which stimulates Na^+ transport via Na^+/H^+ exchange proteins (Gäbel et al., 1991b; Shen et al., 2004). Therefore, HSCFA flux is considered a stimulant of Na^+ transport (Sehested et al., 1999b; Gäbel et al., 2002; Etschmann et al., 2009).

Two Na^+/H^+ exchangers (NHE1 and NHE3) are located on the basolateral and apical membranes of the ruminal epithelium, respectively, which function together to regulate Na^+ transport and cytosolic pH (Gäbel et al., 2002; Graham et al., 2007; Rabbani et al., 2011). After Na^+ is absorbed from the apical membrane, basolateral extrusion occurs via the sodium/potassium pump, Na^+/K^+-ATPase (Leonard-Marek et al., 2010). This pump generates an electro-chemical gradient which drives Na^+ out of the cell via NHE1 and NHE3, an energy-dependent process, indicating that ATP used by the Na^+/K^+-ATPase is required for Na^+ flux (Leonard-Marek et al., 2010). Short chain fatty acids may function as an energy source for this process. Furthermore, Na^+ secretion from the serosal to mucosal side ($J_{SM\text{-}Na}$) is much lower than absorption from the mucosal to serosal side ($J_{MS\text{-}Na}$), and may require a pathway involving basolateral cotransport as well as paracellular transport (Leonard-Marek et al., 2010).

Similar to SCFA absorption, several elements are known to influence apical Na^+ absorption. High concentrate diets fed to ruminants have shown to increase Na^+ absorption. This

has been clearly illustrated in a recent study where sheep transitioned from a high forage to mixed forage/concentrate diet fed up to 12 weeks increased Na^+ absorption significantly from 2.15 μeq/cm^2/h for forage fed sheep to 4.55 μeq/cm^2/h for sheep offered concentrate for 4 weeks (Etschmann et al., 2009). In a different study, expression of NHE1 and NHE3 in the rumen epithelium of concentrate-fed goats increased 20 and 25%, respectively, relative to goats fed roughage only (Yang et al., 2012). In the same study (Yang et al., 2012), *ex vivo* acidification of cultured ruminal epithelial cells caused up-regulation of NHE1 and NHE3, indicating that reduced cytosolic pH stimulates Na^+ transport via NHE1 and NHE3. Similar results were shown in earlier studies (Gäbel et al., 1991b; Shen et al., 2004). Furthermore, high ruminal osmolarity has also shown to increase Na^+ flux from the serosal-to-mucosal side due to reduced barrier function, resulting in a reduction in net Na^+ absorption across ruminal epithelia (Lodemann and Martens, 2006).

2.1.3. Barrier Function of the Ruminal Epithelium

As discussed above, an important role of the ruminal epithelium is the absorption and secretion of nutrients. However, another significant responsibility is to act as barrier against harmful compounds, including bacterial pathogens (Plaizier et al., 2012; Klevenhusen et al., 2013) and antigens such as histamine (Aschenbach and Gäbel, 2000) and LPS (Emmanuel et al., 2007). Barrier function also plays a critical role in regulating nutrient absorption and secretion, where otherwise nutrients would diffuse across the ruminal epithelium according to their concentration gradient. The ruminal epithelium must therefore display structural characteristics that both promote and impede the movement of molecules.

2.1.3.1. Role of Tight Cell Junctions in Ruminal Epithelium Barrier Function

As previously discussed, the localization of known tight-cell junction proteins has been reported to occur for the stratum granulosum and stratum spinosum of the ruminal epithelium. Tight junctions are not made up of single proteins, but are comprised of multiple proteins that bond neighboring epithelial cells (González-Mariscal et al., 2008). Tight junctions are therefore often referred to as “sites of fusion” or “kissing points” (Langbein et al., 2002). These sites of fusion function together to form a barrier that separates the ruminal lumen from the host

circulatory system (Langbein et al., 2002). Proteins involved in the formation of selectively permeable tight junctions within ruminal epithelial tissue include claudins, occludens, zonula occludens, and gap junctions (Graham and Simmons, 2005).

Claudin tight junction proteins have shown to be widely expressed in various epithelia in mammals (González-Mariscal et al., 2008). Claudins exhibit two loops located on their exterior that display a variable number and organization of charged amino acid deposits that determine or regulate the paracellular movement of ions (González-Mariscal et al., 2008). Furthermore, specific claudins form ion channels between cells in support of ion transport (claudin-2 and 16) while others form barriers against ion transport (claudin-7 and 8; González-Mariscal et al., 2008). To date, however, only claudin-1, 4 and 7 have been identified in the ruminal epithelium (Graham and Simmons, 2005; Stumpff et al., 2011). Claudin-1 and 4 are most widely expressed in the stratum granulosum and stratum spinosum, whereas claudin-7 is found predominantly in the stratum corneum (Graham and Simmons, 2005; Stumpff et al., 2011). In the ruminal epithelium, claudin-1 and 4 contribute to the barrier function of the epithelium by preventing the backward flux of such anions across the epithelium (Stumpff et al., 2011). The specific role of claudin-7 and localization in the stratum corneum is still not understood.

Occludens are tight-cell junction proteins comprised of 4 transmembrane domains (Al-Sadi et al., 2011). When epithelial tissue barrier function is strong, occluden proteins form a complex with claudin proteins (Raleigh et al., 2011). However, unlike claudins, which are relatively immobile, occluden proteins are able to commute to various paracellular locations (Shen et al., 2008), and therefore are able to alter the epithelial permeability. Furthermore, movement of occluden proteins from the tight junction into cytoplasmic vesicles frequently occurs due to barrier function loss (Shen et al., 2008), and has been shown to occur due to multiple other stimuli, such as oxidative stress and inflammation (John et al., 2011), occluden overexpression (Furuse et al., 1996), and the presence of a lymphotoxin-like protein (Schwarz et al., 2007). Recently, the structural role of occluden proteins was clearly shown in intestinal epithelial cells both *in vivo* and *ex vivo*, where occluden depletion resulted in increased translocation of harmful molecules, such as LPS and bacterial pathogens, from the apical to basalolateral membrane of cultured Caco-2 cells (Al-Sadi et al., 2011). Furthermore, occluden

attachment to claudin proteins has shown to be regulated by another tight junction protein, zonula occluden-1 (ZO-1; Raleigh et al., 2011).

Zonula occludens (ZO), expressed primarily in the stratum granulosum (Graham and Simmons, 2005), are peripheral tight junction membrane proteins that interact with claudin proteins to offer structural support to claudins (González-Mariscal et al., 2008; Raleigh et al., 2011). In fact, ZO bind directly to occludens, which subsequently bind to claudin proteins to form a robust barrier within the epithelia (Shen et al., 2008; Raleigh et al., 2011). Due to their binding ability, ZO are mobile similar to claudins (Shen et al., 2008). In cultured Caco-2 cells, the interaction between occluden and ZO has shown to be regulated by phosphorylation or dephosphorylation of occluden proteins (Raleigh et al., 2011). When phosphorylated, ZO-1 form a looser attachment to occludens, thereby increasing permeability of the epithelial barrier (Raleigh et al., 2011). Comparatively, occluden dephosphorylation activates the binding of ZO-1 occluden, and subsequently to claudin-1 to form a strong tight junction complex (Raleigh et al., 2011). While some tight-cell junction proteins have been identified in the rumen epithelium, research is required to elucidate epithelial tight-cell junction assembly.

Gap junction proteins are another type of protein expressed in various epithelial tissue (Sáez et al., 2003; White et al., 2003). These proteins are located in between cells and are responsible for paracellular movement of small ions such as potassium and other small molecules including metabolites, sugars, SCFA, as well as cyclic nucleotide signalling molecules (Sáez et al., 2003; White et al., 2003). Gap junction proteins are comprised of multiple protein sub-units that form an hour glass-like shape with a gated channel in the centre (approximately 2 nm in width) that allows paracellular passage of small molecules (Sáez et al., 2003). In vertebrates, connexin 43 is the most widely expressed gap junction protein (Sáez et al., 2003), which remains true for the ruminal epithelium (Graham and Simmons, 2005). Connexin 43 in rumen epithelia is located primarily at the stratum granulosum/stratum spinosum interface, and to a lesser extent the stratum spinosum/stratum basale interface (Graham and Simmons, 2005). Phosphorylation of connexin 43 is believed to regulate whether the channel is open or closed for molecule movement (Sáez et al., 2003). Phosphorylation is also responsible for connexin assembly, membrane insertion, and degradation (Sáez et al., 2003). Protein kinase C (PKC) and mitogen-activated protein kinase (MAPK) are activators of phosphorylation in cultured rat liver

epithelial cells and other non-ruminant epithelial cells (Hossain et al., 1998; Sáez et al., 2003). The enzymes, PKC and MAPK involved in gap junction regulation in epithelial tissue of other species may apply to ruminal epithelial tissue, but to date there is a paucity of information regarding the regulation of gap junction proteins in rumen epithelia.

2.1.3.2. Regulation of Tight Cell Junctions

To date, the mechanisms controlling the alteration of tight junction protein expression, formation, activation, or deactivation following a challenge are not clearly understood. As discussed above, various types of tight junction proteins work together to form a protective barrier between the ruminal lumen environment and circulatory system. Individual tight junction proteins as well as the whole tight junction protein complex are able to transform and relocate. In fact, single or clusters of tight junction proteins continuously undergo remodelling in order to promote or prevent the passage of molecules (Shen et al., 2008). Recently, shown via histomorphometric analysis, it was simply suggested that a reduction in stratum granulosum cell layers was the reason for a decrease in tight junction expression in ruminal epithelia observed in goats fed a high grain diet relative to goats fed a high forage diet (Liu et al., 2013). In the same study, reduced barrier function of ruminal tissue from high grain fed goats relative to high forage fed goats promoted bacteria and LPS translocation *in vivo*. After translocation of these harmful compounds, expression of pro-inflammatory cytokines tumor necrosis factor-α (TNF-α) and interferon-γ (IFN-γ) increased in rumen epithelial tissue (Liu et al., 2013). They suggested that the presence of these cytokines may regulate the localization and expression of tight junction proteins (Liu et al., 2013), a notion that is in agreement with previous work performed on non-ruminant cell lines (Ma et al., 2004; Watson et al., 2005). In fact, in cultured Caco-2 cells it has been shown that TNF-α down-regulates expression of ZO-1 (Ma et al., 2004). Similarly, IFNγ has shown to down-regulate expression of occludin proteins (Watson et al., 2005). Transcriptional regulators, nuclear factor κB (NF-κB) and peroxisome proliferator-activated receptor γ (PPAR-γ), are stimulators of such cytokines in intestinal tissue (Penner et al., 2011). Following stimulation, TNF-α and IFN-γ activate specific isozymes of PKC or MAPK, which subsequently initiate a signaling cascade and phosphorylation to either assemble or disassemble tight junction proteins (González-Mariscal et al., 2008). Barrier function is therefore either

increased or reduced based on the up- or down-regulation of tight junction proteins (González-Mariscal et al., 2008).

Similar to the mechanisms which control the up- or down-regulation of rumen epithelial tight junction proteins, current knowledge on the activation process of rumen epithelial tight junction proteins is limited. However, previous research using other tissues and species may provide suggestions for tight junction activation in the rumen. For example, a recent study performed protein-protein docking using computer software and found that the first of the two extracellular loops exhibited by claudin-4 interacts with ephrin (Eph) receptor, EphA2, to form a claudin-4-EphA2 complex (Bhavaniprasad et al., 2013). This complex stimulates tyrosine kinase activity of EphA2, which initiates phosphorylation of Tyr208, an amino acid located at the end of claudin-4 that is closest to the cytoplasm. The phosphorylation of Tyr208 then reduces the interaction with ZO-1, which offers structural support to claudin proteins, and therefore reduces claudin-4 activation and simultaneously reduces the strength of the tight junction formation (Masamitsu et al., 2005). In another study, EphA2 signalling up-regulated the expression of claudin-2 in the non-small-cell lung carcinoma (NSCLC) cell line (Sukka-Ganesh et al., 2012). Thus, receptors such as EphA2 play a role in claudin activation (Bhavaniprasad et al., 2013).

In a different study, acidic conditions (pH 2) were imposed on human esophageal cells followed by immunofluorescent staining to determine localization of claudin-4 and ZO-1 (Oshima et al., 2012). The acidotic condition imposed caused claudin-4 to migrate from the outer cell membrane to the cytoplasm and nucleus but localization of ZO-1 was not altered (Oshima et al., 2012). Similarly, cultured pig kidney epithelial cells subject to chemical stress (Traweger et al., 2003) or canine kidney epithelial cells exposed to mechanical injury (Islas et al., 2002) have shown to cause migration of ZO-2 to the nucleus of the epithelial cell. To date, however, ZO-2 has not shown expression in rumen epithelial tissue. Yet, ZO-1 and ZO-2 are both members of the membrane-associated guanylate kinase (MAGUK) protein family (González-Mariscal et al., 2008). If the same behaviour applies to ZO-1 in ruminal epithelium after tissue insult as for ZO-2 in non-ruminant epithelial tissue, this movement to the cytoplasm may explain the reduction in ZO-1 expression. Regardless, movement of tight junction proteins away from paracellular space would undoubtedly disrupt the integrity of the epithelium and explain reduced ruminal epithelial barrier function following a dietary challenge.

Furthermore, in a recent review (Penner et al., 2011) butyrate was discussed as a promoter of barrier function in intestinal tissue. More specifically, the review suggested butyrate may play a role in encouraging tight cell junction formation through activation of AMP-activated protein kinase (Peng et al., 2009) and may be a regulator of tight cell junction protein expression (Bordin et al., 2004). Interestingly, butyrate is also known for its role in ruminal epithelial cell proliferation and rumen development (Górka et al., 2011). Still, future research will need to focus on regulatory mechanisms of tight junctions in rumen epithelial tissue in order to confirm that mechanisms controlling ruminant epithelial barrier function are the same as those in non-ruminant epithelial tissue.

2.1.3.3. Factors Affecting Ruminal Barrier Function

Under optimal physiological conditions, the ruminal epithelium is able to maintain its selective permeability. However, common ruminal conditions have been shown to challenge the integrity of the epithelium. For example, ruminal acidosis is a common digestive disorder affecting beef and dairy cattle. While prevalence rates for beef cattle are not available, the prevalence for dairy cattle ranges between 12 and 30% depending on the stage of lactation (Krause and Oetzel, 2006). Ruminal acidosis is characterized by an increase in osmolality (Schweigel et al., 2005; Lodemann and Martens, 2006; Penner et al., 2010) and a reduction in ruminal pH (Nagaraja and Titgemeyer, 2007; Aschenbach et al., 2011; Calsamiglia et al., 2012); both of these factors are known to compromise the selective permeability of the rumen epithelium. For example, exposure of rumen epithelial tissue to hyperosmotic mucosal conditions *ex vivo* in Ussing chambers resulted in increased mannitol flux and tissue conductance (Schweigel et al., 2005; Lodemann and Martens, 2006; Penner et al., 2010) with results indicating reduced selective permeability. Furthermore, a reduction in mucosal pH *ex vivo* also causes increased tissue conductance (Aschenbach and Gäbel, 2000; Wilson et al., 2012), elevated mucosal-to-serosal histamine flux (Aschenbach and Gäbel, 2000), and a reduction in mucosal-to-serosal SCFA flux (Wilson et al., 2012), which again are evidence of increased epithelial permeability.

In a recent study, rumen tissue was collected from mature lactating dairy cows offered a high forage diet (100% chopped hay) or high grain diet (65% grain) in order to evaluate

structural differences due to diet (Steele et al., 2011). Following transition to the high grain diet from the high forage diet, ruminal tissue was evidently more challenged relative to cows fed the high forage diet; exhibiting weak tight junctions between granulosum cells (Steele et al., 2011). In another study using the same forage-to-concentrate ratio, goats were fed for 7 weeks, after which ruminal epithelial tissue was collected to characterize rumen barrier function (Liu et al., 2013). The rumen tissue illustrated eroded tight junction proteins and the loss of stratum granulosum cell layers when analyzed via scanning electron micrographs (Liu et al., 2013). Expression of mRNA for tight junction proteins claudin-4, occluden, and ZO-1 was also down-regulated due to the high grain diet (Liu et al., 2013). Furthermore, the localization of tight junction proteins was different between high forage and high grain fed goats. Using immunofluorescent staining, claudin-1 and -4 and occluden were found on the surface of epithelial cells of ruminal tissue from high forage fed sheep, however, for ruminal epithelium collected from high grain fed sheep these tight junction proteins were highly fragmented and occluden appeared to be localized into the cytoplasm of epithelial cells (Liu et al., 2013). As discussed earlier, occluden proteins are mobile (Shen et al., 2008), and in this case the appearance of occluden in the cytoplasm may have been due to the presence of rumen epithelial inflammation from high grain fed goats.

2.2. Adaptation of the Ruminal Epithelium

The rumen epithelium plays a key role in ruminal acid removal in an effort to deliver nutrients to the epithelium and the rest of the body in order to maintain rumen homeostasis, as previously discussed. However, following a change in diet fermentability, the rumen epithelium must adapt to account for the elevated or reduced SCFA concentration in the rumen.

2.2.1. Morphological Adaptation of the Ruminal Epithelium

One way the ruminal epithelium responds to changes in diet fermentability is by surface area proliferation or degeneration (Dirksen et al., 1985; Mentschel et al., 2001). For example, *in vivo*, butyrate has a positive influence on rumen epithelial proliferation (Mentschel et al., 2001; Górka et al., 2011). Comparatively, studies using cell culture models have shown an inhibitory effect of butyrate on proliferation (Ginsburg et al., 1973; Baldwin, 1999). The discrepancy can

be accounted for by differential conditions imposed *in vivo* relative to *ex vivo*. Therefore, *in vivo*, butyrate may indirectly stimulate rumen epithelial proliferation via activation of hormones and growth promoters, including glucagon (Gálfi et al., 1993), insulin (Sakata et al., 1980; Gálfi et al., 1993), insulin-like growth factor-1 (IGF-1; Shen et al., 2004), and epidermal growth factor (EGF; Baldwin, 1999). These hormones, unless supplemented *in vivo*, are not present, which explains the lack of epithelial proliferation in their absence. Of these hormones, the most dominant promoters of epithelial proliferation are thought to be IGF-1 and EGF, which bind to cell membrane receptors (Baldwin, 1999; Penner et al., 2011). Although the process is not fully understood in rumen epithelial tissue, binding of IGF-1 and EGF to receptors in other cell lines (Caco-2 and DLD-1) have shown to induce a signalling cascade that increase the transcription of extracellular protein kinases, such as serine/threonine kinase (AKT) leading to cell proliferation (Kaulfuss et al., 2009; Penner et al., 2011). Recently, it was also suggested that butyrate can act on insulin-like growth factor binding proteins (IGFBP) to activate IGF-1 (Steele et al., 2011). Furthermore, butyrate may possess anti-apoptosis factors, and thus, when ruminal butyrate concentration is low, cell apoptosis, and subsequent degradation of the ruminal epithelium occurs (Mentschel et al., 2001). This indicates that when feeding high forage diets, which is associated with reduced butyrate production , rumen epithelium degeneration may occur. In a study by Dirksen et al. (1985), proliferative and degenerative processes of the ruminal epithelium of dairy cows were shown prior to and following calving when cows were fed a low and high energy ration, respectively. Mucosa biopsies collected 9 weeks up to calving showed a reduction in the area of cross sections of rumen papillae, relative to after calving when there was a progressive increase (Dirksen et al., 1985). Epithelial degeneration was due to the lower energy diet, which provided less fermentable carbohydrate for acid production, and therefore fewer substrates for epithelial proliferation. Comparatively, the energy rich diet promoted higher carbohydrate fermentation and subsequent epithelial proliferation, which in this study required 4 to 5 weeks of high energy feeding to reach maximum papillae height (Dirksen et al., 1985). The 4 to 5 week delay in maximum proliferation is likely related to cell turnover time in the ruminal epithelium, which has been calculated at 4.3, 10.9, and 16.5 days for sheep transitioning from a high forage to high grain diet, sheep fed a high grain diet, or a high forage diet, respectively (Goodlad, 1981). Similar proliferation and degeneration patterns of rumen epithelium have been shown in additional studies (Liebich et al., 1987; Bannink et al., 2008).

2.2.2. Functional Adaptation of the Ruminal Epithelium

In addition to morphological adaptation, recent evidence shows that enhanced individual cell activity within the ruminal epithelium occurs following a change in diet fermentability (Etschmann et al., 2009; Penner et al., 2011). Ussing chamber experiments have illustrated increased absorptive capacity of the ruminal epithelium as early as 1 week following a change in diet (Etschmann et al., 2009), indicating that functional adaptation precedes morphological adaptation. For example, net Na^+ transport across the ruminal epithelium of sheep increased within 1 week following dietary transition from a high forage to a moderately fermentable diet (Etschmann et al., 2009). This increase in Na^+ transport was accompanied by molecular adaptation, in this case, increased expression of the Na^+/H^+ exchange (NHE) proteins, NHE1 and NHE3 (Etschmann et al., 2009). However, the effect of diet adaptation on ruminal absorption rates remains to be elucidated. A recent study has demonstrated that provision of IGF-1 *ex vivo* acutely increases Na^+ transport via NHE (Shen et al., 2012). This indicates that hormones may strongly influence functional adaptation of the ruminal epithelium and possibly other epithelia, conceivably via up-regulation of transporter proteins.

Furthermore, numerous additional proteins have been identified that may help coordinate functional rumen adaptation following a change in diet. As discussed above, GPR41 and GPR43 proteins interact with butyrate > propionate > acetate, to induce rumen development, insulin and glucagon secretion, and may be involved in the regulation of feed intake (Wang et al., 2009b). The signal transduction cascade induced through GPR41 and GPR43 binding and the resulting hormone release may also partially explain the underlying mechanisms involved in the functional adaptation of the rumen epithelium. Another possible explanation for increased functional adaptation could be through increased expression of proteins involved in transport processes. Regarding SCFA flux, possible transporter proteins include downregulated-in-adenoma (DRA) and PAT1 that are both located on the apical membrane. Additionally, MCT1 and AE2, two transporters capable of transporting SCFA or their metabolites (Müller et al., 2002), are located on the basolateral membrane (Graham et al., 2007; Penner et al., 2011). Potentially, upregulation of these transporters could result in greater transport capability and help to explain functional adaptation of the rumen epithelium.

2.2.3. Cell Turnover in the Ruminal Epithelium

While changes occur both morphologically and functionally in the ruminal epithelium following a change in diet, cell turnover within the epithelium also occurs. In fact, cell turnover time has been measured in sheep transitioned from a high forage to a high concentrate diet (Goodlad, 1981). During the transition period, mean epithelial cell turnover time was nearly 4 times quicker relative to the forage-based diet feeding period, calculated at 4.3 days for sheep transitioning from a high forage to high grain diet, 10.9 days for high grain fed sheep, and 16.5 days for a high forage diet, respectively (Goodlad, 1981). Furthermore, after sheep were fully adapted to the concentrate diet, mean cell turnover time slowed to approximately 1.5 times the speed of that prior to the start of dietary transition (Goodlad, 1981). As discussed previously, IGF and EGF are thought to play a large role in rumen epithelial cell proliferation by attaching to membrane receptors, and subsequently beginning a signaling cascade responsible for cell proliferation (Steele et al., 2011).

2.3. Industry Relevance of Dietary Adaptation

On commercial cattle operations, producers strive for optimal animal performance with the aim of meeting production goals and maintaining profit margins. In order to promote high levels of production, ruminants are often fed starch-rich diets. However, because cattle feature a forestomach capable of fermentation, home to a diverse and sensitive population of microbes, caution must be taken in adapting cattle to such highly fermentable diets. Dietary transition to moderately or highly fermentable diets is therefore essential in enhancing ruminant health and performance. Cattle that often undergo dietary transition include cows transitioning from dry to lactating, weaning dairy and beef calves, and backgrounding and finishing feedlot cattle.

2.3.1. Dietary Adaptation for Transitioning Dairy Cattle

The transition period for dairy cattle is the period spanning 3 weeks prior to calving to 3 weeks following calving (Drackley, 1999). During this 6-week timeframe, dairy cattle are at risk of developing several metabolic diseases as energy requirements increase, without corresponding increases in dry matter intake (DMI), due to the onset of lactation, namely, ketosis, milk fever, fatty liver syndrome, and displaced abomasum (Drackley, 1999; LeBlanc et al., 2005; McArt et

al., 2011). In order to prevent such disease, post-partum dairy cows are often fed a diet considerably higher in fermentable starch than that of the diet received in the dry period (Dann et al., 1999). While this is necessary to meet the high energy demands for lactation and maintain cow health, inadequate dietary adaptation may result in subacute ruminal acidosis (SARA; Fairfield et al., 2007; Penner et al., 2007; Penner and Oba, 2009). In fact, in similarly managed dairy herds in Holland, prevalence of subacute ruminal acidosis, described as ruminal pH between pH 5.5 and 6.0 was up to 40% (Kleen et al., 2009). Economically, the consequences of SARA have been reported at $1/hd/d in US dairy herds (Enemark, 2008). Therefore, dietary transition for transitioning dairy cattle is a crucial step in maximizing cow health and milk production.

2.3.2. Dietary Adaptation for Weaning Dairy Calves

Dairy calves during the weaning period are another example of cattle that undergo dietary transition. Neonatal calves are provided a high quality energy and protein source via milk or milk replacer, essential for initial stages of growth. Dairy calves on commercial dairy operations are commonly weaned from milk as early as 4 weeks of age (Lesmeister and Heinrichs, 2004). In place of milk, the calf requires an alternative high quality and easily digestible feed source to replace the energy and protein received from milk. The replacement diet must also be capable of stimulating ruminal epithelia development. Thus, diets rich in fermentable carbohydrates are fed at weaning (Coverdale et al., 2004) or earlier during the milk-feeding period in order to promote rapid adaptation to solid feed, reduce stress and maximize feed intake at weaning (Lesmeister and Heinrichs, 2004). However, due to the dietary transition from milk to solid and more highly fermentable feed, weaning calves are at risk for ruminal acidosis. Work by Suárez et al. (2006) showed that calves fed a starch-based pelleted concentrate in addition to milk replacer had a lower mean ruminal pH (pH 4.9; $P < 0.05$) relative to calves fed milk replacer only (pH 5.2), or either petin-based (pH 5.1) or neutral detergent fiber (NDF)-based (pH 5.1) concentrate or a combination of all three (starch, pectin, and NDF-based concentrate; pH 5.2) in addition to milk replacer. Comparatively, a recent study showed that calves during the weaning period fed a calf starter ad libitum in addition to milk replacer and hay did not show signs of ruminal acidosis (mean ruminal pH at 6.27; Laarman and Oba, 2011). They suggested that hay feeding during weaning transition may help prevent ruminal acidosis (Laarman and Oba, 2011). Furthermore,

sodium butyrate is well-known for its proliferative effect on ruminal epithelia (Sander et al., 1959; Sakata and Tamate, 1978; Górka et al., 2011), thus, addition of sodium butyrate to milk and solid feed fed to calves is a recommended method of accelerating rumen development (Górka et al., 2011) which may also reduce the risk of ruminal acidosis in weanling dairy calves.

2.3.3. Dietary Adaptation for Calves Entering a Backgrounding Feedlot

Lightweight beef calves weaned and removed from pasture are commonly placed in backgrounding feedlots where the goal is to increase body frame size. Typical backgrounding diets contain approximately 50% concentrate [dry matter (DM) basis; Bevans et al., 2005; Alberta Government, 2012], but concentrate has been included in these diets up to 58% (Schwartzkopf-Genswein et al., 2004). Thus, abrupt dietary transition from a high forage to a moderately fermentable diet is imposed. Consequently, the transition to a backgrounding diet is another situation where cattle may be susceptible to ruminal acidosis; however, ruminal acidosis in this scenario is not due solely to the increase in diet fermentability but also due to low feed consumption. A Minnesota Cattle Feeder Report by Chester-Jones and DiCostanzo (1994) suggests that only 21% of calves are consuming feed on the first day in the feedlot, with a gradual increase to 67 and 85% on days 5 and 10, respectively. Furthermore, Hutcheson and Cole (1986) reported that normal DMI (2.5 to 3.5% of BW) does not occur until 2 to 4 weeks after arrival. Recent research using the temporarily isolated and washed reticulo-rumen technique has shown that feed restriction reduces the absorptive capacity of the ruminal epithelium (Albornoz et al., 2013a; Zhang et al., 2013a) and when feed is provided ad libitum following restriction, ruminal acidosis is likely to occur (Zhang et al., 2013b). Furthermore, ad libitum availability to a moderately fermentable diet following feed restriction is more likely to reduce ruminal pH relative to a high forage diet (Albornoz et al., 2013b). Although cattle entering a backgrounding lot are generally not feed restricted, cattle that go off feed or drastically reduce DMI due to stress upon feedlot arrival and subsequently consume a large quantity of feed are more susceptible to developing ruminal acidosis.

2.3.4. Dietary Adaptation for Finishing Feedlot Cattle

Once cattle have gained sufficient frame growth, they are transitioned to a finishing ration. Finishing feedlot diets contain up to 100% concentrate in order to maximize average daily gain and feed efficiency (Loerch, 1990). However, a series of rations that sequentially increase in concentrate are commonly imposed to ease transition to the highly fermentable diet, referred to as "step-up" diets. A survey was conducted at Texas Tech University where 29 feedlot nutritionists in the United States completed a survey for nutritional recommendations for feedlot cattle (Vasconcelos and Galyean, 2007); results from the survey suggested nutritionists implement an average of 3 diets fed for 7 days each, allowing 21 days to reach the final finishing diet. However, the use of such step-up diets does not abolish the risk of ruminal acidosis in feedlot cattle. Minimum pH values can still decrease as low as 5.0 for cattle provided a series of step-up diets (Bevans et al., 2005). In fact, reduced performance associated with subclinical acidosis has been reported as high as $20 per animal (Schwartzkopf-Genswein et al., 2003).

2.4. Ruminal Fermentation and Potential Outcomes

2.4.1. Ruminal Acidosis

Ruminal acidosis can be a detrimental outcome of abrupt dietary adaptation to a moderately to highly fermentable diet (Nocek, 1997; Penner et al., 2007). Microbial fermentation of carbohydrate in the rumen results in the production of SCFA and, depending on the rate of fermentation and type of acid produced, may result in a significant decrease in ruminal pH. With rapid SCFA production, ruminal pH drops below the physiological norm (pH < 5.8 to 6.2; Nocek, 1997; Nagaraja and Titgemeyer, 2007; Penner et al., 2007). Ruminal acidosis is commonly categorized as either subacute ruminal acidosis (SARA; pH < 5.8 or 5.5) or acute ruminal acidosis (pH < 5.2 or 5.0; Penner et al., 2007; Aschenbach et al., 2011).

2.4.2. Other Diseases Associated with Ruminal Acidosis

Although ruminal acidosis itself is considered a digestive disorder, its presence in ruminants may initiate subsequent disease conditional of its frequency, duration, and magnitude (Nocek, 1997). Laminitis, for instance, is associated with ruminal acidosis. During periods of low ruminal pH and corresponding reduced barrier function, translocation of vasoactive

molecules across the ruminal epithelium from the rumen to portal blood may occur (Nocek, 1997; Klevenhusen et al., 2013). These vasoactive substances, namely histamine and the endotoxin LPS, cause damage to capillaries in the hoof and thus a reduction of oxygen and nutrient supply (Nocek, 1997). This leads to inflammation and lameness known as laminitis (Nocek, 1997). Ruminal acidosis is also linked with liver abscesses, as reduced barrier function caused by low ruminal pH may promote translocation of bacteria (*Fusobacterium necrophorum* and *Arcanobacterium pyogenes*) across the ruminal epithelium increasing risk for colonization of the liver and abscess formation (Nocek, 1997; Plaizier et al., 2009). Moreover, ruminal acidosis has shown to be associated with several other disorders, including diarrhea, dehydration, poor body condition, depression, and reduced rumen motility (Aschenbach et al., 2011). Ruminal acidosis can therefore significantly impact animal health, welfare, and productivity and thus is of sizeable concern on cattle operations.

Bloat is another disease that may occur in feedlot cattle from rapid fermentation of starch in the rumen, and most commonly occurs when cattle are transitioning from a high forage to high grain diet (Hironaka et al, 1973; Cheng et al., 1998). Bloat in feedlot cattle can be described as either free-gas bloat or frothy bloat. Free-gas bloat is due to the accumulation of gas from fermentation of starch in the rumen from either obstruction of the esophagus or cardia or reduced rumen motility due to rapid presence of acidosis (Cheng et al., 1998). Comparatively, frothy bloat in feedlot cattle is caused by the accumulation of foam, which is comprised of bacterial mucopolysaccharides and macromolecules from cell lysis, produced by microbes (Cheng et al., 1976). The foam blocks the cardia and prevents gas eructation (Cheng et al., 1998).

2.5. The Ussing Chamber Technique

As discussed above, dietary adaptation plays an important role in ruminant health and performance. It is therefore essential to understand how the ruminal epithelium adapts to dietary change on a functional level. The Ussing chamber is an *ex vivo* laboratory technique that facilitates our understanding of the *in vivo* mechanisms that underlie ruminal adaptation following a change in diet.

2.5.1. Development and Use of the Ussing Chamber Technique

The Ussing chamber technique was developed by Hans Ussing in the 1950's, as he was interested in understanding the active transport of NaCl across the frog skin (Ussing and Zerhan, 1950). Since his original use of the Ussing chamber, this *ex vivo* technique has been used to measure the movement of molecules across an array of epithelial tissue types, from the apical membrane to the basolateral membrane or, oppositely, from the basolateral membrane to the apical membrane. Examples include the measurement of Na^+ and Cl^- secretion in rabbit and canine ileum (Schwartz et al., 1974), Na^+ absorption in mouse tracheal tissue (Mall et al., 2004), glucose absorption from the jejunum of broiler chickens (Awad et al., 2008), and urea and ammonia flux across the colon of fish (Anderson et al., 2012). Regarding ruminants, the flux of numerous molecules across the rumen epithelium have been measured: Ca^{2+} (Wilkens et al., 2011), Mg^{2+} (Leonard-Marek et al., 1998; Leonard-Marek et al., 2005), Na^+ (Lodemann and Martens, 2006; Etschmann et al., 2009), Cl^- (Gäbel et al., 1991b), urea (Muscher et al., 2010), and SCFA (Aschenbach et al., 2009; Penner et al., 2009a; Wilson et al., 2012; Dengler et al., 2013). With the expansion of Ussing chamber application, significant advances in the understanding of basic cellular mechanisms associated with animal and human medicine and nutrition have been achieved.

2.5.2. Rumen Epithelial Tissue Preparation and Description of the Ussing Chamber

Once the rumen epithelial tissue has been collected from the animal, the underlying muscle layer is commonly removed from the epithelium. This is performed as the submucosa is composed of collagen and cellular elements such as fibroblasts which; 1) acts as a structural diffusion barrier for isotope molecules, 2) reduces the short circuit current conditions that will be applied to the Ussing chamber apparatus, and 3) alters the unidirectional movement of molecules (Binder and Rawlins, 1973; Clarke, 2009). Also, removal of the muscle layer may reduce influence from the intrinsic neuromuscular system (Clarke, 2009).

The Ussing chamber apparatus can be described as having two halves, one which simulates the blood (also referred to as the serosal or basolateral side) and the other that simulates the inside of the rumen (also referred to as the mucosal or apical side; Clarke, 2009; Figure 2.2). The rumen epithelium is mounted in the chamber such that the tissue matches the

serosal and mucosal side appropriately. Small holes are cut in the tissue to fit over pins attached to the chamber, in order to secure the tissue in the centre of the two halves of the chamber. Furthermore, the pins are fastened with rubber gaskets to prevent edge damage to the tissue (Clarke, 2009).

For classical Ussing chambers, each side of the Ussing chamber is attached to an above reservoir that contains a buffer with nutrients to meet essential requirements and in some instances represent *in vivo* conditions. The chamber and exposed surface area, as well as the buffer reservoir are variable in surface area and volume depending on the type of tissue and type of Ussing chambers. Furthermore, the buffer is heated by a water jacket surrounding the buffer solution, which maintains the temperature of the buffer and tissue to physiological temperature (38.5°C in cattle). The buffer solution is also gassed with either carbogen (95% O_2, 5% CO_2) or oxygen, dependent on the aim of the measurement; oxygen gas is used when bicarbonate is absent in the buffer, therefore preventing exogenous production of bicarbonate and maintaining pH at the appropriate level (Clarke, 2009). Gassing also allows for mixing of the buffer solution (Li et al., 2004). By utilizing carbogen gas, the pO_2 concentration (partial pressure of oxygen) is preserved at >400 mmHg, and therefore helps to surmount the lack of hemoglobin that would otherwise be supplied by blood *in vivo* (Clarke, 2009). Additionally, the pCO_2 (partial pressure of carbon dioxide) is similar to that of venous blood, and thus sustains the pH of the buffer at physiological levels (serosal and mucosal at pH 7.4 and 6.2, respectively) by sustaining the HCO_3^- concentration (Clarke, 2009).

Epithelial tissue has the ability to move ions from the basolateral to apical membranes and vice versa (Li et al., 2004). However, there is a natural potential difference across the tissue driven by the Na^+/K^+ ATPase that is located on the basolateral membrane (Li et al., 2004). Thus, the apical side is more positive relative to the basolateral side. To offset the inherent potential difference, Ussing chambers are equipped with a pair of voltage electrodes (calomel electrodes) connected via 3 *M* KCl agar bridges that can be used to measure the voltage potential (V_t) of the tissue. Inside the chamber, the ends of the voltage bridges are located close to the tissue on both the serosal and mucosal side. The voltage electrodes are connected to a voltmeter that reads the V_t (Clarke, 2009). The Ussing chamber also has a pair of current electrodes that are often used to pass current across the tissue in order to clamp the V_t to zero (or to short circuit the tissue known

as short-circuit current; I_{SC}). The I_{SC} is described as the anion and cation flow during the time the V_t is short-circuited (Li et al., 2004). The current electrodes are connected to the interior of the chamber with 3 *M* NaCl salt bridges. On the inside of the chamber, the end of the current bridges are located slightly further away from the tissue relative to the voltage bridges, one on either side of the tissue (Clarke, 2009). In most instances the voltage and current bridges are constructed using 3% agar in the current study, which conveys the voltage and current while providing low resistance (Clarke, 2009). The I_{SC} is variable and adjusted dependent on the V_t as well as the series resistance of circuit and the epithelium (Li et al., 2004; Clarke, 2009). The I_{SC} for the epithelium itself is a calculation that totals all ionic currents across the tissue: $I_{SC} \approx I_{Na+} + I_{K+} + I_{Cl-} + I_{HCO3-} - I_{K+}$, where all ions with the exception of K^+ are inward currents (Clarke, 2009). Furthermore, a brief current can be applied to clamp a specific voltage value, which enables the measurement of transepithelial conductance (tissue conductance, G_t; Clarke, 2009). Tissue conductance, or its inverse, tissue resistance can be used as an indicator of barrier function (Clarke, 2009).

2.5.3. Strengths of the Ussing Chamber

The Ussing chamber is a unique laboratory instrument that has several strengths due to its design. The key strength of the Ussing chamber is its ability to maintain tissue for several hours, during which time precise flux and electrical quantifications can be performed in the absence of external confounding factors, for example, blood flow and hormones (Clarke, 2009). The Ussing chamber has the ability to measure the flux of isotopic markers, which allow the measurement of specific molecules from the mucosal to serosal side of the chamber and vice versa. This is done by injecting a known quantity of radioisotope into the column above one side of the chamber and collecting a sample on the opposite side after a given incubation time period. Samples collected are placed in liquid scintillation vials with liquid scintillation fluid, and subsequently the quantity of radioisotope in the vial is measured by a scintillation counter. Fluorescent dyes may also be used as tracers to label flux measurements, which are analyzed through imaging under a microscope (Clarke, 2009). By measuring the flux of a molecule from both directions, the net

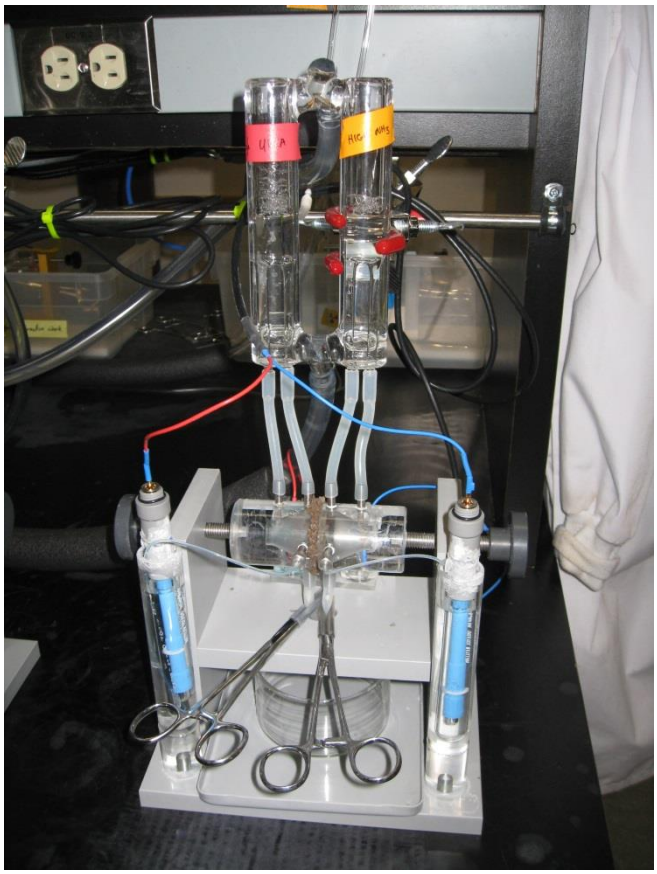

Figure 2.2. Diagram of the Ussing chamber (photo from D.A. Christensen).

flux can be determined in the absence of a concentration gradient. For example, in a recent study (Etschmann et al., 2009) as well as in the study in the forthcoming chapter, Na^+ flux was measured from the mucosal to serosal side (J_{MS-Na}) as well as from the serosal to the mucosal side (J_{SM-Na}) of sheep rumen epithelia, which allowed the calculation of net Na^+ flux (J_{NET-Na}): $J_{NET-Na} = J_{MS-Na} - J_{SM-Na}$. A positive net flux is indicative of net absorption from the mucosal to serosal side. Additionally, through the use of different buffer formulations, pathways of molecule flux can be established, for example, through the use of bicarbonate-containing and bicarbonate-free buffers, the proportion of molecule flux dependent and independent of bicarbonate can be determined (Aschenbach et al., 2009; Penner et al., 2009a). Also, preventing the flux of a specific molecule across the tissue through the use of an inhibitor is another method of determining the pathway. For instance, urea flux via the urea transporter-B can be inhibited by phloretin (Abdoun et al., 2010). However, it should be acknowledged that many inhibitors are not specific to 1 transport pathway. For example, phloretin is also an inhibitor of glucose transport via GLUT transport proteins (Kalsi et al., 2009). Another opportunity is to impose a challenge on the tissue in the Ussing chamber that simulates a physiological challenge, such as reduced ruminal pH (Penner et al., 2010) and hyperosmolarity (Schweigel et al., 2005; Lodemann and Martens, 2006), which provides insight to tissue responsiveness *in vivo* and barrier function. While these responses are induced and evaluated external to the animal, the underlying physiology should be representative of *in vivo* responses.

2.5.4. Limitations of the Ussing Chamber

While the Ussing chamber technique possesses numerous strengths and opportunities to test mechanisms of ion movement across epithelial tissue and measures of barrier function, the *ex vivo* technique certainly has limitations. Firstly, the Ussing chamber provides limited measurements relative to the series of physiological events that occur *in vivo*, such as endocrine and paracrine signalling (Li et al., 2004). Therefore, caution must be taken when evaluating and emphasizing results. With the absence of blood flow in this *ex vivo* technique, nutrient supply is not maintained, as no fermentation occurs to provide substrates; rather, nutrient availability is reduced with increased duration of tissue incubation. For molecules that have strong unidirectional transport such as Na^+ and Cl^- (Sehested et al., 1996; Gäbel et al., 1999), their concentration gradient may be reduced. Furthermore, metabolites from epithelial metabolism are

not cleared due to the lack of blood flow. Hormones and immune agents are also not available due to the lack of blood flow, which has potential to change nutrient absorption or secretion relative to *in vivo*. For example, insulin-like growth factor-1 (IGF-1) is a stimulant of Na^+ absorption (Shen et al., 2012); however, this hormone can be added but buffer solutions are challenging to formulate and prepare consistently. Additionally, drug and reagent contamination of the Ussing chamber is possible due to repetitive use of the chamber. This is due to penetration of these substances into soft plastic such as the tubing that connects the chamber to the buffer columns above as well as the agar-filled voltage and current electrode bridges (Clarke, 2009). Another concern is the possible difference in the responsiveness of the tissue to specific drugs in the Ussing chamber relative to *in vivo*. This is due to 1) the accumulation of mucus on the apical membrane from goblet cells in the Ussing chamber, which act as a diffusion barrier and 2) variable buffer compositions, particularly CO_2/HCO_3^- buffering systems which may promote unidentified physiological changes following drug administration (Clarke, 2009).

Despite these limitations, the Ussing chamber technique has improved over time since its original use in the 1950's and was a reliable tool in the current study to measure functional changes in the rumen epithelium.

2.6. Conclusions

The ruminal epithelium possesses a unique structure that exhibits characteristics that promote the migration of specific molecules that are used by the epithelium itself or subsequently transited to the circulatory system where they are can later be used for essential bodily functions. Simultaneously, the ruminal epithelium inhibits the movement of harmful molecules. The ruminal epithelium is therefore classified as a selectively permeable membrane. Short chain fatty acids are the most valuable energy source for the ruminant, a product that is produced from ruminal fermentation of carbohydrates in the diet. Thus, it is common across numerous types of cattle operations to feed diets containing moderate to high levels of carbohydrates in order to supply the animal with sufficient energy required for growth and lactation. The ruminal epithelium is able to adapt to an increase in diet fermentability, both functionally (short-term adaptation) and morphologically (longer-term adaptation). However, if cattle are not appropriately adapted to such fermentable diets, ruminal acidosis may occur, and ruminal barrier function may be impaired. Rumen epithelium SCFA and Na^+ absorption have

proven to be closely associated, however, the rate that individual SCFA flux pathways and Na^+ transport adapt to an increase in diet fermentability remains to be pursued in cattle.

2.7. Hypothesis

The rate of rumen epithelial adaptation to a moderately fermentable diet occurs rapidly (prior to morphological changes), including rapid increases for SCFA flux and the transport of sodium.

2.8. Objectives

This study was designed to determine the time required for a change in SCFA and Na^+ absorption across the bovine rumen epithelium and to evaluate the rate and degree to which absorption pathways adapt to an increase in diet fermentability relative to changes in surface area.

3.0. SHORT-TERM ADAPTATION OF THE RUMEN EPITHELIUM INVOLVES FUNCTIONAL CHANGES IN SODIUM AND SHORT-CHAIN FATTY ACID TRANSPORT

3.1. Introduction

In order to achieve a high level of performance (e.g. milk production or body weight gain) from ruminants, diets rich in highly fermentable carbohydrates are commonly fed. Fermentation of carbohydrates in the reticulo-rumen yields short-chain fatty acids (SCFA), which serve as the primary energy substrate for ruminants (Bergman, 1990). However, when acid production in the reticulo-rumen exceeds acid clearance, digesta osmolality increases (Owens et al., 1998) and pH decreases (Aschenbach et al., 2011) resulting in ruminal acidosis. Exposure of the ruminal epithelium to hyperosmotic conditions transiently decreases barrier function (Schweigel et al., 2005; Lodemann and Martens, 2006; Penner et al., 2010) and exposure to acidic conditions reduces both absorptive (Gäebel and Martens, 1988) and barrier functions (Aschenbach et al., 2000; Penner et al., 2010). Moreover, the combination of both hyper-osmotic and acidic conditions has been shown to markedly decrease both absorptive and barrier function (Wilson et al., 2012). Despite the potential negative effects associated with ruminal acidosis, absorption of SCFA contributes substantially towards the regulation of ruminal pH (Gäbel et al., 2002; Penner et al., 2009a). Thus, a comprehensive understanding of the regulatory factors affecting SCFA absorption and barrier function of the ruminal epithelium is essential.

Previous studies have largely focused on promoting enlargement of the absorptive surface area by gradually increasing dietary fermentability (Dirsken et al., 1985; Gaebel et al., 1989; Bannink et al., 2008) as a strategy to promote epithelial adaptation. However, it is clear that adaptation involves more than hypertrophy and hyperplasia of the ruminal epithelia. For example, Etschmann et al. (2009) reported that net Na^+ absorption increased by more than 1.7 times within 1 week following a moderate increase in diet fermentability; a timeline that should not result in increased absorptive surface area. Supporting these findings, but in the opposite direction, short-term feed deprivation (48 h; Gäbel et al., 1993) and short-term feed restriction (5 d at 25% of ad libitum dry matter intake; Zhang et al., 2013a) have been reported to markedly reduce SCFA absorption across the reticulo-rumen. Moreover, after feeding a highly fermentable

diet, changes in mRNA abundance for genes encoding proteins involved in SCFA metabolism (Penner et al., 2009b; Schlau et al., 2012; Steele et al., 2012) and Na^+ absorption (Schlau et al., 2012; Yang et al., 2012) have been observed, which indicate functional changes within the ruminal epithelium.

Although the timeline for an increase in Na^+ absorption across the rumen epithelium has been reported (Etschmann et al., 2009), several gaps remain. Firstly, Na^+ absorption is driven by an electrochemical gradient generated from the Na^+/K^+ ATPase; an energy-dependent process. Thus, an increase in net Na^+ absorption must be accompanied by an increase in absorption or metabolism of energetic substrates. It is logical that an increase in SCFA absorption and metabolism may fulfill the energetic requirement, but to the authors' knowledge this has not been investigated. Also, the rate of adaptation for epithelial barrier function has not been assessed. We hypothesized that the rate of ruminal epithelial adaptation to a moderately fermentable diet would occur rapidly, with functional changes (increases in protein-mediated movement of SCFA, increases in transport of sodium, and improved barrier function) preceding increases in absorptive surface area of the ruminal epithelium. The aim of this study was to determine the rate and degree to which the ruminal epithelium adapts to a moderate increase in diet fermentability, including changes in the absorptive surface area, transport rate and pathway for SCFA absorption, rate of Na^+ transport across the ruminal epithelium, and measurements of barrier function. In addition, transcript abundance for proteins involved in SCFA and Na^+ transport, and local inflammatory responses were assessed.

3.2. Materials and Methods

This work was approved by the University of Saskatchewan's Animal Research Ethics Board, and adhered to the Canadian Council on Animal Care guidelines for humane animal use.

3.2.1. Animals, Feeding Regimen, and Housing

Twenty-five weaned Holstein steer calves (213 ± 23.0 kg; approximately 5 to 7 months of age) were used in this study. At the start of the study, all calves were group housed and fed a common high-forage diet (92% chopped grass hay, 8.5% vitamin and mineral supplement) for at

least 5 weeks. Calves were blocked by body weight and assigned to 1 of 2 dietary treatments including the control diet (**CON**; fed for 14 days; n = 5) or a moderately fermentable diet (n = 20). The control diet contained 91.5% hay and 8.5% vitamin and mineral supplement and the moderately fermentable diet contained 41.5% dry-rolled barley grain, 50% hay, and 8.5% vitamin and mineral supplement. Calves assigned to the moderately fermentable diet received the diet for 3 (**G3**; n = 5), 7 (**G7**; n = 5), 14 (**G14**; n = 5), or 21 d **(G21**; n = 5). Diets were formulated to meet calf nutrient requirements (NRC, 2001) to promote growth of 0.5 kg/d. Ingredient and nutrient composition for the CON and moderate grain diet (G3, G7, G14, and G21) are shown in Table 3.1. All calves were fed at 2.25% BW at 0800 h and dry matter intake (**DMI**) was recorded daily. Calves were housed individually in pens (9 m^2) with rubber mats on the floor for 7 d prior to initiation of the feeding protocol. One calf was killed each day with the order of killing balanced among treatments over time. Calves were killed by captive bolt stunning followed by pithing and exsanguination at 1000 h (2 h after feeding) on the last day of the assigned feeding period.

3.2.2. Data and Sample Collection

3.2.2.1. Reticular pH

Reticular pH was measured every 5 min for 48 h prior to killing using the small ruminant pH measurement system (Penner et al., 2009c; Dascor Inc., Escondido, CA, USA). The pH system was orally dosed at the start of the measurement period and recovered from the reticulum when the digestive tract was removed. Pre- and post-measurement standardizations were carried out using pH buffers 7.0 and 4.0 at 39°C. The linear equations derived using the relationship between mV readings in pH buffer solutions 7 and 4 at both the starting and ending standardizations were used to calculate reticular pH assuming linear drift over time.

3.2.2.2. Blood Collection and Analysis

Two blood samples (10 mL each) were drawn from the jugular vein immediately before killing. One blood sample was collected into a lithium heparin (158 IU units) coated vacutainer tube (BD, Franklin Lakes, NJ, USA) and the other into a silica-coated clot-activating vacutainer

Table 3.1. Ingredient and nutrient composition of the control (CON) and moderate grain (G3, G7, G14, and G21) diets.

Item	Diet Treatment	
	CON[*]	G3, G7, G14, and G21[†]
Ingredient, % of DM		
Hay	91.5	50
Barley grain	0	41.5
Vitamin-mineral supplement[‡]	8.5	8.5
Nutrient composition[§]		
DM	87.3	87.9
CP, % of DM	10.6	11.4
NDF, % of DM	48.4	33.5
ADF, % of DM	33.3	20.9
OM, % of DM	92.1	93.6
Starch, % of DM	4.1	24.6
Ether extract, % of DM	1.4	1.5

[*]Control calves (CON; n = 5).

[†]The moderate grain diet was fed for either 3 (G3; n = 5), 7 (G7; n = 5), 14 (G14; n = 5), or 21 (G21; n = 5) days.

[‡]Vitamin-mineral supplement ingredient composition (per 1000 kg): ground barley (404.7), soybean meal (350.0), urea (53.5), limestone (50.9), salt (22.3), tallow (10.0), dynamite (102.1), magnesium oxide (2.87), selenium (1.78), vitamin E (0.74), potassium chloride (0.64), manganese oxide (0.39), vitamin A (0.03), vitamin D (0.03), copper sulfate (0.01), ethylenediamine dihydroiodide (0.01), zinc oxide (0.01), ferrous carbonate (0.01).

[§]Dry matter (DM), crude protein (CP), neutral detergent fiber (NDF), acid detergent fiber (ADF), organic matter (OM).

tube (BD) to retrieve plasma and serum, respectively. Samples were immediately placed on ice until centrifuged at 1,800 × g for 15 min at 4°C, from which serum and plasma were collected and subsequently stored at -20°C until analysis of plasma glucose and insulin and serum BHBA. Plasma insulin was measured in triplicate using a bovine-specific insulin ELISA kit (Mercodia, Uppsala, Sweden). Plasma glucose was quantified using a glucose oxidase-peroxidase enzyme (**PGO** Enzyme Preparation; Sigma-Aldrich Co., St. Louis, MO, USA), which catalyzes o-dianisidine (colorless) to oxidized o-dianisidine (brown; via peroxidase), and glucose to gluconic acid (via glucose oxidase). The intensity of color change is proportionate to the original plasma glucose concentration, which was measured at 450 nm on a SpectraMax Plus^{384} Microplate Reader (Molecular Diagnostics, Inc., Sunnyvale, CA, USA). Each plasma glucose sample was quantified in triplicate with a glucose standard curve on each microplate to ensure accurate glucose quantification. Serum BHBA was analyzed by oxidizing BHBA to acetoacetate and NADH (via β-hydroxybutyrate dehydrogenase; Roche Diagnostics, Laval, QC, Canada). Then, catalyzed by diaphorase, NADH reacted with 2-p-iodophenyl-3-p-nitrophenyl-5-phenyltetrazolum chloride (**INT**) to produce a blue color proportional to the initial BHBA concentration in the serum, which was measured at 340 nm on a microplate reader (SpectraMax Plus^{384}). Each serum sample quantified for BHBA was run in triplicate together with a BHBA standard curve on each microplate.

3.2.2.3. Rumen Tissue and Fluid Collection and Analysis

Immediately after killing, the abdominal cavity was opened and rumen epithelial tissue (300 cm^2) was collected from the caudal dorsal blind sac of the rumen. The caudal dorsal blind sac was selected for the homogenous nature of the density and size of the rumen papillae. The tissue was washed until clean with a pre-heated (38.5°C) buffer (pH 7.4; Table 3.2) gassed with carbogen (95% O_2 and 5% CO_2). Subsequently, the submucosal tissue was gently stripped from the epithelium. The epithelial tissue was then placed in fresh buffer, transported to the laboratory, cut into 9 cm^2 pieces, and mounted between two halves of an Ussing chamber with an exposed surface area of 3.14 cm^2. Additional whole rumen tissue (10 cm^2; preserved in 10% formalin solution) was collected from the ventral sac for analysis of papillae density and surface area measurements. Furthermore, mucosal biopsies from the ventral sac were collected using

Table 3.2. Buffer compositions for washing and transport of tissue and *ex vivo* Ussing chamber experiments.

Substance (mmol/L)	Buffer						
	Sodium and Mannitol[a]		Bicarbonate[b]		Bicarbonate-free[c]		Bicarbonate-free with nitrate[d]
	Serosal	Mucosal	Serosal	Mucosal	Serosal	Mucosal	Mucosal
$CaCl_2$	1.0	1.0	0.0	0.0	0.0	0.0	0.0
$MgCl_2$	1.3	1.3	0.0	0.0	0.0	0.0	0.0
NaCl	15.6	15.6	0.0	0.0	0.0	0.0	0.0
KCl	5.5	5.5	0.0	0.0	0.0	0.0	0.0
Na-gluconate	0.0	0.0	50.6	50.6	69.6	69.6	34.6
K-gluconate	0.0	0.0	5.5	5.5	5.5	5.5	5.5
Ca-gluconate	0.0	0.0	1.0	1.0	1.0	1.0	1.0
Mg-gluconate	0.0	0.0	1.3	1.3	1.3	1.3	1.3
Na-phosphate	0.6	0.6	0.6	0.6	0.6	0.6	0.6
Disodium hydrogen phosphate	2.4	2.4	2.4	2.4	2.4	2.4	2.4
Acetic acid	10.0	10.0	0.0	0.0	0.0	0.0	0.0
Na-D/L-lactate (60%)	5.0	5.0	0.0	0.0	0.0	0.0	0.0
L-glutamine	1.0	1.0	1.0	1.0	1.0	1.0	1.0
HEPES-free acid	10.0	10.0	10.0	10.0	10.0	10.0	10.0
Na-propionate	10.0	10.0	0.0	0.0	0.0	0.0	0.0
Na-butyrate	10.0	10.0	0.0	0.0	0.0	0.0	0.0
Na-bicarbonate	24.0	24.0	24.0	24.0	0.0	0.0	0.0
Glucose	0.0	0.0	10.0	10.0	10.0	10.0	10.0
Na-nitrate	0.0	0.0	0.0	0.0	0.0	0.0	40.0
Acetazoleamide	0.0	0.0	0.0	0.0	0.1	0.1	0.1
Mannitol	100.0	80.0	110.0	90.0	115.0	109.0	109.0
Gluconic acid	0.0	20.0	0.0	20.0	0.0	6.0	1.0
Na-hydroxide	10.0	10.0	0.0	0.0	5.0	5.0	0.0

Table 3.2. (continued). Buffer compositions for washing and transport of tissue and *ex vivo* Ussing chamber experiments.

Substance (mmol/L)	Buffer						
	Wash, transport, sodium, and mannitol[a]		Bicarbonate[b]		Bicarbonate-free[c]		Bicarbonate-free with nitrate[d]
	Serosal	Mucosal	Serosal	Mucosal	Serosal	Mucosal	Mucosal
Antibiotics, mg/L							
Penicillin G Na salt	60.0	60.0	60.0	60.0	60.0	60.0	60.0
Kanamycin sulphate	100.0	100.0	100.0	100.0	100.0	100.0	100.0
Flurocytosine	50.0	50.0	50.0	50.0	50.0	50.0	50.0
Buffer characteristics							
pH	7.4	6.2	7.4	6.2	7.4	6.2	6.2
Temperature (^{o}C)	38.5	38.5	38.5	38.5	38.5	38.5	38.5
Osmolality, mOsmol/L	251±1.36[e]	252±3.23	287±1.42	277±1.64	284±0.58	274±0.80	291±4.81
Gas	C[f]	C	C	C	C	O[g]	O

[a]Buffer for washing tissue at time of collection and subsequent transport to the lab, and sodium and mannitol *ex vivo* Ussing chamber experiments. Antibiotics were not included in the wash/transport buffer, but were for the sodium/mannitol buffer.

[b]Ussing chamber buffer for determination of total acetate and butyrate flux in the presence of bicarbonate (bicarbonate-dependent flux).

[c]Ussing chamber buffer for determination of acetate and butyrate flux in the absence of bicarbonate (bicarbonate-independent flux).

[d]Ussing chamber buffer for determination of acetate and butyrate flux in the absence of bicarbonate but presence of nitrate (bicarbonate-independent nitrate-sensitive flux).

[e]Mean osmolality ± standard error of the mean.

[f]Carbogen gas (95% O_2 and 5% CO_2).

[g]Oxygen gas.

sterile forceps and scissors, rinsed in sterile ice-cold phosphate buffered saline (PBS; pH 7.4) until clean, and placed in RNAlater (Sigma-Aldrich). These mucosal tissue biopsies were held at 4°C for 24 h and then stored at -20°C until analyzed for gene expression.

Rumen fluid (10 mL preserved in 2 mL of 25% [wt/v] metaphosphoric acid) was collected by straining a representative sample of rumen digesta through 2 layers of cheesecloth. Rumen fluid was placed on ice and stored at -20^{o}C until analyzed for SCFA concentration as described by Khorasani et al. (1996), using a gas chromatrography (Agilent Technologies Inc., Santa Clara, CA, USA). The pH of the strained digesta was recorded using an accumet AP110 portable pH meter (Fischer Scientific, Ottawa, ON, Canada) to assess ruminal pH relative to reticular pH.

3.2.2.4. Rumen Papillae Density and Dimension Determination

A 1-cm^2 piece of whole tissue preserved in formalin was used to determine the density of mature and immature papillae. The papillae were classified as either small (papillae that were half or less than half of the size of the average large papillae in each biopsy) or large papillae (papillae that were greater than half of the average large papillae in each biopsy) for each tissue segment. Fifteen large papillae/biospy were cut at the basal attachment using a dissecting microscope (Wild M8 Heerbrugg microscope, Heerbrugg, Switzerland) and scalpel. Excised papillae were used for surface area measurements using an Olympus SZ61 microscope (Olympus Corporation, Tokyo, Japan) equipped with an Olympus DP25 camera (Olympus Corporation). Images were captured at magnification values ranging from 1.2 to 2.5 times depending on papillae size. Papillae length, width, and perimeter were measured using Image-Pro Plus 7.0 (Media Cybernetics Inc., Rockville, MD, USA) software. The area within the papillae perimeter was determined and multiplied by 2 to calculate papillae surface area. Effective surface area was calculated as the large papillae surface area multiplied by the number of large papillae/cm^2 (mm^2/cm^2).

3.2.3. Ussing Chamber Experiments

Within 30 min after killing, rumen epithelial tissue was mounted in a total of 18 Ussing chambers with an exposed surface area of 3.14 cm^2. All tissues were incubated under short-circuit conditions using a computer-controlled voltage-clamp device (Dipl.-Ing. K. Mussler, Scientific Instruments, Aachen, Germany). After mounting, an additional 20 min were allowed for stabilization of tissue conductance (**G_t**) and short circuit current (**I_{SC}**).

The composition of the buffers used for washing and transporting ruminal tissue at the time of collection and for the measurement of Na^+, mannitol, and SCFA flux are shown in Table 3.2. For SCFA absorption, buffers were used to evaluate total SCFA absorption, flux of SCFA in the absence of bicarbonate, and flux of SCFA in the absence of bicarbonate but containing nitrate as described by Aschenbach et al. (2009). All buffers were maintained at 38.5°C using circulating water jackets and buffer solutions were circulated by gas lift. The serosal and mucosal buffer solutions were formulated to mimic physiological conditions at pH 7.4 and 6.2, respectively. Buffers containing bicarbonate were gassed with carbogen and buffers not containing bicarbonate were gassed with 100% O_2. The pH of the serosal and mucosal buffer was adjusted accordingly with NaOH and gluconic acid. All Ussing chamber buffers contained broad-spectrum antibiotics [Penicillin G Na^+ Salt (60 mg/L), Kanamycin sulphate (100 mg/L), and Flurocytosine (50 mg/L)] to inhibit microbial activity. Buffer antibiotics and chemicals were purchased from Sigma-Aldrich, 1-^{14}C-butyrate purchase from Moravek Biochemicals (Moravek Biochemicals Inc., Brea, CA), and all other radiolabelled chemicals from Perkin Elmer Inc. (Woodbridge, ON, Canada).

3.2.3.1. Sodium Flux

The mucosal-to-serosal (**J_{MS-Na}**; 2 chambers) and serosal-to-mucosal (**J_{SM-Na}**; 2 chambers) Na^+ flux across the ruminal epithelium was measured in the absence of a Na^+ concentration gradient. Tissues assigned to J_{MS-Na} and J_{SM-Na} were paired only when G_t differed by less than 20% to determine the net Na^+ flux (**J_{NET-Na}**; calculated as the difference between the J_{MS-Na} and J_{SM-Na}). Labelled Na^+ (80 kBq $^{22}Na^+$/15 mL) was pipetted into either the mucosal or serosal column and tissues were allowed to equilibrate for 45 min prior to the first sample collection in order to measure Na^+ flux (Sehested et al., 1996). A 1 h flux period was used to measure Na^+

flux. Hot samples (taken from the same side as radioactivity addition; n = 2; 100 μL each) and cold samples (taken from the opposite side of radioactivity addition; n = 2; 500 μL each) were collected at the beginning and end of the sampling period.

3.2.3.2. Mucosal to Serosal SCFA Flux

Twelve Ussing chambers were assigned to 1 of 3 buffer solutions: 1) containing HCO_3^-, 2) free of HCO_3^-, or 3) free of HCO_3^- and containing 40 m*M* nitrate as described by Aschenbach et al. (2009). The incubation conditions were used to determine the rate of total, bicarbonate-independent, and bicarbonate-independent nitrate-insensitive mucosal to serosal flux of acetate ($\mathbf{J_{MS\text{-}acetate}}$) and butyrate ($\mathbf{J_{MS\text{-}butyrate}}$) as described by Aschenbach et al. (2009) and Penner et al. (2009a). Briefly, the total $\mathbf{J_{MS\text{-}acetate}}$ and $\mathbf{J_{MS\text{-}butyrate}}$ was determined in bicarbonate-containing buffer and the bicarbonate-dependent flux was calculated as the difference between total flux and the flux in bicarbonate-free buffer. Nitrate-sensitive flux was determined as the difference between the flux measured in bicarbonate-free buffer and the bicarbonate-free buffer with 40m*M* nitrate. The bicarbonate-independent nitrate-insensitive flux was determined as the flux occurring when incubated in bicarbonate-free buffer containing 40 m*M* nitrate.

In addition, half of the chambers assigned to measure $J_{MS\text{-}acetate}$ and $J_{MS\text{-}butyrate}$ were further assigned to 1 of 2 acetate and butyrate concentration treatments: 10 m*M* (**Low**; n = 6) and 50 m*M* (**High**; n = 6), where equimolar concentrations (Low = 5 m*M* acetate and 5 m*M* butyrate and High = 25 m*M* acetate and 25 m*M* butyrate) of acetate and butyrate were added only to the mucosal side. For all incubations, 2-^{3}H-acetate (37 kBq ^{3}H-acetate/15 mL) and 1-^{14}C-butyrate (74 kBq ^{14}C-butyrate/15 mL) were added to the mucosal column, thus both SCFA were measured in parallel. After the addition of ^{3}H-acetate and ^{14}C-butyrate, tissues were provided with a 45-min equilibration period, followed by a 1-h flux period. Hot and cold sample methods and volumes were performed as described above for Na^+ flux samples.

3.2.3.3. Barrier Function

The flux of mannitol (74 kBq 1-^{3}H-mannitol/15 mL) was measured as an indicator of paracellular permeability and thus barrier function of the epithelial tissue. The serosal-to-

mucosal flux ($\mathbf{J_{SM\text{-}mannitol}}$; 2 chambers) of mannitol was measured with a 20 m*M* gradient from the serosal to mucosal side. Tissues were allowed a 45-min isotope equilibration period prior to the first sample collection, which was followed by three 1-h flux periods interspersed by two 30-min treatment application periods. Hot samples (100 μL) were collected at the beginning and end of the entire sampling period, whereas cold samples (500 μL) were collected at the start and end of each flux period. All cold samples were replaced with 500 μL fresh buffer solution to avoid changes in volume and hydrostatic pressure. The first flux period was used to measure baseline (**BASE**) flux rates under control conditions followed by a 30 min duration to apply an acidotic and hyperosmotic challenge on the mucosal side. The mucosal pH was reduced to 5.2 and osmolality was increased to 450 mOsmol/kg by addition of 200 μL 3*M* gluconic acid and 0.41 g mannitol (Penner et al., 2010). The second flux period was used to evaluate mannitol flux while the tissue was exposed to the hyperosmotic and acidotic challenge (**CHAL**). Following the CHAL, the mucosal buffer solution was then drained and fresh buffer solution was added to return conditions back to that imposed during BASE to evaluate recovery (**REC**) under control conditions. A 30-min equilibration period was provided before the start of the REC flux period. This *ex vivo* challenge model was used to simulate rumen acidosis *ex vivo* and follows the procedures previously reported by Penner et al. (2010) and Wilson et al. (2012). Tissues within a buffer treatment were assigned randomly to treatments except for Na^+ in which tissues were paired only when G_t differed by less than 25%.

3.3.3. Quantitative Real-Time PCR

Ruminal tissue was homogenized via a vertical mixer and RNA was extracted using TRIzol reagent according to the TRIzol® Reagent Protocol (Invitrogen, Burlington, ON, Canada). The RNA concentration was quantified using a NanoDrop 2000c Spectrophotometer (Thermo Scientific Inc., Waltham, MA, USA). The average RNA concentration was 1492 ± 1318 ng of RNA/μL and the quality of RNA was confirmed acceptable as measured by the ratio of absorbance at 260:280 nm, where the ratio was 2.06 ± 0.11. Concentrated RNA samples were diluted with RNAase-free water to yield a final concentration of 500 ng/μL and used for cDNA synthesis using the GoScript Reverse Transcription System (Promega Corporation, Madison, WI,

Table 3.3. Target gene name, National Center for Biotechnology Information (NCBI) accession number, and forward and reverse primer sequences, gene function, and sequence source.

Target gene name (abbreviation)	NCBI accession number	Forward and reverse sequences	Gene function	Redesigned or reference
Glyceraldehyde-3-phosphate dehydrogenase (GAPDH)	AB098934	F*: GTCGGAGTGAACGGATTTGG R†: CAATGTCCACTTTGCCAGAGTTAA	Reference gene	Røjen et al., 2011
Toll-like receptor-2 (TLR2)	AY634629	F: CCTTGACCTGTCCAACAAT R: CTGAACCAGGAGGATGATAAG	Innate mucosal immunity	Redesigned
Toll-like receptor-4 (TLR4)	AY634630	F: GGTTTCCACAAAAGCCGTAA R: AGGACGATGAAGATGATGCC	Innate mucosal immunity	Charavaryamath et al., 2011
Acetyl-CoA acetyltransferase (ACAT)	BC102927	F: GGAGATATCTGCGTGGGAAAC R: CGACGAACACTGCCTATTGA	Ketogenesis	Redesigned
Monocarboxylate transporter-1 (MCT1)	NM_001037319	F: CGCGGGATTCTTTGGATTT R: GTCCATCAGCGTTTCAAACAGTAC	SCFA transport	Schlau et al., 2012
Insulin-like growth factor binding protein-3 (IGFBP3)	NM_001075549	F: ATTCCCAACTGCGACAAG R: CGTACTTATCCACACACCAG	IGF axis	Redesigned
Insulin-like growth factor binding protein-5 (IGFBP5)	BC102850	F: CTACAAGAGAAAGCAGTGCAAACC R: TCCACGCACCAGCAGATG	IGF axis	Steele et al., 2012
Sodium-hydrogen exchanger-1 (NHE1)	U49432	F: GAAAGACAAGCTCAACCGGTTT R: GGAGCGCTCACCGGCTAT	Cell pH homeostasis	Penner et al., 2009c
Sodium-hydrogen exchanger-3 (NHE3)	AJ131764.1	F: AGCCTTCGTGCTCCTGACA R: TGACCCCTATGGCCCTGTAC	Cell pH homeostasis	Schlau et al., 2012
G-protein-coupled receptor-41 (GPR41)	NM_005304	F: AACCTCACCCTCTCGGATCT R: GCCGAGTCTTGTACCAAAGC	SCFA receptor	Wang et al., 2009b
G protein-coupled receptor-43 (GPR43)	NP_001157256.1	F:TGCAAGCTTCAGCCATGCCAGACTGGGATAG R: GATGGATCCC-TTCCAAGCCTGCTCAACTCCT	SCFA receptor	Wang et al., 2012

Table 3.3. (continued). Target gene name, National Center for Biotechnology Information (NCBI) accession number, and forward and reverse primer sequences, gene function, and sequence source.

Target gene name (abbreviation)	NCBI accession number	Forward and reverse sequences	Gene function	Redesigned or reference
Tumor necrosis factor-α (TNFα)	AC_000180.1	F*: CAA ACA CTC AGG TCC TCT TC R†: ATG AGG GCA TTG GCA TAC	Pro-inflammatory response	Redesigned
Interleukin-1β (IL-1β)	AC_000168.1	F: CTG AGG AGC ATC CTT TCA TTC R: GTC CTG GAG TTT GCA CTT TAT	Pro-inflammatory response	Redesigned
Interleukin-4 (IL-4)	AC_000164.1	F: GAA TTG AGC TTA GGC GTA TCT A R: CTC GTC TTG GCT TCA TTC A	Anti-inflammatory response	Redesigned
Interleukin-8 (IL-8)	AC_000163.1	F: CTG GCT GTT GCT CTC TTG R: GTG GAA AGG TGT GGA ATG T	Pro-inflammatory response	Redesigned
Interleukin-10 (IL-10)	AC_000173.1	F: GTA TCC ACT TGC CAA CCA R: GAG ACT GGG TCA ACA GTA AG	Anti-inflammatory response	Redesigned
Interleukin-13 (IL-13)	AC_000164.1	F: ACT GCA GTG TCA TCC AAA G R: TTT GGT GTC TCG GAC GTA	Pro-inflammatory response	Redesigned
Interleukin-22 (IL-22)	AC_000162.1	F: TGG CTC AGA AGG CTA GTT R: CTT CGT CAC CTG ATG GAT TC	Pro- and anti-inflammatory response	Redesigned

*F = forward primer.

†R = reverse primer.

USA). The forward and reverse primers used in this study were designed using PrimerQuest software (Integrated DNA Technologies, Inc., Coralville, IA, USA) or sourced from previously published literature. Target genes of interest and their corresponding NCBI accession number, forward and reverse primer sequences, general function, and source are shown in Table 3.3. Amplification efficiencies for each target gene and the reference gene glyceraldehyde-3-phosphate dehydrogenase (**GAPDH**) were determined using serial dilution. The amplication efficiencies ranged between 91.8 and 111.9% with a mean of 102.6%. In addition, consistency across PCR plates was assessed using a mixed cDNA sample run on each plate as an internal control. The interassay CV for the mixed cDNA sample was 3.21% ± 0.30. Quantitative real-time PCR (**qRT-PCR**) was performed on all samples in duplicate using a Stratagene Mx3005P Real-Time PCR System (Agilent Technologies) and SYBR Green probe (Bio-Rad Laboratories Ltd., Mississauga, ON, Canada). There was a 10 min activation period prior to the start of PCR (95°C), followed by 40 cycles each of denaturation (30 s at 95°C), annealing (60 s at 58°C), and elongation (60 s at 72°C). For each calf, the cycle threshold ($\mathbf{C_T}$; number of cycles required for fluorescent signal to cross the threshold) value for GAPDH was subtracted from the C_T value for each target gene to calculate ΔC_T. The corrected fold change value for each target gene and each diet treatment (CON, G3, G7, G14, and G21) was then normalized to the CON for the corresponding gene. Gene expression fold change was calculated using the target gene ΔC_T and assuming a 100% PCR efficiency as per Pfaffl (2001).

3.4. Statistical Analysis

All statistical analyses were carried out using the Mixed Procedure of SAS (SAS v. 9.3 Institute, Inc., Cary, NC). All data were analyzed as a randomized complete block design with polynomial contrasts used to evaluate whether adaptation to dietary change responded in linear, quadratic, or cubic patterns. The model included treatment and block as fixed effects. The relationship between ruminal and reticular pH at time of kill was evaluated by linear regression. The Low and High SCFA concentration *ex vivo* treatment was analyzed using a split-plot design. Interaction between *ex vivo* SCFA concentration treatment and *in vivo* diet treatment was tested. Furthermore, to confirm that the results for G_t and I_{SC} were a result of the *ex vivo* Low and High SCFA treatment imposed, the G_t values prior to acetate and butyrate administration (20 min

following the start of Ussing chamber incubation) were compared. For mannitol flux, *ex vivo* period (BASE, CHAL, and REC) were used as a repeated measure. Treatment differences were designated significant when $P < 0.05$ with all P values shown rather than indicating non-significance. Data are reported as means ± standard error of the mean (SE).

3.5. Results

3.5.1. Body Weight, Dry Matter Intake and Reticulo-Rumen Fermentation

Body weight and DMI were not affected by treatment ($P \geq 0.429$ and $P \geq 0.469$, respectively; Table 3.4) confirming that our experimental model was imposed effectively. However, minimum and mean reticular pH decreased from 6.57 and 6.90 for CON to 6.08 and 6.59 for G7 and increased thereafter resulting in values of 6.31 and 6.79 for G21 (quadratic, $P < 0.001$) showing that even when fed the same diet, reticular pH varies over time. Maximum reticular pH also decreased from 7.22 for CON to 7.05 for G7 and increased thereafter to 7.19 for G21 (quadratic, $P = 0.013$).

Admittedly, most past studies have measured ruminal pH; however, ruminal pH measurements are either obtained using animals fitted with a ruminal cannula or from spot-sample measurements collected after killing. We utilized calves that were not surgically modified and an orally administered pH measurement system that was recovered in the reticulum. Thus, to evaluate whether reticular pH can be used as an indicator of rumen pH, regression analysis was performed using rumen pH spot samples collected immediately after slaughter and the 10-min average of reticular pH corresponding to the same time-point. The results show that ruminal and reticular pH were positively related (Figure 3.1; regression equation $y = 0.87098 + 0.5941x$; $R^2 = 0.548$; $P < 0.001$) indicating that it may be possible to predict rumen pH with reticular pH. Using the equation listed above, mean rumen pH for CON, G3, G7, G14, and G21 are predicted to be 6.57, 6.46, 6.31, 6.39, and 6.48, respectively.

Total ruminal SCFA concentration was not affected by the duration of time fed the moderate grain diet, averaging 84.1 m*M* ($P \geq 0.250$; Table 3.4). This finding was surprising given the large changes in reticular pH from CON to G7 and G21. However, when pH values from the indwelling pH probe were plotted over 48 h prior to kill (Figure 3.2), reticular pH was lowest at

1400 h. This suggests that peak fermentation would not have occurred until 4 h after the time of rumen fluid collection, which may explain the lack of effect of diet on total SCFA concentration from rumen fluid collected at 1000 h. Furthermore, the molar proportion of acetate decreased cubically ($P = 0.008$) from 67.8% for CON to 63.6% for G7, followed by an increase to 64.0% for both G14 and G21. The molar proportion of butyrate increased quadratically ($P = 0.008$) from 9.6 for CON to 13.0% for G14 with a slight decrease to 11.9% for G21. Valerate and caproate increased linearly with increasing days fed the moderate grain diet ($P = 0.019$ and 0.011, respectively). Treatment did not affect propionate ($P \geq 0.117$), isobutyrate ($P \geq 0.269$), and isovalerate ($P \geq 0.460$).

3.5.2. Plasma Glucose, Insulin, Serum β-hydroxybutyric Acid (BHBA) and Plasma Osmolality

To evaluate whether dietary adaptation also affected plasma BHBA, insulin, and osmolality, blood samples were collected immediately before killing. Plasma glucose concentration increased from 68.6 mg/dL for CON to 76.7 mg/dL for G21 (linear $P = 0.012$; Table 3.5), suggesting an increase in substrate supply for gluconeogenesis or possibly direct absorption of glucose. Plasma insulin concentration did not respond similarly to glucose as concentration increased from 0.42 for CON to 1.09 μg/L for G3 and decreased thereafter to 0.54 μg/L for G21 (cubic $P = 0.016$). Dietary treatment did not affect serum BHBA concentration ($P \geq 0.391$) despite changes in ruminal butyrate concentration. Plasma osmolality was not affected ($P \geq 0.210$).

3.5.3. Papillae Density and Surface Area

As the objective of this study was to evaluate functional adaptation, it was essential to determine whether changes in papillae density, papillae dimensions, and effective absorptive surface area were affected under our experimental model. Papillae density in the ventral sac was not affected by diet ($P \geq 0.130$; Table 3.6) nor was the density of small papillae ($P \geq 0.130$). However, there was an increase in the density of large papillae (cubic $P = 0.011$) from 80 for CON to 96 papillae/cm^2 for G21 with the greatest density being 101 papillae/cm^2 for G7. The duration of time consuming the moderate grain diet did not affect mature papillae length ($P \geq$

Table 3.4. Effect of number of days fed moderate grain diet on dry matter intake, reticular pH, and ruminal short-chain fatty acid (SCFA) concentrations.

Item	Treatment[a]					SE[b]	Contrasts[c]		
	CON	G3	G7	G14	G21		L	Q	C
BW, kg	210	210	214	218	218	8.2	0.429	0.788	0.868
DMI[d], kg/d	4.7	4.7	4.8	4.9	4.9	0.20	0.469	0.971	0.878
Reticular pH[e]									
Minimum	6.57	6.29	6.08	6.16	6.31	0.045	0.019	< 0.001	0.086
Mean	6.90	6.77	6.59	6.69	6.79	0.028	0.133	< 0.001	0.123
Maximum	7.22	7.18	7.05	7.13	7.19	0.024	0.638	0.013	0.443
Ruminal SCFA									
Total, m*M*	80.7	79.9	87.5	87.1	85.5	1.70	0.250	0.323	0.907
Acetic acid, %	67.80	64.60	63.60	64.00	64.00	0.400	0.001	0.001	0.008
Propionic acid, %	19.50	21.20	20.80	19.60	20.60	0.402	0.955	0.824	0.117
Isobutyric acid, %	0.79	0.66	0.69	0.68	0.71	0.029	0.665	0.269	0.540
Butyric acid, %	9.64	11.10	12.50	13.00	11.90	0.368	0.018	0.008	0.790
Isovaleric acid, %	0.93	0.78	0.84	0.88	0.88	0.048	0.926	0.635	0.460
Valeric acid, %	1.10	1.32	1.21	1.38	1.43	0.042	0.019	0.653	0.723
Caproic acid, %	0.24	0.34	0.36	0.38	0.41	0.022	0.011	0.252	0.386

[a]Control calves (CON; n = 5) received 91.5% chopped hay and 8.5% vitamin/mineral supplement. Calves assigned to G3, G7, G14, and G21 (n = 5 for each moderate grain diet treatment) received a high energy diet consisting of 41.5% barley grain, 50% chopped hay, and 8.5% vitamin/mineral supplement for 3, 7, 14, or 21 days, respectively.

[b]SE = standard error.

[c]Contrast patterns, L = linear, Q = quadratic, C = cubic.

[d]DMI = feed dry matter intake.

[e]Reticular pH data was collected for two days prior to killing.

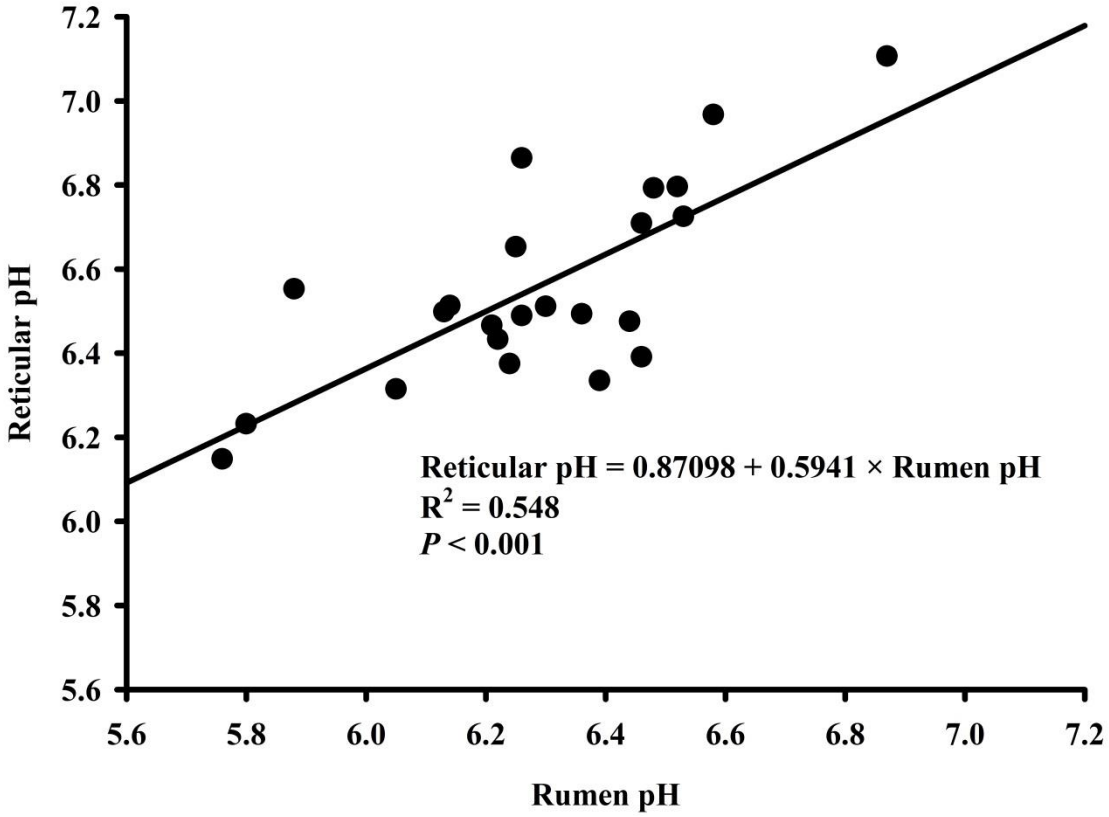

Figure 3.1. Linear regression of ruminal pH measured using a hand-held pH meter at the time of killing and the 10-min average of reticular pH prior to killing measured using an indwelling pH measurement system.

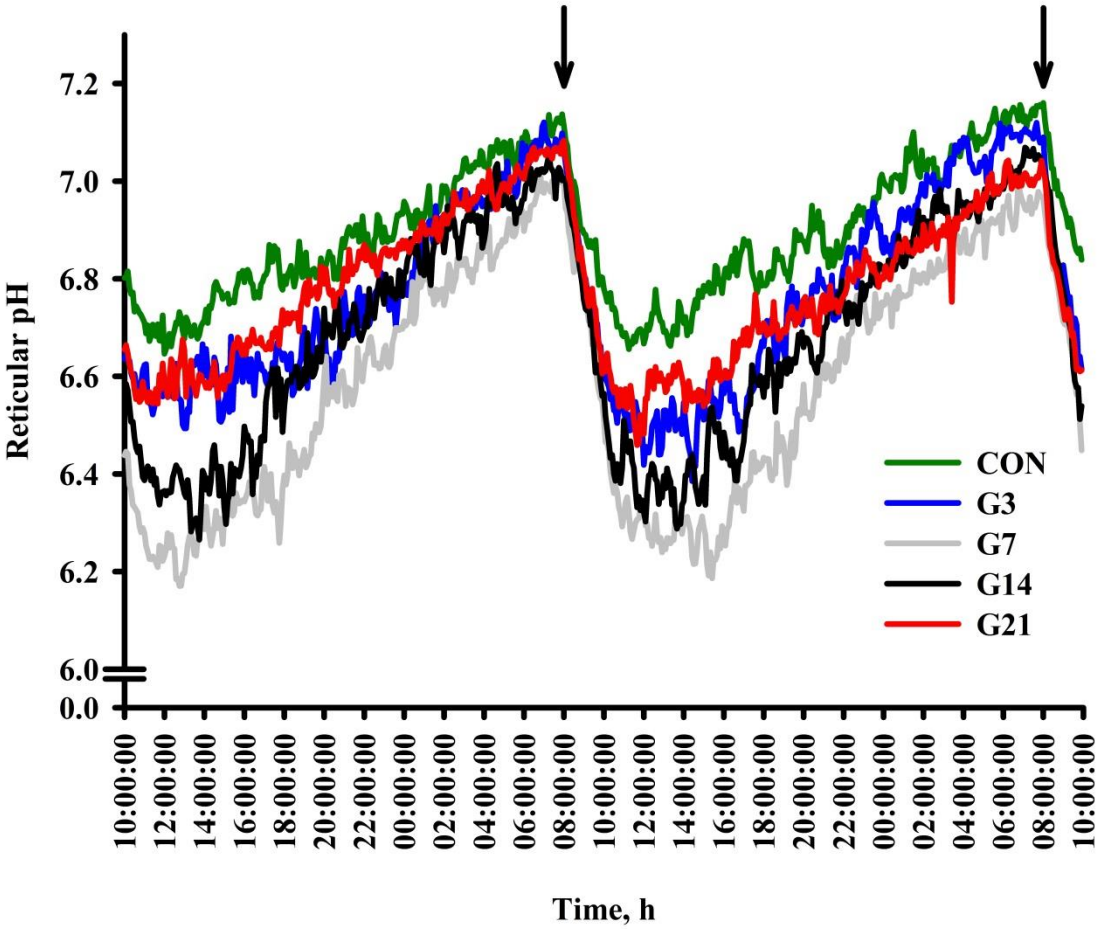

Figure 3.2. Reticular pH for the last 48-h prior to killing. Reticular pH measurements were conducted using an indwelling pH measurement system with 5-min intervals between consecutive measurements. Arrows indicate time of feeding. Control calves (CON; green line) received 91.5% chopped hay and 8.5% vitamin/mineral supplement. Calves assigned to G3 (blue line), G7 (grey line), G14 (black line), and G21 (red line) received a moderately fermentable diet consisting of 41.5% barley grain, 50% chopped hay, and 8.5% vitamin/mineral supplement for 3, 7, 14, or 21 days, respectively. Each line represents the mean reticular pH of 5 calves in a given treatment.

Table 3.5. Effect of number of days fed moderate grain diet on plasma glucose, insulin, osmolality and serum β-hydroxybutyric acid (BHBA).

Blood Parameter	Treatment[*]					SE[†]	Contrasts[‡]		
	CON	G3	G7	G14	G21		L	Q	C
Glucose, mg/dL	68.6	67.4	73.9	71.5	76.7	1.45	0.012	0.992	0.458
BHBA, mg/dL	8.6	12.4	9.1	11.4	11.2	0.74	0.391	0.748	0.686
Insulin, μg/L	0.42	1.09	0.83	0.58	0.54	0.084	0.286	0.100	0.016
Osmolality, mOsmol/kg	292	286	287	283	278	3.1	0.210	0.975	0.771

[*]Control calves (CON; n = 5) received 91.5% chopped hay and 8.5% vitamin/mineral supplement. Calves assigned to G3, G7, G14, and G21 (n = 5 for each moderate grain diet treatment) received a high energy diet consisting of 41.5% barley grain, 50% chopped hay, and 8.5% vitamin/mineral supplement for 3, 7, 14, or 21 days, respectively.

[†]SE = standard error.

[‡]Contrast patterns, L = linear, Q = quadratic, C = cubic.

Table 3.6. Effect of number of days fed moderate grain diet on rumen papillae density and dimensions, and surface area.

Item	Treatment[a]					SE[b]	Contrasts[c]		
	CON	G3	G7	G14	G21		L	Q	C
Papillae density									
Total, no./cm^2	121	119	137	120	150	5.9	0.130	0.573	0.284
Small papillae[d], no./cm^2	40	33	36	61	54	5.3	0.130	0.926	0.224
Large papillae, no./cm^2	80	86	101	59	96	6.4	0.999	0.429	0.011
Large papillae dimensions									
Length, mm	4.37	5.08	3.80	4.12	4.68	0.248	0.992	0.230	0.746
Width, mm	1.73	1.76	1.49	1.87	1.66	0.061	0.936	0.863	0.161
Perimeter, mm	11.16	12.47	9.71	10.70	11.55	0.505	0.937	0.237	0.928
Surface area[e], mm^2	12.95	15.06	9.69	13.07	13.65	0.886	0.882	0.248	0.682
Effective surface area[f], mm^2/cm^2	1069	1334	1022	793	1267	117.9	0.947	0.196	0.265

[a]Control calves (CON; n = 5) received 91.5% chopped hay and 8.5% vitamin/mineral supplement. Calves assigned to G3, G7, G14, and G21 (n = 5 for each moderate grain diet treatment) received a high energy diet consisting of 41.5% barley grain, 50% chopped hay, and 8.5% vitamin/mineral supplement for 3, 7, 14, or 21 days, respectively.

[b]SE = standard error.

[c]Contrast patterns, L = linear, Q = quadratic, C = cubic.

[d]Small papillae were classified as half or less than half of the size of the large papillae based on papillae dimensions for each individual tissue.

[e]Large papillae surface area is the surface area of one side of the papillae multiplied by 2.

[f]Effective surface area is the large papillae surface area multiplied by the number of mature papillae/cm^2.

0.230), width ($P \geq 0.161$), perimeter ($P \geq 0.237$), or 2-dimensional surface area ($P \geq 0.248$). To account for both large papillae surface area and the density of large papillae, we calculated the effective surface area (mm^2/cm^2) and found that it did not differ among treatments ($P \geq 0.196$). While we did observe changes in papillae density, the lack of an effect for effective surface area provides sufficient evidence to indicate that changes observed for $J_{MS\text{-}acetate}$, $J_{MS\text{-}butyrate}$, $J_{NET\text{-}Na}$, and $J_{SM\text{-}mannitol}$ were due to functional changes in the tissue rather than increases in surface area.

3.5.4. Na^+ Flux

The duration of time consuming the moderate grain diet tended to increase $J_{MS\text{-}Na}$ (quadratic, $P = 0.051$ and cubic, $P = 0.070$) from 1.84 for CON to 2.58 μEq/($cm^2 \times h$) for G21 with maximum Na^+ flux at 3.53 μEq/($cm^2 \times h$) for G7 (Table 3.7). The $J_{SM\text{-}Na}$ linearly increased from 0.69 for CON to 1.28 μEq/($cm^2 \times h$) for G21 ($P = 0.020$). Although there were increases for both $J_{MS\text{-}Na}$ and $J_{SM\text{-}Na}$, the $J_{NET\text{-}Na}$ increased (quadratic $P = 0.016$) from 1.15 for CON to 1.30 μEq/($cm^2 \times h$) for G21, with a peak flux at 2.59 μEq/($cm^2 \times h$) for G7. These results are supported by Estchmann et al. (2009) and show rapid increases in $J_{NET\text{-}Na}$ within 1 week of dietary change. The G_t for tissues assigned to the $J_{MS\text{-}Na}$ (quadratic $P = 0.002$) increased from 0.93 for CON to 1.39 mS/cm^2 for G21 with maximum G_t at 1.53 mS/cm^2 for G7, while G_t only tended (linear $P = 0.053$) to increase for tissues assigned $J_{SM\text{-}Na}$ from 0.84 for CON to 1.42 mS/cm^2 for G21. The I_{SC} for tissues assigned to $J_{SM\text{-}Na}$ increased (quadratic $P = 0.004$) from 0.04 for CON to 0.18 μEq/(h x cm^2) for G21 with minimum I_{SC} at -0.08 μEq/(h x cm^2) for G14, however, I_{SC} showed no change across diet treatments for $J_{MS\text{-}Na}$ ($P \geq 0.209$).

3.5.5. SCFA Flux

There was no interaction between SCFA concentration (Low vs. High) and diet (CON, G3, G7, G14, G21; $P > 0.05$) and thus the results presented below focus on the main effects of dietary treatment and the sub-plot effect of SCFA concentration independently.

Table 3.7. Effect of number of days fed moderate grain diet on the mucosal-to-serosal (J_{MS-Na}), serosal-to-mucosal (J_{SM-Na}), and net sodium (J_{NET-Na}) flux.

Item	Treatment[a]					SE[b]	Contrasts[c]		
	CON	G3	G7	G14	G21		L	Q	C
J_{MS-Na}[d]									
Flux, μEq/(cm^2 × h)	1.84	2.35	3.53	2.43	2.58	0.363	0.400	0.051	0.070
Gt[e], mS/cm^2	0.93	1.25	1.53	1.64	1.39	0.131	0.010	0.002	0.796
Isc[f], μEq/(cm^2 × h)	0.02	-0.03	-0.02	-0.04	0.01	0.036	0.968	0.209	0.954
J_{SM-Na}[g]									
Flux, μEq/(cm^2 × h)	0.69	0.84	0.94	0.98	1.28	0.160	0.020	0.895	0.490
Gt, mS/cm^2	0.84	1.27	1.44	1.40	1.42	0.177	0.053	0.100	0.254
Isc, μEq/(cm^2 × h)	0.04	-0.02	0.04	-0.08	0.18	0.044	0.051	0.004	0.056
J_{NET-Na}[h]									
Flux, μEq/(cm^2 × h)	1.15	1.51	2.59	1.45	1.30	0.292	0.734	0.016	0.059

[a]Control calves (CON; n = 5) received 91.5% chopped hay and 8.5% vitamin/mineral supplement. Calves assigned to G3, G7, G14, and G21 (n = 5 for each moderate grain diet treatment) received a high energy diet consisting of 41.5% barley grain, 50% chopped hay, and 8.5% vitamin/mineral supplement for 3, 7, 14, or 21 days, respectively.

[b]SE = standard error.

[c]Contrast patterns, L = linear, Q = quadratic, C = cubic.

[d]Mucosal to serosal sodium flux.

[e]Gt = tissue conductance.

[f]ISc = short circuit current.

[g]Serosal-to-mucosal sodium flux.

[h]J_{NET-Na} = net flux of sodium based on mucosal-serosal and serosal-mucosal fluxes; positive flux indicates net ruminal release from ruminal epithelium to blood.

Table 3.8. Effect of SCFA concentration on acetate and butyrate flux.

Item	Treatment [a]		SE[b]	*P* value
	Low	High		
Total[c]				
Acetate flux, μmol/(cm^2 × h)	0.72	1.54	0.050	< 0.001
Butyrate flux, μmol/(cm^2 × h)	0.91	2.04	0.067	<0.001
Bicarbonate-dependent[d]				
Acetate flux, μmol/(cm^2 × h)	0.39	0.68	0.062	0.002
Butyrate flux, μmol/(cm^2 × h)	0.36	0.71	0.104	0.021
Bicarbonate-independent nitrate-sensitive[e]				
Acetate flux, μmol/(cm^2 × h)	0.06	0.14	0.040	0.130
Butyrate flux, μmol/(cm^2 × h)	-0.07	-0.03	0.083	0.773
Bicarbonate-independent nitrate-insensitive[f]				
Acetate flux, μmol/(cm^2 × h)	0.27	0.72	0.033	<0.001
Butyrate flux, μmol/(cm^2 × h)	0.62	1.36	0.043	<0.001

[a]*Ex vivo* SCFA concentration treatments, Low =10 m*M* and High=50 m*M* ^{14}C-acetate and ^{3}H-butyrate solution. Equimolar concentrations of acetate and butyrate were administered (Low = 5 m*M* acetate and 5 m*M* butyrate and High = 25 m*M* acetate and 25 m*M* butyrate).

[b]SE = standard error.

[c]Total acetate and butyrate flux represents total flux of ^{3}H-acetate and ^{14}C-butyrate in the presence of bicarbonate.

[d]Bicarbonate-dependent acetate and butyrate flux represents flux of ^{3}H-acetate and ^{14}C-butyrate requiring bicarbonate, calculated as the difference between total and bicarbonate-independent flux.

[e]Bicarbonate-independent, nitrate sensitive acetate and butyrate flux represents flux of ^{3}H-acetate and ^{14}C-butyrate in the absence of bicarbonate, calculated as the difference between bicarbonate-independent and bicarbonate-independent, nitrate insenstive flux.

[f]Bicarbonate-independent, nitrate insensitive acetate and butyrate flux represents flux of ^{3}H-acetate and ^{14}C-butyrate in the absence of bicarbonate and presence of nitrate (passive diffusion).

3.5.5.1. Effect of Low and High SCFA Concentration *in vivo* on SCFA Flux

Total $J_{MS\text{-}acetate}$ and $J_{MS\text{-}butyrate}$ were greater when tissues were incubated in High (25 m*M* of each acetate and butyrate; $P < 0.001$; Table 3.8) compared to Low (5 m*M* of each acetate and butyrate) *ex vivo* acetate and butyrate concentrations (1.54 vs. 0.72 μEq/(cm^2 × h) for acetate and 2.04 vs. 0.91 μEq/(cm^2 × h) for butyrate, respectively).

We also evaluated whether the principal pathways for $J_{MS\text{-}acetate}$ and $J_{MS\text{-}butyrate}$ were affected by the concentration of acetate and butyrate, and found that the bicarbonate-dependent $J_{MS\text{-}acetate}$ [0.68 vs. 0.39 μEq/(cm^2 × h); $P = 0.002$] and $J_{MS\text{-}butyrate}$ [0.71 vs. 0.36 and μEq/(cm^2 × h); $P = 0.021$] were nearly twice as large (1.74 and 1.97 times increase for acetate and butyrate, respectively) for High relative to Low (Table 3.8). However, the bicarbonate-independent, nitrate sensitive pathway was not affected by *ex vivo* SCFA concentration for both $J_{MS\text{-}acetate}$ ($P = 0.130$) and $J_{MS\text{-}butyrate}$ ($P = 0.773$). The $J_{MS\text{-}acetate}$ and $J_{MS\text{-}butyrate}$ were measured in the absence of bicarbonate and presence of nitrate to determine the portion of $J_{MS\text{-}acetate}$ and $J_{MS\text{-}butyrate}$ occurring through passive diffusion. The $J_{MS\text{-}acetate}$ and $J_{MS\text{-}butyrate}$ were greater ($P < 0.001$) when buffers contained High compared to Low acetate and butyrate concentrations but the increase (2.7 and 2.2 times) was not as great as the increase in concentration of acetate and butyrate in the buffers (5 times).

3.5.5.2. Effect of the Duration Fed the Moderate Grain Diet on Acetate and Butyrate Flux

The total $J_{MS\text{-}acetate}$ increased (cubic $P = 0.045$; Table 3.9) from CON (1.07 μmol/(cm^2 × h)) to G7 (1.31 μmol/(cm^2 × h)) then decreased to G14 (1.02 μmol/(cm^2 × h)) and increased again to G21 (1.14 μmol/(cm^2 × h)). In contrast to acetate, total $J_{MS\text{-}butyrate}$ increased linearly with advancing days on the moderate grain diet (linear $P = 0.002$; Table 3.9). The bicarbonate-dependent $J_{MS\text{-}acetate}$ and $J_{MS\text{-}butyrate}$ were not affected by treatment ($P = 0.993$ and $P = 0.632$, respectively). Bicarbonate-independent nitrate-sensitive $J_{MS\text{-}acetate}$ and $J_{MS\text{-}butyrate}$ were also not affected by dietary treatment ($P = 0.222$ and $P = 0.215$, respectively), however, the bicarbonate-independent nitrate-insensitive $J_{MS\text{-}acetate}$ and $J_{MS\text{-}butyrate}$ increased (quadratic $P = 0.043$ and 0.005, respectively) with maximal values for $J_{MS\text{-}acetate}$ and $J_{MS\text{-}butyrate}$ occurring on G7 and G14, respectively.

3.5.6. Epithelial Barrier Function

A previous study had reported that sheep fed increasing amounts of concentrate increases the resistance or reduces the sensitivity of ruminal epithelial tissues to a hyper-osmotic challenge (Lodemann and Martens, 2006). However, rumen hyper-osmolality occurs in combination with decreasing pH and the effects of acidification and hyper-osmolality differentially affect epithelium barrier function (Penner et al., 2010). Thus, we tested whether the duration of time on the moderate grain diet influenced the $J_{SM\text{-}mannitol}$ and G_t and whether the susceptibility or responsiveness to a hyper-osmotic (450 mOsmol/kg) and acidic (pH 5.2) challenge was affected. We did not observe an interaction between dietary treatment and *ex vivo* period (BASE, CHAL, and REC) and thus will focus on the Ussing chamber period effects and the main effects of diet.

3.5.6.1. Characterization of the Response of the Ruminal Epithelia to a Hyper-omsotic and Acidic Challenge

During BASE, the $J_{SM\text{-}mannitol}$ was 0.48 μmol/(cm^2 × h) which increased to 1.44 μmol/(cm^2 × h) during CHAL and further increased to 1.89 μmol/(cm^2 × h) during REC (P < 0.001; Table 3.10). Similarly, G_t increased (P < 0.001) from 1.91 for BASE to 4.83 for CHAL and 7.35 mS/cm^2 during REC. From BASE to CHAL, I_{SC} increased from 0.01 to 0.30 µEq/(h × cm^2; P < 0.001), and decreased during REC indicating that ion transport was markedly reduced.

3.5.6.2. Increasing the Duration of Time Fed the Moderate Grain Diet Did Not Improve Barrier Function

Although a past study had reported improved barrier function for sheep fed greater amounts of dietary concentrate (Lodemann and Martens, 2006), we observed an increase for $J_{SM\text{-}mannitol}$ (linear P = 0.045) and G_t (linear P = 0.037) with increasing days fed the moderate grain diet. From CON to G21, $J_{SM\text{-}mannitol}$ increased from 1.00 to 1.67 μmol/(cm^2 × h; Table 3.11) and G_t increased from 3.06 to 6.44 mS/cm^2, respectively. Dietary treatment had no effect on I_{SC} ($P \geq$ 0.455). CHAL to REC. The $\Delta J_{SM\text{-}mannitol}$ from BASE to CHAL ($\Delta J_{SM\text{-}mannitol\text{-}BASE\text{-}CHAL}$) increased linearly ($P$ = 0.028; Table 3.12), however, $\Delta J_{SM\text{-}mannitol}$ from CHAL to REC ($P \geq 0.176$) or BASE to REC ($P \geq 0.102$) did not differ among treatments. The ΔG_t from BASE to CHAL ($\Delta G_{t\text{-}BASE\text{-}CHAL}$)

Table 3.9. Effect of number of days fed moderate grain diet on acetate and butyrate flux.

Item	Treatment[a]					SE[b]	Contrasts[c]		
	CON	G3	G7	G14	G21		L	Q	C
Total[d]									
Acetate flux, μmol/(cm^2 × h)	1.07	1.12	1.31	1.02	1.14	0.079	0.865	0.444	0.045
Butyrate flux, μmol/(cm^2 × h)	1.25	1.35	1.53	1.53	1.72	0.106	0.002	0.670	0.426
Bicarbonate-dependent[e]									
Acetate flux, μmol/(cm^2 × h)	0.61	0.47	0.60	0.48	0.52	0.099	0.579	0.729	0.993
Butyrate flux, μmol/(cm^2 × h)	0.57	0.47	0.38	0.55	0.70	0.164	0.383	0.305	0.632
Bicarbonate-independent nitrate-sensitive[f]									
Acetate flux, μmol/(cm^2 × h)	0.09	0.16	0.12	0.04	0.10	0.063	0.543	0.823	0.222
Butyrate flux, μmol/(cm^2 × h)	-0.06	0.04	0.06	-0.19	0.09	0.132	0.401	0.934	0.215
Bicarbonate-independent nitrate-insensitive[g]									
Acetate flux, μmol/(cm^2 × h)	0.37	0.49	0.59	0.51	0.52	0.053	0.133	0.043	0.115
Butyrate flux, μmol/(cm^2 × h)	0.74	0.84	1.09	1.17	1.12	0.068	<0.001	0.005	0.974

[a]Control calves (CON; n = 5) received 91.5% chopped hay and 8.5% vitamin/mineral supplement. Calves assigned to G3, G7, G14, and G21 (n = 5 for each moderate grain diet treatment) received a high energy diet consisting of 41.5% barley grain, 50% chopped hay, and 8.5% vitamin/mineral supplement for 3, 7, 14, or 21 days, respectively.

[b]SE = standard error.

[c]Contrast patterns, L = linear, Q = quadratic, C = cubic.

[d]Total acetate and butyrate flux represents total flux of ^{3}H-acetate and ^{14}C-butyrate in the presence of bicarbonate.

[e]Bicarbonate-dependent acetate and butyrate flux represents flux of ^{3}H-acetate and ^{14}C-butyrate requiring bicarbonate, calculated as the difference between total and bicarbonate-independent flux.

[f]Bicarbonate-independent nitrate-sensitive acetate and butyrate flux represents flux of ^{3}H-acetate and ^{14}C-butyrate in the absence of bicarbonate, calculated as the difference between bicarbonate-independent and bicarbonate-independent, nitrate insenstive flux.

[g]Bicarbonate-independent nitrate-insensitive acetate and butyrate flux represents flux of ^{3}H-acetate and ^{14}C-butyrate in the absence of bicarbonate and presence of nitrate (passive diffusion).

Table 3.10. Effect of *ex vivo* acidotic and hyperosmotic challenge on serosal to mucosal mannitol flux ($J_{SM\text{-}mannitol}$).

Item	Period[a]			SE[b]	*P* value
	BASE	CHAL	REC		
$J_{SM\text{-}mannitol}$[c], μmol/(cm^2 × h)	0.48^{z} [d]	1.44^{y}	1.89^{x}	0.102	<0.001
Gt[e], mS/cm^2	1.91^{z}	4.83^{y}	7.35^{x}	0.451	<0.001
Isc[f], μEq/(cm^2 × h)	0.01^{y}	0.30^{x}	-0.01^{y}	0.033	<0.001

[a]*Ex vivo* periods, BASE = initial flux period. CHAL = hyperosmostic and acidotic challenge by addition of 0.41 g mannitol and 200 μL gluconic acid on mucosal side. REC = mucosal buffer drained following challenge and replaced with fresh buffer. All periods were measured by the same 2 Ussing chambers.

[b]SE = standard error.

[c]Serosal to mucosal mannitol flux.

[d]Means with differing subscripts are different ($P < 0.05$).

[e]Gt = tissue conductance.

[f]Isc = short circuit current.

Table 3.11. Effect of number of days fed moderate grain diet on serosal to mucosal mannitol flux ($J_{SM\text{-}mannitol}$).

Item	Treatment[a]					SE[b]	Contrasts[c]		
	CON	G3	G7	G14	G21		L	Q	C
$J_{SM\text{-}mannitol}$[d], μmol/(cm^2 × h)	1.00	1.25	1.15	1.28	1.67	0.205	0.045	0.603	0.501
Gt[e], mS/cm^2	3.06	4.94	3.83	5.21	6.44	0.959	0.037	0.854	0.607
Isc[f], μEq/(cm^2 × h)	0.09	0.11	0.15	0.08	0.08	0.043	0.562	0.455	0.464

[a]Control calves (CON; n = 5) received 91.5% chopped hay and 8.5% vitamin/mineral supplement. Calves assigned to G3, G7, G14, and G21 (n = 5 for each moderate grain diet treatment) received a high energy diet consisting of 41.5% barley grain, 50% chopped hay, and 8.5% vitamin/mineral supplement for 3, 7, 14, or 21 days, respectively.

[b]SE = standard error.

[c]Contrast patterns, L = linear, Q = quadratic, C = cubic.

[d]Serosal to mucosal mannitol flux.

[c]Contrast patterns, L = linear, Q = quadratic, C = cubic.

[e]Gt = tissue conductance.

[f]Isc = short circuit current.

Table 3.12. Effect of number of days fed a moderate grain diet on change in tissue conductance (ΔG_t) of ruminal epithelia exposed to an acidotic and hyperosmotic challenge.

Item	Treatment[a]					SE[b]	Contrasts[c]		
	CON	G3	G7	G14	G21		L	Q	C
$\Delta G_{t\text{-BASE-CHAL}}$[d]	0.50	1.09	0.86	0.87	1.48	0.127	0.028	0.521	0.161
$\Delta G_{t\text{-CHAL-REC}}$[e]	0.67	0.28	0.51	0.56	0.22	0.083	0.328	0.752	0.176
$\Delta G_{t\text{-BASE-REC}}$[f]	1.17	1.37	1.37	1.42	1.70	0.113	0.102	0.675	0.732

[a]Control calves (CON; n = 5) received 91.5% chopped hay and 8.5% vitamin/mineral supplement. Calves assigned to G3, G7, G14, and G21 (n = 5 for each moderate grain diet treatment) received a high energy diet consisting of 41.5% barley grain, 50% chopped hay, and 8.5% vitamin/mineral supplement for 3, 7, 14, or 21 days, respectively.

[b]SE = standard error.

[c]Contrast patterns, L = linear, Q = quadratic, C = cubic.

[d]Change in tissue conductance 30 min after mucosal acidotic and hyperosmotic challenge minus change in tissue conductance before mucosal hyperosmotic and acidotic challenge.

[e]Change in tissue conductance 30 min after buffer exchange minus change in tissue conductance before buffer exchange.

[f]Change in tissue conductance 30 min after buffer exchange minus change in tissue conductance before mucosal hyperosmotic and acidotic challenge.

tended to increase linearly from CON to G21 ($P = 0.052$; Table 11). From CHAL to REC, ΔG_t increased linearly ($\Delta G_{t\text{-CHAL-REC}}$; $P = 0.013$) and from BASE to CHAL, as did ΔG_t for BASE to CHAL ($\Delta G_{t\text{-BASE-REC}}$; $P = 0.012$). These data suggest that increasing the duration of time fed the moderate grain diet did not improve resistance or reduce tissue sensitivity to an induced challenge *ex vivo*.

3.5.7. Gene Expression

Duration of time fed the moderate grain diet affected the expression of IL-1β, which increased (linear $P = 0.014$) from 1.00 for CON to 1.54 for G21 (Table 3.13) whereas mRNA expression for other inflammatory proteins IL-4, IL-8, IL-10, IL-13, and IL-22 were not affected ($P > 0.100$). Moreover, TNFα was not affected by the duration of time calves were fed the moderate grain diet ($P \geq 0.158$). Toll-like receptor 2 tended to increase (linear $P = 0.062$) from 1.00 for CON to 3.66 for G21, while TLR-4 was not affected ($P \geq 0.406$).

The fold change of IGFBP5 decreased (cubic $P = 0.010$) from 1.00 for CON to 0.36 for G21, while IGFBP3 was not affected by diet treatment ($P \geq 0.120$). The Na^+/H^+ exchangers, NHE1 and NHE3, both tended to decrease in expression with increased duration consuming the moderate grain diet (quadratic $P = 0.058$ and cubic $P = 0.061$, respectively) which is not supported by the increases in $J_{NET\text{-}Na}$ that were observed. Comparatively, G-coupled protein receptors, GPR41 and GPR43, tended to increase expression from CON to G21 (cubic $P = 0.096$ and linear $P = 0.054$, respectively) while genes involved in energy metabolism and SCFA transport, namely ACAT and MCT1, were not affected by treatment ($P \geq 0.260$ and $P \geq 0.369$, respectively).

3.6. Discussion

The ruminal epithelium adapts to dietary change in two manners: through changes in individual cell activity (functional adaptation; Etschmann et al., 2009; Penner et al., 2011) and alterations in ruminal epithelial surface area through hyperplasia and hypertrophy (Dirksen et al., 1985; Bannink et al., 2008). It is currently suggested that functional adaptation precedes morphological adaptation (Etschmann et al., 2009); however, few studies evaluated functional adaptation and the underlying mechanisms are largely unknown. For example, while Etschmann

Table 3.13. Effect of number of days fed moderate grain diet on expression of target genes related to rumen adaptation.

Target gene expression[*]	Treatment[†]					SE[‡]	Contrasts[§]		
	CON	G3	G7	G14	G21		L	Q	C
TNFα	1.00	1.44	0.72	0.84	1.54	0.138	0.514	0.158	0.368
IL-1β	1.00	2.38	1.16	1.62	3.29	0.248	0.014	0.149	0.115
IL-4	1.00	1.00	0.80	0.95	1.30	0.173	0.601	0.528	0.965
IL-8	1.00	3.30	1.21	1.43	2.96	0.363	0.402	0.470	0.135
IL-10	1.00	1.07	0.61	0.91	1.56	0.142	0.255	0.137	0.866
IL-13	1.00	1.70	1.38	0.72	1.40	0.259	0.891	0.838	0.264
IL-22	1.00	0.79	0.64	2.16	1.47	0.343	0.327	0.837	0.273
TLR2	1.00	2.80	2.47	2.99	3.66	0.379	0.062	0.603	0.408
TLR4	1.00	1.37	1.28	1.43	1.37	0.109	0.406	0.515	0.768
ACAT	1.00	0.52	0.83	0.68	1.12	0.113	0.512	0.260	0.897
MCT1	1.00	0.83	0.89	0.94	1.28	0.100	0.369	0.392	0.966
IGFBP3	1.00	0.96	1.00	1.40	0.89	0.099	0.772	0.197	0.120
IGFBP5	1.00	0.47	0.48	0.70	0.36	0.082	0.049	0.450	0.010
NHE1	1.00	0.59	0.49	0.65	0.74	0.081	0.600	0.058	0.171
NHE3	1.00	0.51	0.53	0.65	0.53	0.070	0.166	0.191	0.061
GPR41	1.00	2.00	1.78	0.81	1.94	0.266	0.797	0.815	0.096
GPR43	1.00	1.87	3.45	3.46	4.38	0.550	0.054	0.536	0.636

[*]Gene expression expressed as fold change.

[†]Control calves (CON; n = 5) received 91.5% chopped hay and 8.5% vitamin/mineral supplement. Calves assigned to G3, G7, G14, and G21 (n = 5 for each moderate grain diet treatment) received a high energy diet consisting of 41.5% barley grain, 50% chopped hay, and 8.5% vitamin/mineral supplement for 3, 7, 14, or 21 days, respectively.

[‡]SE = standard error.

[§]Contrasts, L = linear, Q = quadratic, C = cubic.

et al. (2009) reported a rapid and marked increase in $J_{NET\text{-}Na}$ within 1 week of dietary change, they did not measure epithelial surface area and papillae density and therefore cannot confirm whether morphological adaptation occurred. In the current study, functional activity of the ruminal epithelium was determined by measuring SCFA, Na^+, and mannitol transport rates and expression of mRNA encoding for proteins involved in dietary adaptation and inflammatory responses. As well, the extent to which individual SCFA transport pathways were utilized was quantified. Furthermore, morphological measurements of epithelial surface area were quantified to verify whether the responses observed may be attributable to the absorptive surface area or whether they were truly an indication of functional adaptation.

3.6.1. The Rate of Adaptation was Rapid and Independent of Morphological Changes

Following dietary shift from the high forage to moderate grain diet, reticular pH decreased in a quadratic manner with an initial reduction followed by a gradual increase in pH with advancing days on feed. Similarly, Steele et al. (2011) reported an initial reduction in ruminal pH followed by a gradual increase when dairy cattle were abruptly transitioned to a more fermentable diet. Given that SCFA absorption is strongly related to ruminal pH (Penner et al., 2009a), it could be expected that the marked increase in $J_{MS\text{-}acetate}$ and $J_{MS\text{-}butyrate}$ on G7 helped to stabilize pH. However, it is also possible that the microbial communities were adapting to the change in substrate supply and may account for a portion of the response.

Despite changes in reticular pH with advancing days on the moderate grain diet, we did not observe differences for total SCFA concentration. While this is unexpected, it is likely an artefact of the timing of sampling. Based on reticular pH curves, it appears that fermentation was maximized between 3 and 7 h post-feeding. However, in our study, calves were killed 2 h post-feeding and rumen fluid was collected at that time. Thus, it is likely that our sampling time point occurred prior to maximal ruminal fermentation and thus diminished the ability to detect treatment differences for SCFA concentration. That said, changes in the molar proportion of individual SCFA were evident. As could be expected, when feeding diets containing a greater proportion of starch, we observed a reduction in the molar proportion of acetate (Sutton et al., 2003; Penner et al., 2009b), and correspondingly an increase in butyrate. These data confirm that an abrupt dietary change and adaptation to that diet involves shifts in rumen fermentation; a critical aspect of our model to evaluate functional adaptation.

Maximal ruminal epithelial surface area has been shown to occur 4 to 6 weeks after an increase in dietary fermentability for dairy cattle (Dirksen et al., 1985; Bannink et al., 2008) and goats (Shen et al., 2004; Wang et al., 2009a). The short timeframe imposed in the current study (maximum of 3 weeks) allowed for evaluation of functional adaptation. We provided further evidence that functional adaptation of the ruminal epithelium occurs with a lack of differences among treatments for papillae surface area and the effective surface area. It is acknowledged that the density of large papillae increased, although this had no effect on total absorptive surface area. Thus, we interpret these findings to indicate that changes in the flux of Na^+, SCFA, and mannitol were due to functional changes rather than changes influenced by surface area enlargement.

Supporting the results obtained by Etschmann et al. (2009), we observed a rapid and marked increase in $J_{Net\text{-}Na}$ with a 31% increase within 3 d and a 125% increase within 7 d. These values are comparable to the 73% increase in $J_{NET\text{-}Na}$ reported by Etschmann et al. (2009) within 1 week of dietary change. Interestingly, $J_{NET\text{-}Na}$ decreased from G7 to G21 due to a reduction in $J_{MS\text{-}Na}$ and an increase in $J_{SM\text{-}Na}$. The reasons for the reduction after G7 are not clear especially considering that the relative expression of mRNA for NHE1 and NHE3 tended to increase during this timeframe. A discrepancy between the expression of NHE1 and NHE3 and $J_{NET\text{-}Na}$ was also evident between CON and G7 as we observed a reduction for mRNA expression while $J_{NET\text{-}Na}$ increased. The latter results differ from previous studies showing that exposure to concentrate increased the expression of NHE1 and NHE3 by 20 and 25%, respectively compared to goats not offered concentrate (Yang et al., 2012). However, no studies known to the authors have measured both functional activity and expression of NHE1 or NHE3 in the same rumen tissue suggesting that the increase in mRNA abundance for NHE1 and NHE3 may not correlate well to functional characteristics. Others have also reported no effect of diet on the abundance of NHE1 (Penner et al., 2009b; Schlau et al., 2012) and NHE3 (Penner et al., 2009b). In addition, mRNA expression is affected by changes in fermentation intensity with lower expression for goats killed 16 h after feeding relative to those killed 2 h post-feeding (Yang et al., 2012). Thus, an alternative explanation for the lack of correlation between $J_{NET\text{-}Na}$ and mRNA abundance for NHE1 and NHE3 could be that our sampling time point occurred prior to maximal mRNA abundance despite observed increases in $J_{NET\text{-}Na}$ with advancing days on the moderate grain diet. Others have also reported that NHE1 expression was not affected by diet fermentability even

when SCFA transport rates were affected (Penner et al., 2009b). A recent study (Amith and Fliegel, 2013) discusses phosphorylation as a regulatory mechanism of NHE1. Much of the NHE1 regulation occurs on its cytosolic domain, where several protein kinases have shown to phosphorylate specific amino acid sites and thereby activate (ex. Protein kinase p160ROCK) or inhibit (ex. Protein kinase B) NHE1 activity (Amith and Fliegel, 2013). Collectively, these results highlight the challenge of relying on mRNA abundance as an indicator of cellular or tissue functional activity.

Sodium transport across the ruminal epithelium is well characterized (Gäbel et al., 1989, 1991; Sehested et al., 1999; Etschmann et al., 2009; Shen et al., 2012) and is driven by the Na^+/K^+-ATPase located on the basolateral membrane (Graham and Simmons, 2005). Several factors influence Na^+ transport including luminal osmolality (Schwiegel et al., 2005), SCFA concentration (Sehested et al., 1999), and more recently it has been demonstrated that IGF-1 acutely stimulates Na^+ transport (Shen et al., 2012). However, in the current study mRNA abundance of IGFBP5 was down regulated and IGFBP3 was not affected with increasing days fed the grain diet. While these receptors influence epithelial growth (Firth and Baxter, 2002; Shen et al., 2004), IGF-1 also acutely stimulates Na^+ absorption in the rumen (Shen et al., 2012). This opposes results previously showing up-regulation of IGFBP5 within 1 week of abrupt grain adaptation in mature non-lactating dairy cows (Steele et al., 2011) and as early as 4 d after inducing a grain challenge in second lactation lactating dairy cows (Steele et al., 2012). Sehested et al. (1999b) reported a positive correlation between $J_{NET\text{-}butyrate}$ and $J_{NET\text{-}Na}$. The indirect coupling between $J_{NET\text{-}butyrate}$ and $J_{NET\text{-}Na}$ can be attributed to the requirement for removal of H^+ from the cytosol to prevent intracellular acidification with passive diffusion of SCFA (Gäbel et al., 1991b; Aschenbach et al., 2011) and perhaps a stimulatory effect of butyrate metabolism on cell ATP status thereby increasing Na^+/K^+-ATPase activity. Indeed, in addition to the increase for $J_{NET\text{-}Na}$, we observed increases for both $J_{MS\text{-}acetate}$ and $J_{MS\text{-}butyrate}$. We interpret this finding to indicate that SCFA flux serves as the driving factor promoting $J_{NET\text{-}Na}$ by 1) providing a fuel source for generation of ATP, 2) by promoting Na^+ absorption in order to regulate intracellular pH, or a combination of both. While the above speculation is supported by the increase in the bicarbonate-independent nitrate-insensitive $J_{MS\text{-}acetate}$ and $J_{MS\text{-}butyrate}$ flux with advancing days on the moderate grain diet, the lack of differences for the abundance of mRNA encoding for ACAT and MCT1 are not supportive of the above speculation. However, several other studies have also

reported no differences for ACAT and MCT1 with large differences in dietary fermentability (Steele et al., 2012; Malhi et al., 2013), despite ACAT and MCT1 being potential regulators of ketogenesis and basolateral export, respectively.

Known mechanisms for SCFA uptake by the ruminal epithelium include bicarbonate-SCFA anion exchange, passive diffusion, and a bicarbonate-independent nitrate-sensitive pathway (Sehested et al., 1999; Aschenbach et al., 2009; Aschenbach et al., 2011). Basolateral extrusion mechanisms for SCFA into portal circulation include bicarbonate-SCFA anion exchange (Aschenbach et al., 2011), a SCFA-permeable conductance channel (Stumpff et al., 2009), and co-transport with H^+ via MCT1 (Müller et al., 2002; Graham et al., 2007; Aschenbach et al., 2011). In the present study, we evaluated the $J_{MS\text{-}acetate}$ and $J_{MS\text{-}butyrate}$ and partitioned that flux into bicarbonate-dependent, bicarbonate-independent nitrate-sensitive, and bicarbonate-dependent nitrate-insensitive to represent the uninhibited flux, bicarbonate dependent flux, bicarbonate-independent nitrate-sensitive flux, and passive diffusion as described by Aschenbach et al. (2009). For the first time, we have shown that of the mechanisms involved in $J_{MS\text{-}acetate}$ and $J_{MS\text{-}butyrate}$, passive diffusion was the primary mechanism influencing the increase in flux with advancing days on feed.

Corresponding to increased $J_{MS\text{-}acetate}$ and $J_{MS\text{-}butyrate}$ as the duration of time consuming grain increased, there was a tendency for an increase in the mRNA for GPR43 and a tendency for increased expression of GPR41. The potency of acetate, propionate, and butyrate are equivalent as agonists for GPR41 and GPR43 (Brown et al., 2003), therefore the increase in ruminal butyrate with advancing days fed the moderate grain diet may have been sufficient to initiate the increase in expression of these receptors. Furthermore, GPR41 and GPR43 may play a role in mediating rumen epithelial growth by regulating SCFA absorption via cAMP (Gäbel et al., 1999; Wang et al., 2012). Recently, GPR43 up-regulation occurred in bovine neutrophils treated with propionate (Carretta et al., 2013), suggesting propionate is a strong stimulant of immune response in bovine tissue, supporting previous proposals (Wang et al., 2009b). Although propionate was not affected based on the sampling time period following feeding in the current study, propionate concentration in the rumen may have differed at peak fermentation, causing up-regulation of GPR41 and GPR43 in the ruminal epithelium.

Barrier function decreased with increasing duration consuming the grain diet, as illustrated by increases in G_t and mannitol flux. It has been widely observed that diets high in fermentable carbohydrate challenge barrier function of the ruminal epithelium (Penner et al., 2011; Steele et al., 2011; Liu et al., 2013). Rapid ruminal carbohydrate fermentation and subsequent increases in SCFA concentration cause tight junction proteins and gap junctions in the ruminal epithelium to break down, leading to increased permeability (Liu et al., 2013). Activation of GPR41 and GPR43 via increased ruminal SCFA concentration may have promoted an inflammatory response (Oh and Lagakos, 2011) and subsequent increase in epithelial permeability. However, results from the current study differ from previous work where under normal physiological osmostic conditions, ruminal epithelium from concentrate-supplemented sheep showed no change in G_t, whereas ruminal tissue from forage-fed sheep displayed increases in G_t (Lodemann and Martens 2006; Etschmann et al., 2009).

Following the *ex vivo* mucosal hyperosmotic and acidotic challenge, barrier function was reduced, again shown by increases in G_t and mannitol flux. The reduction in barrier function is in agreement with earlier Ussing chamber studies where hyperosmotic and acidotic challenges were imposed on rumen epithelia (Schweigel et al., 2005; Lodemann and Martens 2006; Penner et al., 2010; Wilson et al., 2012). Furthermore, when mucosal solution was drained and replaced with buffer solution simulating normal physiological conditions, G_t and mannitol flux were not reversible. Previous findings have also shown a lack of recovery of G_t following an *ex vivo* acidotic challenge (Penner et al., 2010; Wilson et al., 2012). Other studies suggest the increase in G_t under high osmotic pressure *ex vivo* returns to baseline values after physiological mucosal osmotic pressure is re-imposed (Schweigel et al., 2005; Lodemann and Martens 2006; Penner et al., 2010). In the latter two studies, an acidotic challenge was either not carried out and thus pH of both the control and hyperosmotic mucosal buffer solutions were 7.3-7.5 (Lodemann and Martens 2006), or the acidotic challenge was performed separately from the osmotic challenge (Penner et al., 2010). The simultaneous acidotic and hyperosmotic challenge in the current study may have caused non-reversible damage to the epithelia. Or perhaps the mucosal pH conditions used in our study may have been too low to promote reversibility of barrier function. More time may also be necessary to measure a return to baseline values under such pH and hyperosmotic conditions. Furthermore, in the current study, tissue was collected two hours following feeding; however, this timeframe was not discussed in previous literature (Schweigel et al., 2005;

Lodemann and Martens 2006). Ruminal osmotic pressure *in vivo* can change drastically, from < 250 before feeding to > 400 mOsmol/kg after feeding, but the degree of change in osmotic pressure is variable depending on rate of feed consumption and water intake (Warner and Stacey 1968). Although these variables were not measured in the current study, ruminal osmotic conditions prior to tissue collection may have affected *ex vivo* tissue response to hyperosmotic and acidotic challenges.

Supporting the reduction in barrier function with advancing days on the moderate grain diet, IL-1β, a pro-inflammatory cytokine (Dinarello, 1996), showed greater expression with increasing days fed the moderate grain diet. Although there is a paucity of information on the expression of IL-1β during dietary adaptation in ruminants, IL-1β has been shown to increase the permeability of intestinal tight junctions of Caco-2 cells (Al-Sadi and Ma, 2007). If IL-1β acts similarly in the ruminal epithelium, it may play a role in reducing barrier function. Inducers of IL-1 expression in the gut include hyperosmolarity, T and B cells, and other interleukin proteins (Dinarello, 1996); indicating that these factors may have played a role in IL-1β up-regulation in calves fed grain for a longer duration. Additionally, TLR2, responsible for recognizing bacterial by-products and initiating an innate immune response (Abreu 2010), tended to increase with duration fed the grain diet. Recently, mRNA for TLR2 and TLR4 were expressed higher in acidosis-resistant relative to acidosis-susceptible steers, suggesting that acidosis-resistant steers may have more mild inflammation or greater immunity (Chen et al., 2012). In the current study TLR2 was more highly expressed as duration consuming the grain diet increased. Therefore, reduced barrier function may be present, but higher expression of TLR2 could indicate elevated immune response activation for calves consuming grain for a longer duration.

In the current study, calves fed the grain diet for 14 days posed numerous interesting results, indicating that substantial changes occur in the ruminal epithelium 2 weeks following change in diet fermentability. Briefly, G14 illustrated the highest proportion of small papillae, suggesting surface area proliferation of the ruminal epithelium. Calves consuming the grain diet for 14 days also posed a drop in $J_{MS\text{-}Na}$, resulting in a large decrease in $J_{NET\text{-}Na}$. Furthermore, reduced total $J_{MS\text{-}acetate}$ was exhibited by G14 and a significant reduction in bicarbonate-independent $J_{MS\text{-}acetate}$ and $J_{MS\text{-}butyrate}$ occurred after G7. The flux of SCFA has been shown to drive Na^+ transport (Lodemann and Martens 2006), which may explain the simultaneous

decrease in both SCFA and Na^+ transport across the ruminal epithelium after 14 d of grain feeding, however, the lack of up-regulation of Na^+/H^+ exchangers does not support this explanation. The decrease in bicarbonate-independent $J_{MS\text{-}acetate}$ and $J_{MS\text{-}butyrate}$ transport following G7 may indicate increased use of protein-mediated transport. Additionally, G14 represented a reduction in GPR41 expression, which may be indicative of reduced SCFA flux. Contrastingly, G14 showed a drastic increase in IGFBP5 expression, which may be indicative of cell proliferation. Cumulatively, reduced epithelial capacity for SCFA and Na^+ flux at G14 suggest that functional activity of individual cells may be partially inhibited despite increases in transport ability shortly after diet change.

3.7. Conclusion

In summary, $J_{MS\text{-}acetate}$, $J_{MS\text{-}butyrate}$, and $J_{NET\text{-}Na}$ across the ruminal epithelium increased after dietary transition to a moderately fermentable diet. These increases in epithelial activity were shown independent of surface area proliferation, indicating that functional adaptation occurs prior to morphological adaptation. However, barrier function of the ruminal epithelium was reduced by the moderate grain diet as indicated by increased $J_{SM\text{-}mannitol}$, tissue conductance, as well as up-regulation of inflammatory response proteins. In the future, a greater understanding of the reliance on individual flux pathways, the relationship between functional adaptation and surface area proliferation, and expression of regulatory genes initiating changes in cell activity within the ruminal epithelium will enhance knowledge of dietary adaptation and improve feeding management in ruminant production systems.

4.0. GENERAL DISCUSSION

4.1. Relevance to Ruminant Production

Ruminant research over the past couple of decades has put increased focus on the relationship between ruminant health and nutrition. These two aspects of ruminant production are closely related, indicating that one may largely affect the other during various points of the ruminant production cycle. As previously discussed, diets high in fermentable carbohydrates are commonly fed to cattle in backgrounding and finishing feedlots to promote rapid body growth or in dairy cattle to support high milk production (Lesmeister and Heinrichs, 2004; Bevans et al., 2005; Penner et al., 2007). However, carbohydrate-rich diets may increase the risk for ruminal acidosis, a digestive problem that may compromise both animal health and performance (Plaizier et al., 2009; Lechartier and Peyraud, 2010). Feeding regimes on intensive cattle operations must therefore sustain animal health and promote optimal performance. However, to achieve these goals, feeding cattle on on-farm requires an understanding of the basic mechanisms underlying ruminant physiology and nutrition.

As discussed in earlier chapters, results in this thesis offer novel discoveries in regards to rumen adaptation in addition to results that confirm that previous work performed using other ruminant species are also applicable to cattle. As previously described, the current study models scenarios in ruminant production where cattle are transitioned from a high forage to moderately fermentable (50% concentrate) diet, with the aim of applying this basic research to improve our understanding of dietary management and rumen epithelial function.

Based on the morphological results alone from the current research, it may be beneficial to more rapidly adapt cattle to a moderately fermentable diet in order to promote quicker rumen epithelial surface area proliferation and therefore increased rumen absorptive capacity, as there was no change in papillae density and dimensions, and effective surface area within 21 days following diet change. However, changes in the activity of the epithelium on a cellular (i.e. functional) level during dietary adaptation clearly responds more rapidly relative to morphological adaptation. The net absorption of Na^+ and the mucosal to serosal flux of acetate and butyrate across the ruminal epithelium increased by 2.25, 1.22, and 1.22 times, respectively; within the first week following dietary transition from the high forage to moderate grain diet.

These results indicate that functional adaptation occurs prior to and in the absence of morphological adaptation, and that the ruminal epithelium has a substantial ability to account for increases in diet fermentability through increased absorption. Furthermore, lipophilic diffusion of acetate and butyrate across the epithelium from the mucosal to serosal side increased 71 and 66%, respectively, from CON to G21; relative to the transport of SCFA via protein-mediated transport which did not show a significant change. Comparatively, previous studies have measured SCFA absorption pathways in sheep and showed that transport proteins are a primary mechanism of acetate absorption (Aschenbach et al., 2009; Penner et al., 2009) and bicarbonate-independent transport was the main absorption pathway for butyrate (Penner et al., 2009). Section 3.0. describes the first study to determine SCFA absorption pathways in cattle, and that increases in total acetate and butyrate absorption was primarily due to passive diffusion. This may be a short-term mechanism to cope with increased ruminal SCFA concentration prior to longer-term increased protein-mediated pathway up-regulation and epithelial surface area proliferation. Based on these absorption results, perhaps cattle in the appropriate scenario can be transitioned to a diet containing greater than 50% concentrate. For example, if a dairy producer is aware of a high producing cow in the herd, this cow may be fed a diet containing 55-60% concentrate upon lactation. For large dairy operations, several high producing dairy cows that calve close together may be grouped separately from the rest of the herd and fed this higher energy transition period ration.

However, the current study also showed a reduction in barrier function with increasing time consuming the moderate grain diet, as indicated by the linear increase in epithelial permeability to mannitol and the increase in tissue conductance. Furthermore, the elevated quantity of IL-1β and TLR2 (3.11 and 3.56 x increase from CON to G21, respectively) mRNA indicate that an inflammatory response may have been initiated and that bacterial by-products (i.e. histamine and LPS; Aschenbach and Gäbel, 2000; Emmanuel et al., 2007) may have been present on the surface of the epithelium (Dinarello, 1996; Abreu, 2010). Reduced barrier function following a rapid change in diet fermentability indicates an increase in tissue permeability. The rumen is rich in antigenic factors such as bacteria (Tan et al., 1994; Nagaraja et al., 2005; Metzler-Zebeli et al., 2013), bacterial endotoxins (Nagaraja et al., 1978; Nagaraja and Titgemeyer 2007), and amines (Nocek, 1997; Nagaraja and Titgemeyer 2007), which, when barrier function is compromised, have an elevated risk of passage into portal circulation

(Aschenbach and Gäbel, 2000; Takayama et al., 2000; Emmanuel et al., 2007; Klevenhusen et al., 2013). Antigenic compounds such as histamine may also directly compromise barrier function (Aschenbach et al., 1998). In terms of practical production, reduced barrier function may put the ruminant at risk of laminitis from elevated blood histamine and LPS levels or liver abscesses from translocation of bacteria such as Fusobacterium necrophorum and Arcanobacterium pyogenes from the rumen to the blood (Nocek, 1997; Plaizier et al., 2009), and ultimately, reduced health and performance. Furthermore, although there was a reduction in barrier function with increasing duration fed the moderate grain diet, absorption was not affected and ruminal acidosis was not induced. Therefore, moderate increases in diet fermentability, such as that in the current study, support current feeding recommendations for ruminants transitioning to a higher production expectation (i.e. transitioning dairy cattle and beef cattle entering a backgrounding feedlot).

As discussed earlier, the ruminal epithelium is a selectively permeable membrane that performs two essential roles: 1. the absorption of nutrients from the ruminal lumen into the bloodstream and, oppositely, from the blood to the lumen (Gäbel et al., 2002; Aschenbach et al., 2009), and 2. prevention of the transfer of harmful compounds from the lumen to the blood (Aschenbach and Gäbel, 2000; Plaizier et al., 2012). Collectively, results shown in this thesis indicate that although the ruminal epithelium may initiate a rapid increase in absorptive capacity for Na^+ and SCFA following an abrupt increase in diet fermentability, barrier function (i.e. permeability) of the epithelium is compromised for at least 21 days following diet change. This indicates that the two roles of the ruminal epithelium, absorption and barrier function, follow different timelines, which poses a challenge when adapting cattle to moderately to highly fermentable rations.

4.1.1. Dietary Adaptation during Stressful Production Time Points

With the above conclusions in mind, it is important to consider that diet change is often associated with stressful time points in the production cycle of cattle when the immune system is already challenged. Additional stress, such as those associated with the diet, must therefore be minimized during critical periods in order to maintain health and maximize production. For example, the prevention of reduced ruminal pH through proper feeding management may help avoid early lactation dairy cattle from going off feed, and thus prevent common transition-related

problems such as ketosis, an accumulation of ketones (i.e. BHBA) in the blood due to rapid fat mobilization (Goff, 2006; McArt et al., 2011), and displaced abomasum (Shaver, 1997; Cameron et al., 1998; LeBlanc et al., 2005). Such diseases during the transition period reduce lactation milk yield (Rajala-Schultz et al., 1999), decrease conception rates (Walsh et al., 2007), and increase involuntary culling (Gröhn et al., 1998), which contribute to reduced farm profitability. Also, the prevention of ruminal acidosis in backgrounding and finishing feedlot cattle helps to avoid repetition of rumen acidosis, which may occur when cattle drastically reduce feed intake due to ruminal acidosis and subsequently consume a large quantity of highly fermentable feed, followed by another period of reduced feed intake (Schwartzkopf-Genswein et al., 2003; Plaizier et al., 2012). When repetitive ruminal acidosis is prevented, feed consumption and efficiency may increase. Furthermore, as discussed above, the passage of bacteria and other toxic substances (i.e. histamine and endotoxins such as LPS) into the blood across tissue with an elevated permeability due to acidic ruminal conditions may result in laminitis (Nocek, 1997; Garner et al., 2002; Plaizier et al., 2009) and liver abscesses (Tan et al., 1994; Nagaraja and Chengappa, 1998; Nagaraja et al., 2005; Plaizier et al., 2009) in cattle on intensive dairy and beef operations. Therefore, by understanding basic mechanisms of ruminant nutrition, metabolism, and physiology, and their interactions, cattle on commercial operations can be fed in a manner that imposes minimal immune and health stress while simultaneously maintaining a high level of performance during critical periods of production.

4.2. Future Research Directions

Although results from the research provided within this thesis offer insight to understanding the timeline and roles of functional and morphological adaptation in ruminants, future work is still necessary to explain several gaps in the literature and questions that have unfolded from the current study. Future research is needed to explain the reasons and mechanisms occurring between 7 and 14 d following diet transition that cause a decrease in absorptive capacity relative to the substantial increase during the first week. Furthermore, the regulation and use of protein-mediated SCFA absorption warrants further understanding to explain the heavy reliance of SCFA absorption on passive diffusion in the current study. Further investigation on the expression and regulation of sodium-hydrogen exchange proteins, NHE1 and NHE3, is also necessary, as the tendency for the reduction in expression with increasing time

spent consuming the moderate grain diet in this study is not in agreement with results from previously published research. Work is also needed to further describe the mechanisms and timeline underlying surface area proliferation in a variety of dietary scenarios. A better understanding of these mechanisms may reduce the time gap between functional and morphological adaptation, and subsequently reduce the diet adaptation period required on-farm, for example, adapting cattle to a finishing feedlot ration over a shorter time period. Moreover, by repetition of the current study, it would be interesting to evaluate the same variables but 1. decrease the diet fermentability (< 50% concentrate) to determine at what level of concentrate inclusion would the reduction in barrier function have been prevented, and 2. increase the diet fermentability (> 50% concentrate) to establish a limit to concentrate level inclusion, which together may establish a minimum and maximum diet fermentability which can be applied in ration formulation.

5.0. CONCLUSIONS

This thesis has indicated that a moderate and abrupt increase in diet fermentability increases rumen epithelial absorptive capacity in the absence of an increase for epithelial surface area. The increase in absorption of SCFA and Na^+ occurs within 1 week following diet change. However, despite the rapid increase in nutrient absorption, barrier function of the rumen epithelium was reduced for at least 3 weeks after diet change. Results in this thesis therefore suggest that ration formulation during critical points in the production cycle of dairy and beef cattle, namely; the transition period, weaning, time of entrance into a backgrounding feedlot, and adaptation to a finishing feedlot ration, requires moderate increases in diet fermentability. As a result, rumen epithelial absorptive and barrier functions will be optimized and ruminant health and production will be maximized.

6.0. LITERATURE CITED

Abdoun K, Stumpff F, Rabbani I, Martens H. Modulation of urea transport across sheep rumen epithelium in vitro by SCFA and CO_2. *Am J Physiol Gastrointest Liver Physiol* 298: G190-G202, 2010.

Abreu MT. Toll-like receptor signalling in the intestinal epithelium: how bacterial recognition shapes intestinal function. *Nat Rev Immunol* 10: 131–144, 2010.

Alberta Government. Nutrition and management: Feeding lightweight calves. Retrieved on July 16, 2013 from http://www1.agric.gov.ab.ca/$department/deptdocs.nsf/all/beef11684, 2012.

Albornoz RI, Aschenbach JR, Barreda DR, Penner GB. Feed restriction reduces short-chain fatty acid absorption across the reticulo-rumen of beef cattle independent of diet. *J Anim Sci* 91: 4730-4738, 2013.

Albornoz RI, Aschenbach JR, Barreda DR, Penner GB. Moderate decreases in the forage-to-concentrate ratio before feed restriction and increases thereafter independently improve the recovery from a feed restriction insult in beef cattle. *J Anim Sci* 91: 4739-4749, 2013b.

Allen MS. Relationship between fermentation acid production in the rumen and the requirement for physically effective fiber. *J Dairy Sci* 80: 1447–1462, 1997.

Al-Sadi R, Khatib K, Guo S, Ye D, Youssef M, Ma T. Occluden regulates macromolecule flux across the intestinal epithelial tight junction barrier. *Am J Physiol Gastrointest Liver Physiol* 300: G1054-G1064, 2011.

Al-Sadi RM, Ma TY. I-1β causes an increase in intestinal epithelial tight junction permeability. *J Immunol* 178: 4641-4649, 2007.

Amith SR, Fliegel L. Regulation of the Na^+/H^+ exchanger (NHE1) in breast cancer metastasis. *Cancer Res* 73: 1259-1264, 2013.

Anderson WG, Nawata CM, Wood CM, Piercey-Normore MD, Weihrauch D. Body fluid osmolytes and urea and ammonia flux in the colon of two chondrichthyan fishes, the ratfish, Hydrolagus colliei, and spiny dogfish, Squalus acanthias. *Comp Biochem Physiol* 161: 27–35, 2012.

Aschenbach JR, Bilk S, Tadesse G, Stumpff F, Gäbel G. Bicarbonate-dependent and bicarbonate-independent mechanisms contribute to nondiffusive uptake of acetate in the ruminal epithelium of sheep. *Am J Physiol Gastrointest Liver Physiol* 296: G1098-G1107, 2009.

Aschenbach JR, Fürll B, Gäbel G. Histamine affects growth of sheep ruminal epithelial cells kept in primary culture. *Zentralbl Veterinarmed A* 45: 411-416, 1998.

Aschenbach JR, Gäbel, G. Effect and absorption of histamine in sheep rumen: significance of acidotic epithelial damage. *J Anim Sci* 78: 464-470, 2000.

Aschenbach JR, Penner GB, Stumpff F, Gäbel, G. RUMINANT NUTRITION SYMPOSIUM: Role of fermentation acid absorption in the regulation of ruminal pH. *J Anim Sci* 89: 1092-1107, 2011.

Ash R, Baird GD. Activation of volatile fatty acids inbovine liver and rumen epithelium. *Biochem* 136: 311–319, 1973.

Awad WA, Razzazi-Fazeli E, Bo¨hm J, Zentek J. Effects of B-trichothecenes on luminal glucose transport across the isolated jejunal epithelium of broiler chickens. *J Anim Phys* Nut 92: 225-230, 2008.

Baldwin RL VI. The proliferative actions of insulin, insulin like growth factor-I, epidermal growth factor, butyrate and propionate on ruminal epithelial cells in vitro. *Small Rumin Res* 32: 261–268, 1999.

Bannink A, France J, Lopez S, Gerrits WJJ, Kebreab E, Tamminga S, Dijkstra J. Modelling the implications of feeding strategy on rumen fermentation and functioning of the rumen wall. *Anim Feed Sci Technol* 143: 3-26, 2008.

Barcroft J, McAnally RA, Phillipson AT. Absorption of volatile acids from the alimentary tracts of the sheep and other animals. *J Exp Biol* 20: 120-129, 1944.

Bergman EN. Energy contributions of volatile fatty acids from the gastrointestinal tract in various species. *Physiol Rev* 70: 567-590, 1990.

Bergman EN, Reid RS, Murray MG, Brockway JM, Whiteflow FG. Interconversions and production of volatile fatty acids in the sheep rumen. *Biochem* 97: 53-58, 1965.

Bevans DW, Beauchemin KA, Schwartzkopf-Genswein KS, McKinnon JJ, McAllister TA. Effect of rapid or gradual grain adaptation on subacute acidosis and feed intake by feedlot cattle. *J Anim Sci* 83: 1116-1132, 2005.

Bhavaniprasad V, Febin Prabhu Dass J, Jayanthi S. Activation mechanism of claudin-4 by ephrin type-A receptor 2: a molecular dynamics approach. *Mol Biosyst* 9: 2627-2634, 2013.

Bilk S, Huhn K, Honscha KU, Pfannkuche H, Gäbel G. Bicarbonate exporting transporters in the ovine ruminal epithelium. *Comp Physiol B* 175: 365-374, 2005.

Binder HJ, Rawlins CL. Electrolyte transport across isolated large intestinal mucosa. *Am J Physiol* 225: 1232–1239, 1973.

Bondzio A, Gabler C, Badewien-Rentzsch B, Schulze P, Martens H, Einspanier R. Identification of differentially expressed proteins in ruminal epithelium in response to a concentrate-supplemented diet. *Am J Physiol Gastrointest Liver Physiol* 301: G260-G268, 2011.

Bordin M, D'Atri F, Guillemot L, Citi, S. Histone deacetylase inhibitors up-regulate the expression of tight junction proteins. *Mol Cancer Res* 2: 692–701, 2004.

Brown AJ, Goldsworthy SM, Barnes AA, Eilert MM, Tcheang L, Daniels D, Muir AI, Wigglesworth MJ, Kinghorn I, Fraser NJ, Pike NB, Strum JC, Steplewski KM, Murdock PR, Holder JC, Marshall FH, Szekeres PG, Wilson S, Ignar DM, Foord SM, Wise A, Dowell SJ. The orphan G protein-coupled receptors GPR41 and GPR43 are

activated by propionate and other short chain carboxylic acids. *J Biol Chem* 278: 11312–11319, 2003.

Bugaut M. Occurrence, absorption and metabolism of short chain fatty acids in the digestive tract of mammals. *Comp Biochem Physiol B* 86: 439–472, 1987.

Calsamiglia S, Blanch M, Ferret A, Moya D. Is subacute ruminal acidosis a pH related problem? Causes and tools for its control. *Anim Feed Sci Tech* 172: 42-50, 2012.

Cameron REB, Dyk PB, Herdt TH, Kaneene JB, Miller R, Bucholtz HF, Liesman JS, Vandehaar MJ, Emery RS. Dry cow diet, management, and energy balance as risk factors for displaced abomasum in high producing dairy herds. *J Dairy Sci* 81: 132-139, 1998.

Carretta MD, Conejeros I, Hidalgo MA, Burgos RA. Propionate induces the release of granules from bovine neutrophils. *J Dairy Sci* 96: 2507–2520, 2013.

Chen Y, Oba M, Guan LL. Variation of bacterial communities and expression of Toll-like receptor genes in the rumen of steers differing in susceptibility to subacute ruminal acidosis. *Vet Microbiol* 159: 451–459, 2012.

Cheng KJ, Hironaka R, Jones GA, Nicas T, Costerton JW. Frothy feedlot bloat in cattle: production of extracellular polysaccharides and development of viscosity in cultures of *Streptococcus bovis*. *Can J Microbiol* 22: 450-459, 1976.

Cheng KJ, McAllister TA, Popp JD, Hristov AN, Mir Z, Shin HT. A review of bloat in feedlot cattle. *J Anim Sci* 76: 299-308, 1998.

Chester-Jones H, DiCostanzo A. A perspective on nutrition and management of incoming feedlot cattle. *Minnesota Cattle Feeder Report* B-414, 1994.

Clarke LL. A guide to Ussing chamber studies of mouse intestine. *Am J Physiol Gastrointest Liver Physiol* 296: G1151-G1166, 2009.

Coverdale JA, Tyler HD, Quigley JD III, Brumm JA. Effect of various levels of forage and form of diet on rumen development and growth in calves. *J Dairy Sci* 87: 2554–2562, 2004.

Dengler F, Rackwitz R, Benesch F, Pfannkuche H, G€abel G. Bicarbonate-dependent transport of acetate and butyrate across the basolateral membrane of sheep rumen epithelium. *Acta physiologica* doi: 10.1111/apha.12155., 2013.

Dinarello, CA. Biologic basis for interleukin-1 in disease. *Blood* 87: 2095–2147, 1996.

Dirksen G, Liebich H, Mayer K. Adaptive changes of the ruminal mucosa and functional and clinical significance. *Bovine Practice* 20: 116–120, 1985.

Doranalli K, Penner GB, Mutsvangwa T. Feeding oscillating dietary crude protein concentrations increases nitrogen utilization in growing lambs and this response is partly attributable to increased urea transfer to the rumen. *J Nutr* 141: 560-567, 2011.

Drackley JK. Biology of dairy cows during the transition period: The final frontier? *J Dairy Sci* 82: 2259–2273, 1999.

Emmanuel DGV, Madsen KL, Churchill TA, Dunn SM, Ametaj, BN. Acidosis and lipopolysaccharide from *Escherichiacoli* B:055 cause hyperpermeability of rumen and colon tissues. *J Dairy Sci* 90: 5552–5557, 2007.

Enemark JM. The monitoring, prevention and treatment of sub-acute ruminal acidosis (SARA): a review. *Vet J* 176: 32-43, 2008.

Etschmann B, Suplie A, Martens H. Change of ruminal sodium transport in sheep during dietary adaptation. *Arch Anim Nutr* 63: 26–38, 2009.

Fairfield AM, Plaizier JC, Duffield TF, Lindinger MI, Bagg R, Dick P, McBride BW. Effects of a prepartum administration of a monensin controlled release capsule on rumen pH, feed intake, and milk production of transition dairy cows. *J Dairy Sci* 90: 937–945, 2007.

Faix S, Faixova Z. *In vitro* transfer of L-alanine, L-histidine and carnosine across the rumen epithelium of sheep. *Acta Vet Brno* 70: 243–246, 2001.

Firth SM, Baxter RC. Cellular actions of the insulin-like growth factor binding proteins. *Endocr Rev* 23: 824–854, 2002.

Furuse M, Fujimoto K, Sato N, Hirase T, Tsukita S. Overexpression of occludin, a tight junction-associated integral membrane protein, induces the formation of intracellular multilamellar bodies bearing tight junction-like structures. *J Cell Sci* 109: 429 – 435, 1996.

Gäbel G, Aschenbach JR. Influence of food deprivation on the transport of 3-O-methyl-alpha-D-glucose across the isolated ruminal epithelium of sheep. *J Anim Sci* 80: 2740-2746, 2002.

Gäbel G, Aschenbach JR, Müller F. Transfer of energy substrates across the ruminal epithelium: implications and limitations. *Anim Health Res Rev* 3: 15-30, 2002.

Gäbel G, Bell M, Martens H. The effect of low mucosal pH on sodium and chloride movement across the isolated rumen mucosa of sheep. *J Exp Phys* 74: 35-44, 1989.

Gäbel G, Bestmann M, Martens H. Influences of diet, short-chain fatty acids, lactate and chloride on bicarbonate movement across the reticulorumen wall of sheep. *Zentralbl Veterinarmed A* 38: 523–529, 1991a.

Gäbel G, Butter H, Martens H. Regulatory role of cAMP in transport of Na^+, Cl^- and short-chain fatty acids across sheep ruminal epithelium. *Exper Physiol* 84: 333-345, 1999.

Gäbel G, Marek M, Martens H. Influence of food deprivation on SCFA and electrolyte transport across sheep reticulorumen. *Zentralbl Veterinarmed A* 40: 339-344, 1993.

Gäbel G, Sehested J. SCFA Transport in the Forestomach of Ruminants. *Comp Biochem Physiol* 118: 367–374, 1997.

Gäbel G, Vogler S, Martens H. Short-chain fatty acids and $C0_2$ as regulators of Na^+ and Cl^- absorption in isolated sheep rumen mucosa. *J Comp Physiol B* 161: 419-426, 1991b.

Gäebel G, Bell M, Martens H. The effect of low mucosal pH on sodium and chloride movement across the isolated rumen mucosa of sheep. *J Exp Phys* 74: 35-44, 1989.

Gaebel G, Martens H. Reversibility of acid induced changes in absorptive function of sheep rumen. *J Vet Med* 35: 157-160, 1988.

Gálfi P, Gäbel G, Martens H. Influences of extracellular matrix components on the growth and differentiation of ruminal epithelial cells in primary culture. *Res Vet Sci* 54: 102–109, 1993.

Garner MR, Flint JF, Russell JB. *Allisonella histaminiformans* gen. nov., sp. nov.; A novel bacterium that produces histamine, utilizes histidine as its sole energy source, and could play a role in bovine and equine laminitis. *Syst Appl Microbiol* 25: 498–506, 2002.

Ginsburg E, Salomon D, Sreevalsan T, Freese E. Growth inhibition and morphological changes caused by lipophilic acids in mammalian cells. *Proc Nat Acad Sci USA* 70: 2457-2461, 1973.

Goff JP. Major advances in our understanding of nutritional influences on bovine health. *J Dairy Sci* 89: 1292–1301, 2006.

González-Mariscal L, Tapia R, Chamorro D. Crosstalk of tight junction components with signaling pathways. *Biochimica et Biophysica Acta* 1778: 729–756, 2008.

Goodlad RA. Some effect of diet on the mitotic index and the cell cycle of the ruminal epithelium of sheep. *Exper Physiol* 66: 487-499, 1981.

Górka P, Kowalski ZM, Pietrzak P, Kotunia A, Jagusiak W, Holst JJ, Guilloteau P, Zabielski R. Effect of method of delivery of sodium butyrate on rumen development in newborn calves. *J Dairy Sci* 94: 5578–5588, 2011.

Gozho N, Mutsvangwa T. Influence of carbohydrate source on ruminal fermentation characteristics, performance, and microbial protein synthesis in dairy cows. *J Dairy Sci* 91: 2726–2735, 2008.

Graham C, Gatherar I, Haslam I, Glanville M, Simmons NL. Expression and localization of monocarboxylate transporters and sodium/proton exchangers in bovine rumen epithelium. *Am J Physiol Regul Integr Comp Physiol* 292: R997-R1007, 2007.

Graham C, Simmons NL. Functional organization of the bovine rumen epithelium. *Am J Physiol Regul Integr Comp Physiol* 288: R173-R181, 2005.

Gröhn YT, Eicker SW, Ducrocq V, Hertl JA. Effect of diseases on the culling of Holstein dairy cows in New York state. *J Dairy Sci* 81: 966–978, 1998.

Hinders RG, Owen FG. Relation of ruminal parakeratosis development to volatile fatty acid absorption. *J Dairy Sci* 48: 1069-1073, 1965.

Hironaka R, Miltimore JE, McArthur JM, McGregor DR, Smith ES. Influence of particle size of concentrate on rumen conditions associated with feedlot bloat. *Can J Anim Sci* 53: 75-80, 1973.

Hossain MZ, Ao P, Boynton AL. Platelet-derived growth factor-induced disruption of gap junctional communication and phosphorylation of connexin43 involves protein kinase C and mitogen-activated protein kinase. *J Cell Physiol* 176: 332–341, 1998.

Hutcheson DP, Cole NA. Management of transit stress syndrome in cattle: Nutritional and environmental effects. *J Anim Sci* 62: 555-560, 1986.

Islas S, Vega J, Ponce L, Gonzalez-Mariscal L. Nuclear localization of the tight junction protein ZO-2 in epithelial cells. *Exp Cell Res* 274: 138–148, 2002.

John LJ, Fromm M, Schulzke JD. Epithelial barriers in intestinal inflammation. *Antioxid Redox Signal* 15: 1255-1270, 2011.

Kalsi KK, Baker EH, Fraser O, Y-L Chung, Mace OJ, Tarelli E, Philips BJ, Baines DL. Glucose homeostasis across human airway epithelial cell monolayers: role of diffusion, transport and metabolism. *Pflugers Arch Eur J Physiol* 457: 1061–1070, 2009.

Kaulfuss S, Burfeind P, Gaedcke J, Scharf JG. Dual silencing of insulin-like growth factor-I receptor and epidermal growth factor receptor in colorectal cancer cells is associated with decreased proliferation and enhanced apoptosis. *Mol Cancer Ther* 8: 821–833, 2009.

Khorasani GR, Okine, EK, Kennelly, JJ. Forage source alters nutrient supply to the intestine without influencing milk yield. *J Dairy Sci* 79: 862–872, 1996.

Kirat D, Masuoka J, Hayashi H, Iwano H, Yokota H, Taniyama H, Kato S. Monocarboxylate transporter 1 (MCT1) plays a direct role in short-chain fatty acids absorption in caprine rumen. *J Physiol* 576: 635–647, 2006.

Kleen JL, Hooijer GA, Rehage J, Noordhuizen JP. Subacute ruminal acidosis in Dutch dairy herds. *Vet Rec* 164: 681-683, 2009.

Klevenhusen F, Hollmann M, Podstatzky-Lichtenstein L, Krametter-Frotscher R, Aschenbach JR, Zebeli Q. Feeding barley grain-rich diets altered electrophysiological properties and permeability of the ruminal wall in a goat model. *J Dairy Sci* 96: 2293–2302, 2013.

Kramer T, Michelberger T, Gürtler H, Gäbel G. Absorption of short chain fatty acids across ruminal epithelium of sheep. *J Comp Physiol B* 166: 262–269, 1996.

Krause KM, Oetzel GR. Understanding and preventing subacute ruminal acidosis in dairy herds: A review. *Anim Feed Sci Technol* 126: 215–236, 2006.

Kristensen NB, Danfær A, Agnergaard N. Absorption and metabolism of short-chain fatty acids in ruminants. *Arch Anim Nutr* 5: 165-175, 1998.

Kristensen NB, Danfaer A, Agergaard N. Diurnal patterns of ruminal concentrations and portal appearance rates of short-chain fatty acids in sheep fed hay or a concentrate/straw diet in two meals daily. *Acta Agric Scand Sect A, Anim Sci* 46: 227–238, 1996.

Kristensen NB, Harmon DL. Splanchnic metabolism of volatile fatty acids absorbed from the washed reticulorumen of steers. *J Anim Sci* 2: 2033-2042, 2004.

Laarman AH, Oba M. Short communication: Effect of calf starter on rumen pH of Holstein dairy calves at weaning. *J Dairy Sci* 94: 5661-5664, 2011.

Langbein L, Grund C, Kuhn C, Praetzel S, Kartenbeck J, Brandner JM, Moll I, Franke WW. Tight junctions and compositionally related junctional structures in mammalian stratified epithelia and cell cultures derived therefrom. *Euro J Cell Biol* 81: 419-435, 2002.

Lavker RM, Matoltsy AG. Formation of horney cells. Cell Biol 44: 501-512, 1970.

LeBlanc SJ, Leslie KE, Duffield TF. Metabolic predictors of displaced abomasum in dairy cattle. *J Dairy Sci* 88: 159-170, 2005.

Lechartier C, Peyraud JL. The effects of forage proportion and rapidly degradable dry matter from concentrate on ruminal digestion in dairy cows fed corn silage–based diets with fixed neutral detergent fiber and starch contents. *J Dairy Sci* 93: 666–681, 2010.

Leonhard-Marek S, Becker G, Breves B, Schröder, B. Chloride, gluconate, sulfate, and short-chain fatty acids affect calcium flux across the sheep forestomach epithelium. *J Dairy Sci* 90: 1516–1526, 2007.

Leonard-Marek S, Gäbel G, Martens H. Effects of short chain fatty acids and carbon dioxide on magnesium transport across sheep rumen epithelium. *Exp Physiol* 83: 155-164, 1998.

Leonhard-Marek S, Stumpff F, Brinkmann I, Breves G, Martens H. Basolateral Mg^{2+}/Na^{+} exchange regulates apical nonselective cation channel in sheep rumen epithelium via cytosolic Mg^{2+}. *Am J Physiol Gastrointest Liver Physiol* 288: G630-G645, 2005.

Leonard-Marek S, Stumpff F, Martens H. Transport of cations and anions across forestomach epithelia: conclusions from in vitro studies. *Animal* 4: 1037-1056, 2010.

Lesmeister KE, Heinrichs AJ. Effects of corn processing on growth characteristics, rumen development, and rumen parameters in neonatal dairy calves. *J Dairy Sci* 87: 3439-3450, 2004.

Liebich HG, Dirksen G, Arbel A, Dori S, Mayer E. Feed-dependent changes in the rumen mucosa of high-producing cows from the dry period to eight weeks post partum. *Zentralbl Veterinarmed A* 34: 661-672, 1987.

Loerch SC. Effects of feeding growing cattle high-concentrate diets at a restricted intake on feedlot performance. *J Anim Sci* 68: 3086-3095, 1990.

Li H, Shepparda DN, Hug MJ. Transepithelial electrical measurements with the Ussing chamber. *J Cyst Fibros* 3: 123-126, 2004.

Liu J, Xu T, Liu Y, Zhu W, Mao S. High-grain diet causes massive disruption of ruminal epithelial tight junctions in goats. *Am J Physiol Regul Integr Comp Physiol* (June 5, 2013). doi:10.1152/ajpregu.00068.

Livak KJ, Schmittgen TD. Analysis of relative gene expression data using real-time quantitative PCR and the 2−ΔΔCT method. *Methods* 25: 402–408, 2001.

Lodemann U, Martens H. Effects of diet and osmotic pressure on Na+ transport and tissue conductance of sheep isolated rumen epithelium. *Exp Physiol* 91.3: 539–550, 2006.

López S, Hovell FD, Dijkstra J, France J. Effects of volatile fatty acid supply on their absorption and on water kinetics in the rumen of sheep sustained by intragastric infusions. *J Anim Sci* 81: 2609–2616, 2003.

Ma TY, Iwamoto GK, Hoa NT, Akotia V, Pedram A, Boivin MA, Said HM. TNF-alpha-induced increase in intestinal epithelial tight junction permeability requires NF-kappa B activation. *Am J Physiol-Gastr L* 286: G367-G376, 2004.

Malhi M, Gui H, Yao L, Aschenbach JR, Gäbel G, Shen Z. Increased papillae growth and enhanced short-chain fatty acid absorption in the rumen of goats are associated with transient increases in cyclin D1 expression after ruminal butyrate infusion. *J Dairy Sci* (October 10, 2013). doi: 10.3168/jds.2013-6700.

Mall M, Grubb BR, Harkema JR, O'Neal1 WK, Boucher RC. Increased airway epithelial Na^+ absorption produces cystic fibrosis-like lung disease in mice. *Nature Med* 10: 487-493, 2004.

Masamitsu T, Reiko K, Ryuichi S. EphA2 phosphorylates the cytoplasmic tail of claudin-4 and mediates paracellular permeability. *Biol Chem* 280: 42375–42382, 2005.

Matthews JC, Webb KE Jr. Absorption of L-carnosine, L-methionine, and L-methionylglycine by isolated sheep ruminal and omasal epithelial tissue. *J Anim Sci* 73: 3464-3475, 1995.

McArt JAA, Nydam DV, Ospina PA, Oetzel GR. A field trial on the effect of propylene glycol on milk yield and resolution of ketosis in fresh cows diagnosed with subclinical ketosis. *J Dairy Sci* 94: 6011–6020, 2011.

Mentschel J, Leiser R, Mulling C, Pfarrer C, Claus R. Butyric acid stimulates rumen mucosa development in the calf mainly by a reduction of apoptosis. *Arch Tierernahr* 55: 85–102, 2001.

Metzler-Zebeli BU, Schmitz-Esser S, Klevenhusen F, Podstatzky-Lichtenstein L, Wagner M, Zebeli Q. Grain-rich diets differently alter ruminal and colonic abundance of microbial populations and lipopolysaccharide in goats. *Anaerobe* 20: 65-73, 2013.

Muscher AS, Schroder B, Breves G, Huber K. Dietary nitrogen reduction enhances urea transport across goat rumen epithelium. *J Anim Sci* 88: 3390–3398, 2010.

Müller F, Huber K, Pfannkuche H, Aschenbach JR, Breves G, Gaebel G. Transport of ketone bodies and lactate in the sheep ruminal epithelium by monocarboxylate transporter 1. *Am J Physiol Gastrointest Liver Physiol* 283: G1139–G1146, 2002.

Nagaraja TG, Bartley EE, Fina LR, Anthony HD, Bechtle RM. Evidence of endotoxins in the rumen bacteria of cattle fed hay or grain. *J Anim Sci* 47: 226–234, 1978.

Nagaraja TG, Chengappa MM. Liver abscesses in feedlot cattle: a review. *J Anim Sci* 76: 287-298, 1998.

Nagaraja TG, Narayanan SK, Stewart GC, Chengappa MM. Fusobacterium necrophorum infections in animals: pathogenesis and pathogenic mechanisms. *Anaerobe* 11: 239-246, 2005.

Nagaraja TG, Titgemeyer EC. Ruminal acidosis in beef cattle: The current microbiological and nutritional outlook. *J Dairy Sci* 90: E17-E38, 2007.

Nocek JE. Bovine acidosis: Implications on laminitis. *J Dairy Sci* 80: 1005–1028, 1997.

NRC. Nutrient requirements of beef cattle. 7th rev. ed. Natl Acad Press Washington, DC, 2000.

Obara Y, Dellow D, Nolan J. Effects of energy-rich supplements on nitrogen kinetics in ruminants. Page 551 in Physiological Aspects of Digestion and Metabolism in Ruminants. T. Tsuda, Y. Sasaki, and R. Kawashima, ed. Academic Press, San Diego, CA, 1991.

Oh DY, Lagakos WS. The role of G-protein-coupled receptors in mediating the effect of fatty acids on inflammation and insulin sensitivity. *Curr Opin Clin Nutr Metab Care* 14: 322-327, 2011.

Oshima T, Koseki J, Chen X, Matsumoto T, Miwa H. Acid modulates the squamous epithelial barrier function by modulating the localization of claudins in the superficial layers. *Lab Invest* 92: 22-31, 2012.

Owens FN, Secrist DS, Hill WJ, Gill DR. Acidosis in cattle: a review. *J Anim Sci* 76: 275-286, 1998.

Peng L, Li Z-R, Green RS, Holzman IR, Lin J. Butyrate enhances the intestinal barrier by facilitating tight junction assembly via activation of AMP-activated protein kinase in Caco-2 cell monolayers. *J Nutr* 139: 1619–1625, 2009.

Penner GB, Aschenbach JR, Gäbel G, Oba M. Technical note: evaluation of continuous ruminal pH measurement system for use in non-cannulated small ruminants. *J Anim Sci* 87: 2363-2366, 2009c.

Penner GB, Aschenbach JR, Gäbel G, Rackwitz R, Oba M. Epithelial capacity for apical uptake of short chain fatty acids is a key determinant for intraruminal pH and the susceptibility to subacute ruminal acidosis in sheep. *J Nutr* 139: 1714-1720, 2009a.

Penner GB, Beauchemin KA, Mutsvangwa T. The severity of ruminal acidosis in primiparous Holstein cows during the periparturient period. *J Dairy Sci* 90: 365-375, 2007.

Penner GB, Oba M. Increasing dietary sugar concentration may improve dry matter intake, ruminal fermentation, and productivity of dairy cows in the post-partum phase of the transition period. *J Dairy Sci* 92: 3341-3353, 2009.

Penner GB, Oba M, Gabel G, Aschenbach JR. A single mild episode of subacute ruminal acidosis does not affect ruminal barrier function in the short term. *J Dairy Sci* 93: 4838–4845, 2010.

Penner GB, Steele MA, Aschenbach JR, McBride BW. RUMINANT NUTRITION SYMPOSIUM: Molecular adaptation of ruminal epithelia to highly fermentable diets. *J Anim Sci* 89: 1108-1119, 2011.

Penner GB, Taniguchi M, Guan LL, Beauchein KA, Oba M. Effect of dietary forage to concentrate ratio on volatile fatty acid absorption and the expression of genes related to volatile fatty acid absorption and metabolism in ruminal tissue. *J Dairy Sci* 92: 2767-2781, 2009b.

Pfaffl MW. A new mathematical model for relative quantification in real-time RT-PCR. *Nucleic Acids Res* 29: 2002-2007, 2001.

Plaizier JC, Khafipour E, Li S, Gozho GN, Krause DO. Subacute ruminal acidosis (SARA), endotoxins and health consequences. *Anim Feed Sci Tech* 172: 9-21, 2012.

Plaizier JC, Krause DO, Gozho GN, McBride BW. Subacute ruminal acidosis in dairy cows: the physiological causes, incidence and consequences. *Vet J* 176: 21-31, 2009.

Rabbani I, Siegling-Vlitakis C, Noci B, Martens H. Evidence for NHE3-mediated Na transport in sheep and bovine forestomach. *Amer J Physiol – Regu Physiol* 30: R313-R319, 2011.

Rajala-Schultz PJ, Gröhn YT, McCulloch CE. Effects of milk fever, ketosis, and lameness on milk yield in dairy cows. *J Dairy Sci* 82: 288–294, 1999.

Raleigh DR, Boe DM, Yu D, Weber CR, Marchiando AM, Bradford EM, Wang Y, Wu L, Schneeberger EE, Shen L, Turner JR. Occludin S408 phosphorylation regulates tight junction protein interactions and barrier function. *J Cell Biol* 193: 565-582, 2011.

Sáez JC, Berthoud VM, Branes MC, Martinez AG, Beyer EC. Plasma Membrane Channels Formed by Connexins: Their Regulation and Functions. *Physiol Rev* 83: 1359–1400, 2003.

Sakata T, Hikosaka K, Shiomura Y, Tamate H. Stimulatory effect of insulin on ruminal epithelium cell mitosis in adult sheep. *Br J Nutr* 44: 325–331, 1980.

Sakata T, Tamate H. Rumen epithelial cell proliferation accelerated by rapid increase in intraruminal butyrate. *J Dairy Sci* 61: 1109-1113, 1978.

Sander EG, Warner RG, Harrison HN, Loosli JK. The stimulatory effect of sodium butyrate and sodium propionate on development of rumen mucosa in the young calf. *J Dairy Sci* 42: 1600-1605, 1959.

Schlau N, Guan LL, Oba M. The relationship between rumen acidosis resistance and expression of genes involved in regulation of intracellular pH and butyrate metabolism of ruminal epithelial cells in steers. *J Dairy Sci* 95: 5866–5875, 2012.

Schwartzkopf-Genswein KS, Beauchemin KA, Gibb DJ, Crews DH Jr, Hickman DD, Streeter M, McAllister TA. Effect of bunk management on feeding behavior, ruminal acidosis and performance of feedlot cattle: A review. *J Anim Sci* 81(Suppl. 2): E149–E158, 2003.

Schwartzkopf-Genswein KS, Beauchemin KA, McAllister TA, Gibb DJ, Streeter M, Kennedy AD. Effect of feed delivery fluctuations and feeding time on ruminal acidosis, growth performance, and feeding behavior of feedlot cattle. *J Anim Sci* 82: 3357–3365, 2004.

Schwartz CJ, Kimberg DV, Sheerin HE, Field M, Said SI. Vasoactive Intestinal Peptide Stimulation of Adenylate Cyclase and Active Electrolyte Secretion in Intestinal Mucosa. *J Clin Investig* 54: 536-544, 1974.

Schwarz BT, Wang F, Shen L, Clayburgh DR, Su L, Wang Y, Fu YX, Turner JR. LIGHT signals directly to intestinal epithelia to cause barrier dysfunction via cytoskeletal and endocytic mechanisms.*Gastroenterol* 132: 2383-2394, 2007.

Schweigel M, Freyer M, Leclercq S, Etschmann B, Lodemann U, Böttcher A, Martens H. Luminal hyperosmolarity decreases Na transport and impairs barrier function of sheep rumen epithelium. *J Comp Physiol B* 174: 575–591, 2005.

Schweigel M, Kuzinski J, Deiner C, Kolisek M. Rumen epithelial cells adapt magnesium transport to high and low extracellular magnesium conditions. *Magnes Res* 22: 133-150, 2009.

Sehested J, Diernaes L, Møller PD, Skadhauge E. Ruminal transport and metabolism of short-chain fatty acids (SCFA) in vitro: effect of SCFA chain length and pH. *Compar Biochem Physiol A* 123: 359–368, 1999a.

Sehested J, Diernæs L, Møller PD, Skadhauge E. Transport of butyrate across the isolated bovine rumen epithelium – interaction with sodium, chloride and bicarbonate. *Comp Biochem Physiol A* 123: 399-408, 1999b.

Sehested J, Diernæs L, Møller PD, Skadhauge E. Transport of sodium across the isolated bovine rumen epithelium: interaction with short-chain fatty acids, chloride and bicarbonate. *Exp Phyiol* 81: 79-94, 1996.

Shaver RD. Nutritional risk factors in the etiology of left displaced abomasum in dairy cows: a review. *J Dairy Sci* 80: 2449-53, 1997.

Shen Z, Martens H, Schweigel-Röntgen M. Na^+ transport across **rumen** epithelium of hay-fed sheep is acutely stimulated by the peptide IGF-1 in vitro. *Exp Physiol* 97: 497-505, 2012.

Shen Z, Seyfert HM, Lorhke B, Schneider F, Zitnan R, Chudy A, Kuhla S, Hammon HM, Blum JW, Martens H, Hagemeister H, Voigt J. An energy-rich diet causes rumen papillae proliferation associated with more IGF-1 receptors and increased plasma IGF-1 concentrations in young goats. *J Nutr* 134: 11-17, 2004.

Shen L, Weber CR, Turner JR. The tight junction protein complex undergoes rapid and continuous molecular remodeling at steady state. *J Cell Biol* 181: 683–695, 2008.

Steele MA, Croom J, Kahler M, AlZahal O, Hook SE, Plaizier K, McBride BW. Bovine rumen epithelium undergoes rapid structural adaptations during grain-induced subacute ruminal acidosis. *Am J Physiol Regul Integr Comp Physiol* 300: R1515–R1523, 2011.

Steele MA, Dionissopoulos L, AlZahal O, Doelman J, McBride BW. Rumen epithelial adaptation to ruminal acidosis in lactating cattle involves the coordinated expression of insulin-like growth factor-binding proteins and a cholesterolgenic enzyme. *J Dairy Sci* 95: 318–327, 2012.

Steven DH, Marshall AB. Organisation of the rumen epithelium. In: *Physiology of Digestion and Metabolism in the Ruminant*, edited by Phillipson AT. Newcastle upon Tyne, UK: Oriel, 1970.

Stumpff F, Georgi M-I, Mundhenk L, Rabbani I, Fromm M, Martens H, Günzel D. Sheep rumen and omasum primary cultures and source epithelia: barrier function aligns with expression of tight junction proteins. *J Exper Biol* 214: 2871-2882, 2011.

Stumpff F, Martens H, Bilk S, Aschenbach JR, Gäbel G. Cultured ruminal epithelial cells express a large-conductance channel permeable to chloride, bicarbonate, and acetate. *Pflugers Arch* 457: 1003-1022, 2009.

Suárez BJ, Van Reenen CG, Beldman G, van Delen J, Dijkstra J, Gerrits WJ. Effects of supplementing concentrates differing in carbohydrate composition in veal calf diets: I. Animal performance and rumen fermentation characteristics. *J Dairy Sci* 89: 4365-4375, 2006.

Sukka-Ganesh B, Mohammed KA, Kaye F, Goldberg EP, Nasreen N. Ephrin-A1 inhibits NSCLC tumor growth via induction of Cdx-2 a tumor suppressor gene. *BMC Cancer* 12: 309-322, 2012.

Sutton JD, Dhanoa MS, Morant SV, France J, Napper DJ, Schuller E. Rates of production of acetate, propionate, and butyrate in the rumen of lactating dairy cows given normal and low-roughage diets. *J Dairy Sci* 86: 3620-3633, 2003.

Takayama Y, Kanoe M, Maeda K, Okada Y, Kai K. Adherence of Fusobacterium necrophorum subsp. necrophorum to ruminal cells derived from bovine rumenitis. *Letters Appl Microbiol* 3: 308-311, 2000.

Tan ZL, Nagaraja TG, Chengappa MM. Biochemical and biological characterization of ruminal *Fusobacterium necrophorum. FEMS Microbiol Letters* 120: 81-86, 1994.

Tappeiner, H. Untersuchungen iiber die garbing der cellulose insbesondere iiber deren losting in darmkanale. *Z Biol* 20: 52-134, 1884.

Traweger A, Fuchs R, Krizbai IA, Weiger TM, Bauer HC, Bauer H. The tight junction protein ZO-2 localizes to the nucleus and interacts with the heterogeneous nuclear ribonucleoprotein scaffold attachment factor-B. *J Biol Chem* 278: 2692–2700, 2003.

Ussing HH, Zerhan K. Active transport of sodium as the source of electric current in the short-circuited isolated frog skin. *Acta Physiol Scand* 23: 110-127, 1951.

Vasconcelos JT, Galyean ML. Nutritional recommendations of feedlot consulting nutritionists: The 2007 Texas Tech University survey. *J Anim Sci* 85: 2772-2781, 2007.

Walsh RB, Walton JS, Kelton DF, LeBlanc SJ, Leslie KE, Duffield TF. The effect of subclinical ketosis in early lactation on reproductive performance of postpartum dairy cows. *J Dairy Sci* 90: 2788–2796, 2007.

Wang A, Gu Z, Heid B, Akers RM, Jiang H. Identification and characterization of the bovine G protein-coupled receptor GPR41 and GPR43 genes. *J Dairy Sci* 92: 2696-2705, 2009b.

Wang A, Si H, Liu D, Jiang H. Butyrate activates the cAMP-protein-kinase A-cAMP response element-binding protein signaling pathway in Caco-2 cells. *J Nutr* 142: 1-6, 2012.

Wang YH, Xu M, Wang FN, Yu ZP, Yao JH, Zan LS, Yang FX. Effect of dietary starch on rumen and small intestine morphology and digesta pH in goats. *Livest Sci* 122: 48-52, 2009a.

Warner ACI, Stacy BD. The fate of water in the rumen. *Br J Nut* 22: 389-410, 1968.

Watson CJ, Hoare CJ, Garrod DR, Carlson GL, Warhurst G. Interferon-gamma selectively increases epithelial permeability to large molecules by activating different populations of paracellular pores. *J Cell Sci* 118: 5221-5230, 2005.

White TW. Nonredundant gap junction functions. *Physiol* 18: 95-99, 2003.

Wilkens MR, Mrochen N, Breves G, Schröder B. Gastrointestinal calcium absorption in sheep is mostly insensitive to an alimentary induced challenge of calcium homeostasis. *Compar biochem physiol* 158: 199-207, 2011.

Wilson DJ, Mutsvangwa T, Penner GB. Supplemental butyrate does not enhance the absorptive or barrier functions of the isolated ovine ruminal epithelia. *J Anim Sci* 90: 3153-3161, 2012.

Yang W, Shen Z, Martens H. An energy-rich diet enhances expression of Na^+/H^+ exchanger isoform 1 and 3 messenger RNA in rumen epithelium of goat. *J Anim Sci* 90: 307-317, 2012.

Zhang S, Albornoz RI, Aschenbach JR, Barreda DR, Penner GB. Short-term feed restriction impairs the absorptive function of the reticulo-rumen and total tract barrier function in beef cattle. *J Anim Sci* 91: 1685-1695, 2013a.

Zhang S, Aschenbach JR, Barreda DR, Penner GB. Recovery of absorptive function of the reticulo-rumen and total tract barrier function in beef cattle after short-term feed restriction. *J Anim Sci* 91: 1696-1706, 2013b.